FGFR1-Dependency Prediction by Genomic and Functional Analysis in Squamous Cell Lung Cancer

Inaugural-Dissertation

zur

Erlangung des Doktorgrades

Der Mathematischen-Naturwissenschaftlichen Fakultät

der Universität zu Köln

vorgelegt von

Florian Malchers

aus Bonn

März 2014

Berichterstatter (Gutachter)

1. Gutachter: Prof. Dr. Manolis Pasparakis
2. Gutachter: Prof. Dr. Roman K. Thomas

Tag der mündlichen Prüfung: 22.05.2014

Zusammenfassung in deutscher Sprache

Amplifikationen (Vervielfältigungen genetischen Materials) des menschlichen 8p12-Lokus (FGFR1) treten in etwa 20% aller Plattenepithelkarzinome der Lunge auf. Diese könnten in einer ansonsten unzureichend behandelbaren Klasse von Lungentumoren mit einer therapierbaren FGFR1-Abhängigkeit einhergehen. Allerdings ist derzeit der Zusammenhang zwischen einer 8p12-Amplifikation und einer therapeutisch behandelbaren FGFR1-Abhängigkeit unklar. In dieser Studie wurden mit Hilfe von zwei Computerprogrammen genetische Kopienzahlveränderungen von Plattenepithelkarzinomen der Lunge analysiert. Dadurch konnte ein heterogenes Amplifikations-Muster des 8p12-Lokus dargestellt werden. Es zeigte sich, dass nur eine kleine Anzahl der 8p12-Amplifikationen zentriert auf FGFR1 vorlagen. Dies konnte bei anderen häufig vorkommenden Amplifikationen wie EGFR (7p11) oder CCND1 (19q12) nicht beobachtet werden. RNA-Sequenzierung von FGFR1-amplifizierten Tumoren führte zur Identifizierung primär exprimierter FGFR1-Splice-Varianten. Ferner konnte eine Ligandenabhängigkeit von FGFR1-amplifizierten Tumorzellen gezeigt werden. FGFR1-Überexpression führte zu einer mäßigen Transformation von NIH3T3-Zellen. Der transformierende Phänotyp dieser Zellen konnte durch die Co-Expression von MYC deutlich verstärkt und gegenüber FGFR-Hemmung empfindlich gemacht werden. Daraus folgend wurde gezeigt, dass FGFR1-amplifizierte und FGFR Inhibitoren empfindliche Zelllinien MYC regulieren und hoch exprimieren. In einer großen Kohorte von Tumorbiopsien korrelierte die FGFR1-Amplifikation mit einer FGFR1-Proteinphosphorylierung. Jedoch exprimierte nur ein kleiner Teil beträchtliche Mengen von MYC, was vermuten ließ, dass nur diese Patienten von einer FGFR-Inhibitortherapie profitieren würden. Die Behandlung eines Patienten mit einem FGFR1-amplifizierten und MYC-positiven Plattenepithelkarzinom führte nach sechs Wochen teilweise zu einer Remission.

Danksagung

Ich danke meiner gesamten Familie, besonders meiner Frau Laura, meinen Kindern und Eltern sowie meinen Brüdern.

Auch folgenden Personen gebührt besonderer Dank:

Jakob Schöttle, Dr. Martin Peifer, Dr. Danila Seidel, Dr. Julie George, Dr. Johannes Heukmann, Dr. Oliver Gautschi, Dr. Lukas Heukamp sowie Dr. Felix Dietlein

Ganz besonders möchte ich noch Prof. Dr. Roman Thomas für seine Ausbildung und Betreuung, seine große Geduld sowie für das freundschaftliche Verhältnis danken

ABBREVIATIONS 7

1 ABSTRACT 9

2 INTRODUCTION 11

2.1 CANCER 11
2.1.1 LUNG CANCER 14
2.1.2 HISTOLOGY OF LUNG CANCER 15
2.2 SOMATIC MUTATIONS 16
2.3 ONCOGENES AND TUMOR SUPPRESSOR GENES 18
2.4 CELL SIGNALING AND PROTEIN KINASES 21
2.4.1 RECEPTOR TYROSINE KINASES 23
2.4.2 FIBROBLAST GROWTH FACTOR RECEPTORS 25
2.5 GROWTH FACTORS 30
2.5.1 FIBROBLAST GROWTH FACTORS 31
2.6 TRANSCRIPTION FACTORS 35
2.7 KINASE INHIBITORS AND TARGETED THERAPY 37

3 OBJECTIVE OF THIS STUDY 39

4 MATERIAL AND METHODS 40

4.1 REAGENTS 40
4.2 APOPTOSIS ASSAYS 40
4.3 cDNA TRANSCRIPTION 40
4.4 CELL LINE STIMULATION 41
4.5 CELL LINES 41
4.6 COMPUTATIONAL ANALYSIS 42
4.7 ELISA ASSAY 43
4.8 FGFR1 CLONING AND SITE-DIRECTED MUTAGENESIS 43
4.9 IMMUNOBLOTTING 44
4.10 IMMUNOHISTOCHEMISTRY 44
4.11 QUANTITATIVE REAL-TIME PCR 45
4.12 RNAI AND STABLE TRANSDUCTION 45
4.13 SOFT-AGAR ASSAY 45
4.14 STABLE cDNA EXPRESSION 46
4.15 VIABILITY ASSAYS AND COMPOUND ACTIVITY PREDICTION 46
4.16 VIRUS PRODUCTION 46
4.17 WHOLE TRANSCRIPTOME SEQUENCING (RNASEQ) 47
4.18 XENOGRAFT MOUSE MODELS 48
4.19 PRIMER LIST 49

5 RESULTS 53

5.1 HETEROGENIC AMPLIFICATION PATTERN OF THE 8P12 LOCUS 53

5.2 Activation of the MAPK Pathway by FGFs 55
5.3 Secretion of FGF2 and 4 by *FGFR1*-amplified Tumor Cells 57
5.4 Ligand Dependency of H1581 Cells 59
5.5 FGFs Requirement of H1581 Cells for Tumor Formation 62
5.6 FGF Signaling is Saturated in *FGFR1*-amplified Lung Cancer Cells 63
5.7 Identification of FGFR1 Splice Variants Expressed in 8p12-Amplified Tumors 65
5.8 MYC Induced Transformation Supported by Oncogenic FGFR1 Expression 67
5.9 Initiation of Tumor Formation by FGFR1 69
5.10 Regulation of MYC in FGFR1-Depended Cell Lines 71
5.11 Prediction of FGFR Inhibitor Sensitivity by FGFR1 and MYC Expression 73
5.12 FGFR1 and MYC Expression in Primary 8p12-Amplified Lung Tumors 75
5.13 Clinical Case 76

6 DISCUSSION 79

7 SUMMARY 82

8 REFERENCES 83

8.1 Additional sources 92

9 PUBLICATIONS 94

APPENDIX I

Abbreviations

ABL	c-abl oncogene one
AD	Adenocarcinoma
AKT	v-akt murine thymoma viral oncogene homolog 1
Apaf1	Apoptotic protease activating factor 1
ARF	Adenosyl-ribosylierungs-faktor
ATP	Adenosine triphosphate
Bax	BCL2-associated X protein
BCR	Breakpoint cluster region
CD95	Fas-receptor
CEF	Chicken embryo fibroblasts
CLCGP	Clinical Lung Cancer Genome Project
CT	Computer tomography
CYP7A1	Cholesterol 7alpha-hydroxylase
DBD	DNA-binding domain
DNA	Deoxyribonucleic acid
EGF	Epidermal growth factor
EGFR	Epidermal growth factor receptor
Eph	Ephedrine
ERBB2	v-erb-b2 erythroblastic leukemia viral oncogene homolog 2
Erk	Extracellular-signal regulated kinase
FCS	Fetal Calf Serum
FDG-PET	Fluordesoxyglucose - Positron Emission Tomography
FGF	Fibroblast growth factor
FGFR1	Fibroblast growth factor receptor 1
FGFR2	Fibroblast growth factor receptor 2
FGFR3	Fibroblast growth factor receptor 3
FGFR4	Fibroblast growth factor receptor 3
FGFRs	Fibroblast growth factor receptors
Flt3	Receptor-type tyrosine-protein kinase
FRS2	Fibroblast growth factor receptor substrate 2
Gab1	GRB2-associated-binding protein 1
GDNF	Glial cell line-derived neurotropic factor
GFs	Growth factors
GLUT1	Glucose transporter 1
Grb2	Growth factor receptor-bound protein 2
HGF	Hepatocyte growth factor
HSPG	Heparin sulfate proteoglycan
IG	Immunoglobulin
IGF	Insulin-like growth factor
IGV	Integrative Genome Viewer

KD	Kinase domain
Kgf2	Keratinocyte growth factor 2
Kit	v-kit Hardy-Zuckerman 4 feline sarcoma viral oncogene homolog
LC	Large-Cell Carcinoma
MAPK	Mitogen-activated protein kinase
Mbp	Mega base pairs
MOMP	Mitochondrial outer membrane permeabilization
mRNA	Messenger ribonucleic acid
MuSK	Muscle-specific kinase
NGF	Nerve growth factor
Noxa	Phorbol-12-myristate-13-acetate-induced protein 1
NSCLC	Non-small cell lung cancer
p107	Retinoblastoma-like protein 1
p130	Retinoblastoma-like protein 2
p21	Cyclin-dependent kinase inhibitor 1
p38	P38 mitogen-activated protein kinases
p53	Tumor protein p53
PDGF	Platelet derived growth factor
PKB	Protein kinase B
PKC	Protein kinase C
PLC	phospholipase C
PPARα	Peroxisome proliferator-activated receptor-α
PUMA	P53 upregulated modulator of apoptosis
Raf	Rapidly accelerated fibrosarcoma
Ras	Rat sarcoma
RB	Retinoblastoma-protein
RKI	Robert Koch Institute
RNA	Ribonucleic acid
RSV	Rous sarcoma virus
RPMI	Roswell Park Memorial Institute medium
SCC	Squamous cell lung cancer
SCF	Stem cell factor
SCLC	Small Cell Lung Cancer
Sef	Similar expression to fgf
SPHK1	Sphingosine kinase 1
SSD	Signal-sensing domain
STAT	Signal transducers and activators of transcription
TAD	Trans activation domain
TGF	Transforming growth factor
Tie2	Angiopoietin-1 receptor
TKD	Tyrosine kinase domain
VEGF	Vascular endothelial growth factor

1 Abstract

Amplifications of 8p12 occur in approximately 20% of squamous cell lung cancer (SCC) samples and may define a FGFR1 dependent, therapeutically amenable class of this tumor entity with poor outcome. However, association of 8p12-amplification with therapeutically tractable FGFR1 dependency is presently unclear. In this study copy number data of squamous cell lung cancer were analyzed using GISTIC (Genomic Identification of Significant Targets in Cancer) and visualized by IGV (Integrative Genomics Viewer). Thereby we were able to show the heterogeneity of the 8p12 locus. In spite of focal amplified regions, only a minority of 8p12 amplicons appeared to be centered on *FGFR1* – which could not be observed for other recurrent amplified loci, e.g. *EGFR* (7p11) or *CCND1* (19q12). Further, RNA sequencing of *FGFR1*-amplified tumors identified splice variants expressed by *FGFR1*-amplified carcinomas. Moreover, *FGFR1*-amplified tumor cells were found to be ligand dependent and overexpression of FGFR1 in NIH3T3 cells had weak transforming capacities. The transforming phenotype was strongly enhanced by *MYC* co-expression and also sensitized these cells to FGFR inhibition. Finally, MYC was regulated and expressed at high levels in several *FGFR1*-amplified and inhibitor-sensitive cell lines. While *FGFR1* amplification correlated with FGFR1 protein phosphorylation in a large set of tumor biopsies, only a subset of all amplified tumors exhibited high expression of MYC, suggesting that only these patients will benefit from an FGFR inhibitor therapy. Treatment of a patient who suffered from an *FGFR1*-amplified and MYC positive squamous cell lung cancer led to a partial response after six weeks. Thus, these findings may help to identify patients, who profit from FGFR inhibition (Figure 1).

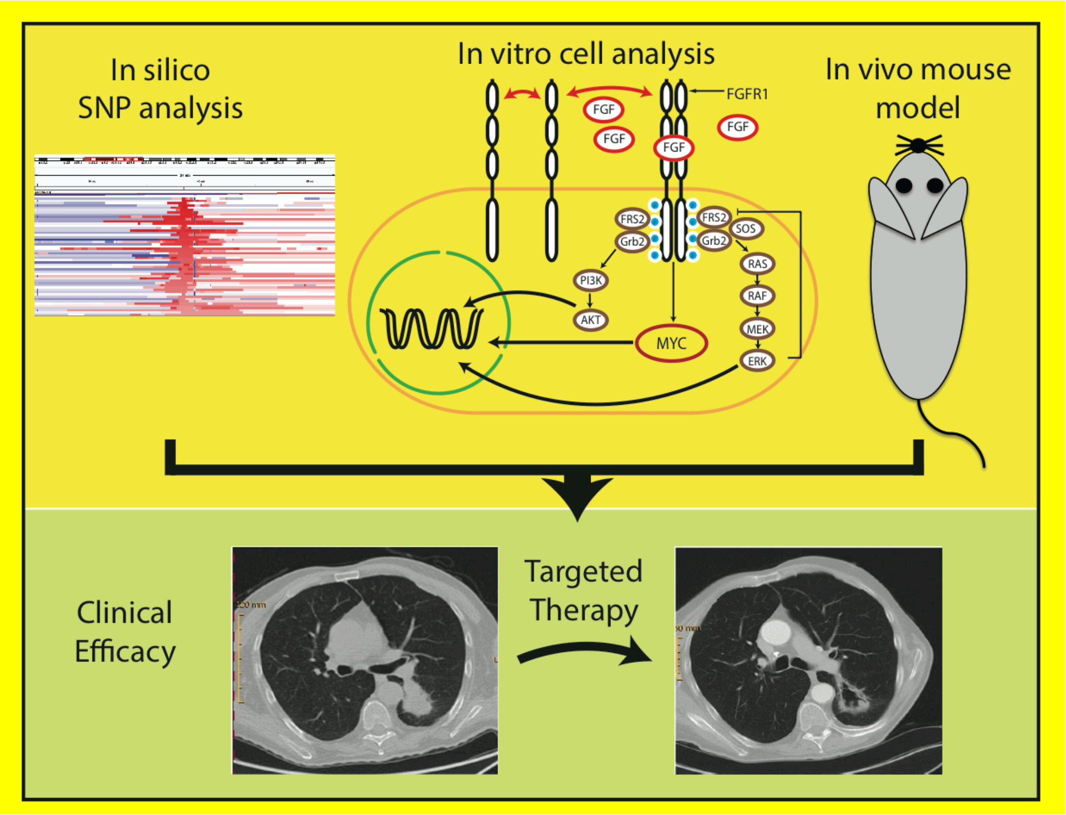
In silico SNP analysis
In vitro cell analysis
FGFR1
FGF
FGF
FGF
FGF
FRS2
Grb2
FRS2
Grb2
SOS
PI3K
AKT
MYC
RAS
RAF
MEK
ERK
In vivo mouse model
Clinical Efficacy
Targeted Therapy

Figure 1: Graphical Abstract. FGFR1-Dependency Prediction by Genomic and Functional Analysis in Squamous Cell Lung Cancer.

2 Introduction

2.1 Cancer

According to the German Statistical Federal Office and the Robert-Koch-Institute, in 2012 exclusively in Germany more than 490.000 people suffered from cancer and 228.000 people died by the disease (https://www.destatis.de, http://www.rki.de) (Ogino et al., 2007; Robert-Koch-Institut, 2013). Therefore, cancer is the second leading cause of death in Germany after cardiovascular disease (https://www.destatis.de).

Cancer is mainly characterized as a disease of the genome. It is the common name for any malignancies of tissue with uncontrolled growth and destructive infiltration into surrounding tissue (metastasis). In general, early cancer detection and treatment increases the chance of cure (Robert-Koch-Institut, 2013). In Germany, the observation of increased incident rates of cancer, as a consequence of an increased aging society and due to better diagnosis, is accompanied by a decline of death rates. This is caused by early cancer detection and better treatment options. The risk of getting cancer significantly increases with age (http://www.gbe-bund.de).

There are two major groups of malignant neoplasms: solid, hard tumors and malignant diseases of the blood and blood-forming organs (haematological malignancies) such as leukemia, malignant lymphoma, and multiple myeloma. In principle, every dividing cell from any tissue is able to degenerate and therefore cause cell transformation and promote cancer. However, most tumors arise from degenerated epithelial cells, like the surface cells of the skin, mucosa and glandular cells (carcinoma) or from connective tissue cells, such as cartilage, bone and muscle cells (sarcomas) (http://www.rki.de, http://www.krebsdaten.de).

The predominant causes of cancer are genomic alterations such as mutations (Greenman et al., 2007). Mutations can be caused by chemicals, viruses and radiation or occur without external cause during normal cell division. Through mutations a “healthy” cell becomes a “defective” cell with a durable proliferating phenotype (Garraway and Lander, 2013). This permanent cell division leads to tumor formation and unbounded tumor growth. Most tumors settle cells via the blood and lymphatic system to distant organs where they form metastases (secondary tumors) (Mantovani et al., 2008).

Cell division is a natural and constant process occurring in all living organisms. For an organized cell division, a machinery of genes that control the process of proliferation is necessary. Simplified, proto-oncogenes promote cell division while tumor suppressor genes suppress cell division. Both types of genes act together in a sophisticated balance with multiple control mechanisms. However, if one of the opponents is defective – e.g., a proto-oncogene becomes an oncogene by mutation – the system is out of balance and the cell begins to proliferate in an uncontrolled manner. Such genetic defects are relatively common, but are usually corrected by cellular repair mechanisms (Hanahan and Weinberg, 2011). If the cell is no longer able to repair the damage, it will be destroyed by endogenously or exogenously initiated apoptosis, a cell death program. But even these security systems can be damaged or altered. Thereby, they are unable to exert their cellular growth control function (Green and Kroemer, 2009; Lengauer et al., 1998). Hundreds of genes that enable tumor growth and metastatic dissemination are found to show six hallmarks: evasion of growth suppressors, activation of invasion and metastasis, enabled replicative immortality, induction of angiogenesis, resistance of cell death (apoptosis) and toleration of proliferative signaling (Hanahan and Weinberg, 2011)

(Figure2).

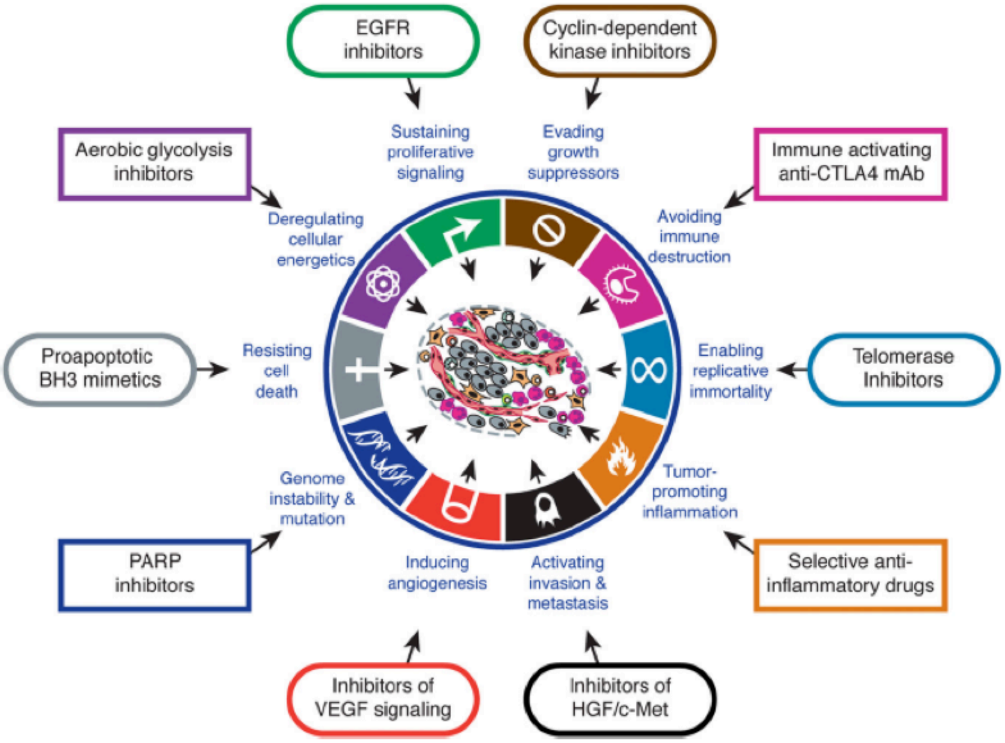
EGFR inhibitors
Cyclin-dependent kinase inhibitors
Aerobic glycolysis inhibitors
Sustaining proliferative signaling
Evading growth suppressors
Immune activating anti-CTLA4 mAb
Deregulating cellular energetics
Avoiding immune destruction
Proapoptotic BH3 mimetics
Resisting cell death
Enabling replicative immortality
Telomerase Inhibitors
Genome instability & mutation
Tumor-promoting inflammation
PARP inhibitors
Inducing angiogenesis
Activating invasion & metastasis
Selective anti-inflammatory drugs
Inhibitors of VEGF signaling
Inhibitors of HGF/c-Met

Figure 2: Illustration describes six hallmarks capabilities deregulated in cancer (sustaining proliferating signaling, evading growth suppressors, activating invasion and metastasis, enabling replicative immortality, inducing angiogenesis, resistance to cell death), two emerging hallmarks (deregulating cellular energetics and avoiding immune destruction), and two consequential characteristics of neoplasia facilitate acquisition of both core and emerging hallmarks (genome instability and mutation, tumor promoting inflammation). Drugs are illustrative examples that interfere with each of the acquired capabilities and are in clinical trials or in some cases approved for clinical use in treating certain forms of human cancer. Figure from Hanahan and Weinberg, 2011.

These six hallmarks have to be essentially and fundamentally deregulated in cell physiology to raise cancer. However, in the past years two additive hallmarks emerged in the cancer field: deregulation of cellular energetics and avoided immune destruction as well as two enabling characteristics -genome instability and tumor-promoting inflammation (Hanahan and Weinberg, 2011) (Figure 2).

In summary, cancer results from cumulative disruption of the cellular growth control machinery.

2.1.1 Lung Cancer

In Germany lung cancer is the second most common cancer type for men and the third most frequent cancer type for women. However, it is by far the leading cause of cancer related deaths for men and the second deadly cancer type for woman (Robert-Koch-Institut, 2013). Smoking is the main risk factor of lung cancer. Up to 90% of incidents are caused by tobacco smoke (Khuder, 2001; Rubin, 2011). In contrast to tobacco-induced lung cancers, they can also arise from asbestos, radioactive gas (radon), silica and nickel dust as well as from polycyclic aromatic hydrocarbons. In addition, several lung cancer cases cannot be explained by chemical carcinogenesis. Therefore, even in non-smokers, lung cancer is the seventh deadly cancer type world wide (Blume-Jensen and Hunter, 2001; Sun et al., 2007). In 2010, approximately 35.000 men and 17.000 women were affected by lung cancer and about 29.000 men and 13.500 women died of it in Germany alone (Robert-Koch-Institut, 2013). Lung cancer is usually diagnosed at late stages and thus has very low cure rates (Siegel et al., 2012). The late detection of lung cancer is due to late perceptual symptoms, e.g. persistent cough or coughing up blood. After the diagnosis of lung cancer, the relative 5-year overall survival rates are 15% (Schiller et al., 2002). The life expectancy of patients is highly dependent on the stage and subtype of the disease (TNM-Classification). The TNM-Classification is class-divided in tumor size and invasiveness (T), infestation of regional lymph nodes (N) and distant metastasis (M) (Detterbeck et al., 2013; FRCS et al., 2011; Koboldt et al., 2012). If lung cancer is detected in the local stadium, the 5-year overall survival rate is around 50%. However, if already distant metastases have occurred, the 5-year overall survival rate drops to 5%. In general, the stage distribution in men and woman is quite similar and is characterized by a high proportion (about 40%) of T4 stages (Garraway and Lander, 2013; Robert-Koch-Institut, 2013; Schiller et al., 2002; Siegel et al., 2012).

2.1.2 Histology of Lung Cancer

Lung cancer is currently classified into four major subtypes: small cell lung cancer (SCLC), adenocarcinoma (AD), squamous cell lung cancer (SCC) and large cell carcinoma (LC) (Green and Kroemer, 2009; Hanahan and Weinberg, 2011; Petersen, 2011; Travis et al., 2011). This classification is clinically important due to the different methods of treatment (Ihde, 1992; McWhirter et al., 1993). However, the different forms can also merge and coexist (Zakowski et al., 2006).

Small cell lung cancer is a highly aggressive lung tumor subtype and is diagnosed in 15-20% of all lung cancer cases. It is characterized by fast dividing small cells, arising from the airway bronchioles, and early metastasizing (Gustafsson et al., 2008; Reiner, 2007). The patients respond well to classical chemotherapy and radiation but in nearly all cases resistance and therefore relapse appears within short time. Combined deactivation of the tumor suppressors *TP53* and *RB1* seam to be the main genetic characteristic of this lung cancer subtype (Peifer et al., 2012; Schaffer et al., 2010).

Adenocarcinoma (AD) is the most frequent histological form of lung cancer and is diagnosed in approximately 40-50 % of all lung cancer cases. It arises from epithelial cells from the periphery of the alveoli (Travis, 2011). Several driving lesions are known for lung adenocarcinomas and some of them, such as *EGFR* and *EML4-ALK* alterations, are therapeutically treatable in clinical practice (Buettner et al., 2013; Ding et al., 2008; Mok et al., 2009; Robert-Koch-Institut, 2013; Soda et al., 2007; Sun et al., 2007).

Squamous cell lung cancer (SCC) is the second most frequent lung cancer subtype. SCC is diagnosed in approximately 30 % of all lung cancer cases and arises from epithelial cells from the main bronchus. In nearly all cases *TP53* is altered and mutations in *DDR2*, *FGFR2* and *NFE2L2* are frequently observed. Furthermore, amplifications of *FGFR1* and *SOX2* are recurrently described (Detterbeck et al., 2013; FRCS et al., 2011; Hammerman et al., 2012; Schiller et al., 2002; The Clinical Lung Cancer Genome Project (CLCGP) and Network Genomic Medicine (NGM), 2013). In contrast to adenocarcinomas this cancer subtype lacks therapeutically treatable lesions.

Large cell carcinoma (LC) is poorly differentiated and a rare subtype of lung cancer. LC accounts for approximately 10 % of all lung cancer subtypes. It has frequent amplifications in *NKX2-1*, *CCNE1* and *MYC.* The identity of this subtype has been recently questioned and it is likely that LC will be subdivided in AD and SCC (The Clinical Lung Cancer Genome Project (CLCGP) and Network Genomic Medicine (NGM), 2013).

2.2 Somatic Mutations

Mutations are alterations in the nucleotide sequence that can contribute phenotypic changes. A mutation is called somatic if it is absent in the germline (Manning, 2002; Wheeler and Wang, 2013). Furthermore, they are specified based either on a coding DNA reference sequence or on a protein-level amino acid sequence (Blume-Jensen and Hunter, 2001; Ogino et al., 2007). Mutations within the DNA are denoted by the position followed by the event, e.g. nucleotide exchange “c. 437 A>T” meaning “codon 437 adenine is replaced by thymidine” or deletions “c. 437_438 delAG” meaning “codon 437 adenine and 438 guanine are deleted”. Mutations within the protein levels are described by the single letter code of the amino acid followed by the position and the event, e.g. amino acid exchange “A437T” meaning “Alanine 437 is replaced by Threonine” (Ogino et al., 2007).

The types of mutation are highly diverse. Point mutations are single nucleotide exchanges and commonly caused by chemicals or radiation. They can be silent, missense or nonsense mutated. If a gene is silently mutated the triplet code is unaffected and represents the same amino acid. The protein code stays unchanged. In contrast, a missense or nonsense mutation always affects the amino acid code. Missense mutations lead to an amino acid change, e.g. L858R, whereas nonsense mutations generally truncate the protein due to induction of an early stop codon, e.g. G542X. Point mutations are also known as nucleotide insertions or deletions, whereby single or several nucleotides are added or removed. They usually occur during defective replication or are caused by transposable elements. The protein phenotype is always affected and a shift in the reading frame is likely (Lengauer et al., 1998; Yang et al., 2013).

Other mutations are affecting chromosomal regions, chromosomal arms or whole chromosomes. Duplications of chromosomal regions are called amplifications (Lengauer et al., 1998). They can also be caused by other mechanisms, such as by creation of double minutes and other, sometimes highly complex structural rearrangements. Amplifications often increase the expression of genes within the amplified region. On the contrary, entirely or partly removed chromosomes are called deletions. They cause a loss of genetic material within the deleted region. A special case of deletion is the loss of heterozygosity. The cell that previously had two different alleles (heterozygote) loses one, by deletion or recombination, and becomes homozygous at this particular locus. Furthermore, a frequently observed mutation in cancer is the exchange of genetic material between two non-homologous chromosomes. Here, two chromosomes cross over and translocate in a balanced or unbalanced fashion. During an unbalanced translocation genetic material is lost and can, for example, lead to fusion genes or to a loss of tumor suppressors. Translocations can also occur in a balanced fashion without loosing genetic material. Balanced translocations can also destroy tumor suppressors, bring proto-oncogenes under regulation of another promoter or create fusion genes (Travis, 2011; Yang et al., 2013).

2.3 Oncogenes and Tumor Suppressor Genes

The word oncogene is derived from oncogenic gene and was termed in 1969 by Robert Huebner and George Todaro (The Emperor of All Maladies, p. 363). It describes a type of gene, which has the potential to cause cancer. Proto-oncogenes are genes that encode for proteins which have physiological importance in signal transduction and cell division (mitosis) regulating cell growth and differentiation. Oncogenes are mutated or overexpressed proto-oncogenes.

In 1911, Francis Peyton Rous discovered the Rous sarcoma virus (RSV) and thus for the first time described a retrovirus which is able to induce tumors in animals. Injection of a cell free filtrate from chicken sarcomas into healthy Plymouth Rock chickens promoted oncogenesis and induced sarcomas (Rubin, 2011). The first oncogene *v-SRC* was found and Rous was awarded the Nobel price in 1966. Further, Harry Rubin found that RSV is able to transform chicken embryo fibroblasts (CEF) in vitro forcing them to produce a steady stream of progeny virus particles over a long period of time. In contrast, it was known that most other viruses enter into host cells, multiply and kill their hosts quickly (The biology of cancer, p 61). From here on, tumor progression could be studied in cell culture under the microscope and lead to the discovery of many other RNA and DNA tumor viruses.

Years later, in 1979, John Michael Bishop and Harold Elliot Varmus found that even normal chicken cells have structurally closely related copies of *v-SRC*. Therefore, they used a homologous *src* DNA probe derived from RSV to hybridize chicken DNA originally following the fate of the *src* gene after cells were infected with RSV (The biology of cancer, p 75). The detected proto-oncogene was called *c-SRC* (cellular *src*) and revolutionized the current thinking about how cancer emerges. It became clear that endogenous cellular proto-oncogenes play significant roles in cancer development.

Today several cellular proto-oncogenes are known and the run to discover new oncogenes is still an ongoing process (Blume-Jensen and

Hunter, 2001; Huse and Kuriyan, 2002). The formation from a proto-oncogene to an oncogene is defined by its activation. Activation can be caused by:

1. Increased enzyme activity or loss of regulatory elements e.g. *EGFR* mutations (e.g. L858R, exon 19 deletion) or *BRAF* (e.g. V600E) (Solit et al., 2005).

2. Increased amounts of a certain protein caused by simple overexpression, prolonging mRNA stability or gene duplication, e.g. v-erb-b2 erythroblastic leukemia viral oncogene homolog 2 (*ERBB2*) or sphingosine kinase 1 (SPHK1 mRNA stabilized by *v-src*) (Koboldt et al., 2012; Lemmon and Schlessinger, 2010).

3. Chromosomal translocations, where either a proto-oncogene is translocated to the physical proximity of another promoter and therefore overexpressed or fused to a second gene creating of a fusion gene (encoding for a fusion protein with increased oncogenic activity), e.g. *IGH-MYC* rearrangements in Burkitt's lymphoma or *Bcr-Abl* fusion gene (Philadelphia Chromosome) (Lemmon and Schlessinger, 2010; McWhirter et al., 1993).

Since the early 1970s it is known that cancer arises as a result of somaticly mutated or deregulated proto-oncogenes. People claimed that there must be counterparts, which might oppose proto-oncogenetic effects. Several experiments suggested that particular genes were able to suppress tumorigenicity (Sherr, 2004). Today, numerous tumor suppressor genes have been identified. Tumor suppressor genes regulate a wide range of cellular activities, including cell cycle control, DNA damage detection, DNA repair, protein degradation, ubiquitination, mitogenic signaling, cell differentiation, migration and specification. Altogether, a tumor suppressor gene controls cell growth and prevents tumor development.

A typical tumor suppressor gene is recessive. They have to become inactivated on both alleles to raise cancer. Loss of function mutations in common tumor suppressor genes are frequently observed in many different tumor types. Inheritance of one mutated allele increases the risk of tumor formation, because only one additional mutation is required to inactivate the tumor suppressor gene and its function. Hence, mutated tumor suppressors in germlines cause high risk of tumor susceptibility and can be the reason for familial cancer syndrome (Sherr, 2004).

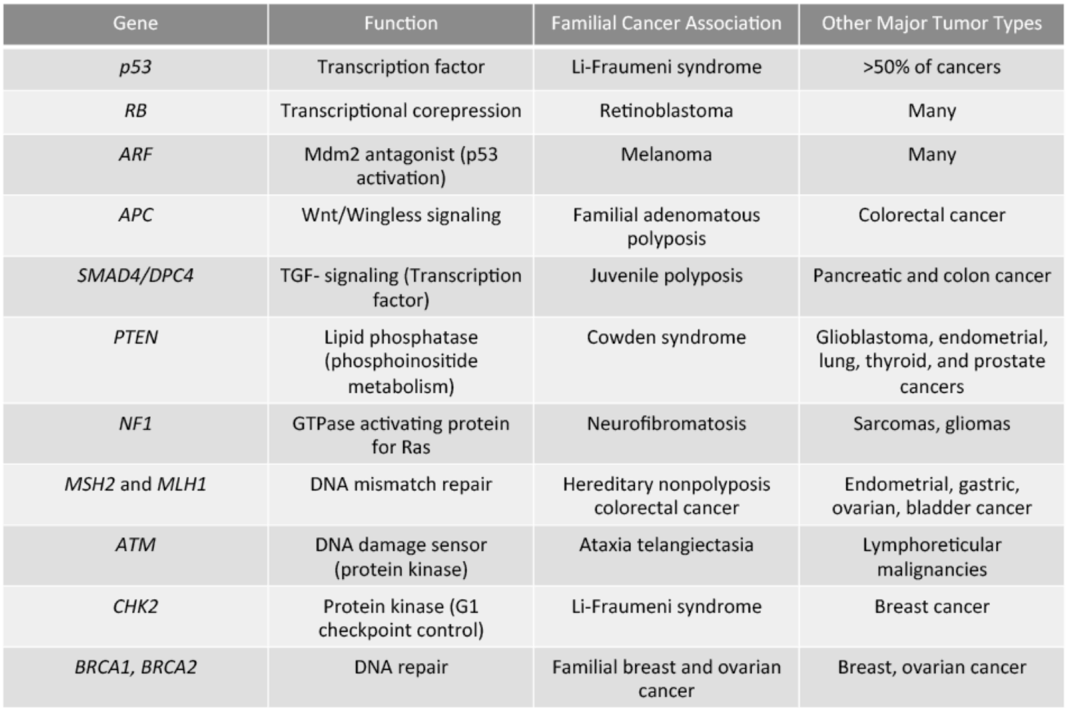

Gene	Function	Familial Cancer Association	Other Major Tumor Types
p53	Transcription factor	Li-Fraumeni syndrome	>50% of cancers
RB	Transcriptional corepression	Retinoblastoma	Many
ARF	Mdm2 antagonist (p53 activation)	Melanoma	Many
APC	Wnt/Wingless signaling	Familial adenomatous polyposis	Colorectal cancer
SMAD4/DPC4	TGF- signaling (Transcription factor)	Juvenile polyposis	Pancreatic and colon cancer
PTEN	Lipid phosphatase (phosphoinositide metabolism)	Cowden syndrome	Glioblastoma, endometrial, lung, thyroid, and prostate cancers
NF1	GTPase activating protein for Ras	Neurofibromatosis	Sarcomas, gliomas
MSH2 and *MLH1*	DNA mismatch repair	Hereditary nonpolyposis colorectal cancer	Endometrial, gastric, ovarian, bladder cancer
ATM	DNA damage sensor (protein kinase)	Ataxia telangiectasia	Lymphoreticular malignancies
CHK2	Protein kinase (G1 checkpoint control)	Li-Fraumeni syndrome	Breast cancer
BRCA1, BRCA2	DNA repair	Familial breast and ovarian cancer	Breast, ovarian cancer

Figure 3: Table of tumor suppressor genes. Table lists prominent tumor suppressor genes. Abridged and modified from Sherr, 2004.

The first tumor suppressor gene, discovered by Alfred G. Knudson, was the *RB1* (Retinoblastoma) gene (The biology of cancer, p. 214). In 1971 he claimed that retinoblastoma is caused by a two-mutation event. He and others showed that people with germline deletions of chromosome 13q14 run a higher risk for retinoblastoma. Today it is known that *RB1*, together with *p107* and *p130*, is part of a complex regulating cell cycle, apoptosis and differentiation. Since then, several other tumor suppressor genes were found, which play fundamental role in cancerogenesis (The biology of cancer, p. 215) (Figure 3).

2.4 Cell Signaling and Protein Kinases

Processing and transduction of information is essential for all cells. Cells take action of internal and environmental (external) information, e.g. nutrients, hypoxia, apoptosis, etc. Allosteric changes are the basis of signal transmission and its regulation governs communication within, across, and between cells (Nussinov and Tsai, 2013). Allostery is a universal phenomenon of all dynamic proteins and describes conformational changes, in which binding of an effector alters the function of the protein (Tsai et al., 2009). Effectors can adjust through non-covalent events, such as binding ions, lipids, cAMP, drugs, proteins, RNA, DNA, from light absorption and covalent events, such as phosphorylation or reactions with small molecules (Kar et al., 2010; Nussinov and Tsai, 2013). Thus, allosteric events regulate the activity of proteins and thereby affect downstream its signaling pathways.

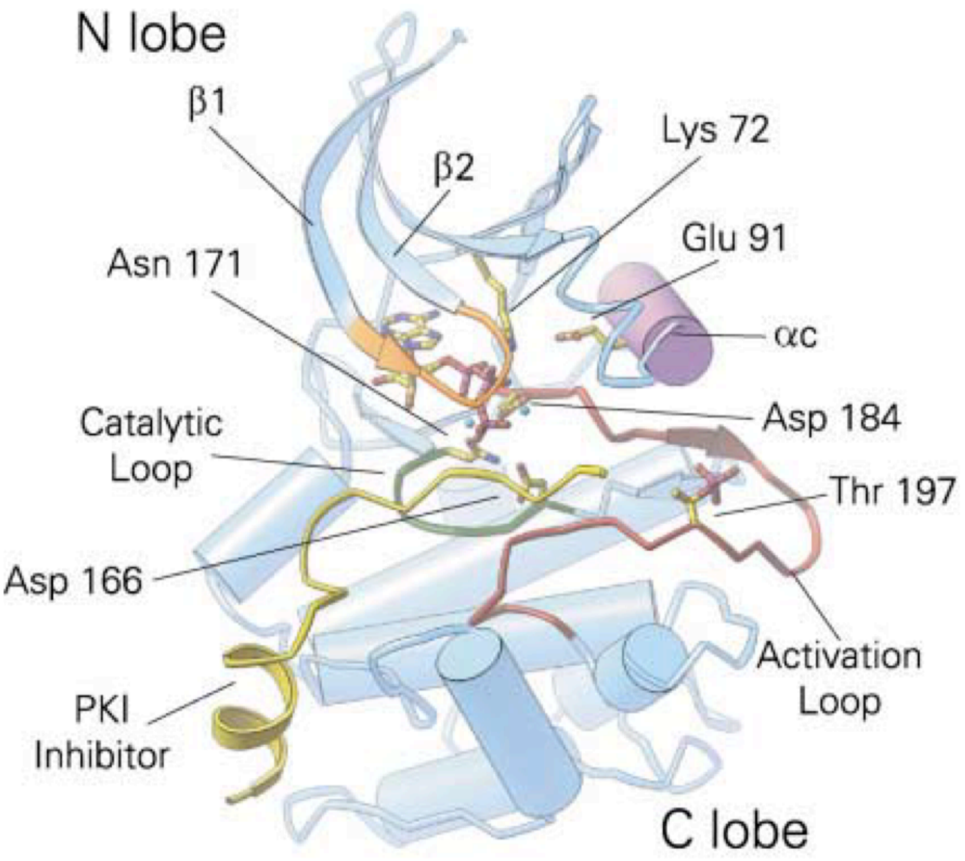

Figure 4: Crystal structure of protein kinase A (PKA, a serine/threonine kinase) (Zheng et al., 1993). Key structural elements within the kinase domain are colored as follows: activation loop, red; αC helix, purple; P loop, orange; PKI peptide inhibitor (mimic substrate), yellow and catalytic loop, green. The P-loop connects β1 and β2. Figure from Huse and Kuriyan, 2002.

Protein kinases account for one of the largest gene families in eukaryotes and at least 518 human kinases are known (Manning, 2002). They are altered in nearly every cancer type (Blume-Jensen and Hunter, 2001). Kinases are highly specific in their substrate phosphorylation and can be subclassified in tyrosine- and serine-/threonine-kinases. SRC is a well-known tyrosine kinase. Famous examples of serine/threonine kinases are AKT or Raf. All kinase domains have similar structures with an N-lobe and a C-lobe (Figure 4) and are highly comparable in the activated kinase conformation (Lemmon and Schlessinger, 2010). They correspond in their regulatory elements incorporating a catalytic subunit, which is located in a slot between the N-lobe and the C-lobe. The catalytic subunit includes the αC-helix, which is associated to the kinase N-lobe, and a conserved phosphate-binding loop (P-loop), which contains a glycine rich motive (GXGXXG) that is required for catalysis of phosphotransfer. ATP is bound between the rift of the N and C lobe and sits below the P-loop connecting β1 and β2 (Huse and Kuriyan, 2002). In addition, the catalytic subunit comprises an activation loop (Figure 4) within a conserved tripeptide motive (DFG….APE) (Nolen et al., 2004). Kinases have been described as key regulators of certain cellular processes, such as differentiation, proliferation, migration, cell-cycle control as well as cell survival, apoptosis and metabolism (Blume-Jensen and Hunter, 2001; Lemmon and Schlessinger, 2010; The Clinical Lung Cancer Genome Project (CLCGP) and Network Genomic Medicine (NGM), 2013). Generally, kinases catalyze and transfer the terminal phosphate (γ) group from a nucleoside triphosphate donor, such as ATP, to the amino acid tyrosine, serine or threonine. The phosphorylation can cause numerous effects although it affects mostly three-dimensional conformational changes and alters the function of the targeted (phosphorylated) protein (Huse and Kuriyan, 2002). Furthermore, most signals are enhanced by secondary messengers such as cyclic AMP (adeninmonophosphat), cyclic GMP (Guaninmonophosphat), calcium ions, inositol 1,4,5-trisphphosphate (IP3) and diacylglycerol (DAG) (Lemmon and Schlessinger, 2010). These secondary messengers trigger reactions that activate further proteins such as kinases or transcription factors.

2.4.1 Receptor Tyrosine Kinases

The receptor tyrosine kinases (RTKs) are located in the lipid bilayer membrane of the cell and mediate signals from the outer milieu to the inside of the cell. There are 58 known RTKs in humans, which are divided into 20 subfamilies (Lemmon and Schlessinger, 2010). In general, except for the family of insulin receptors, the RTKs are present as inactive monomers.

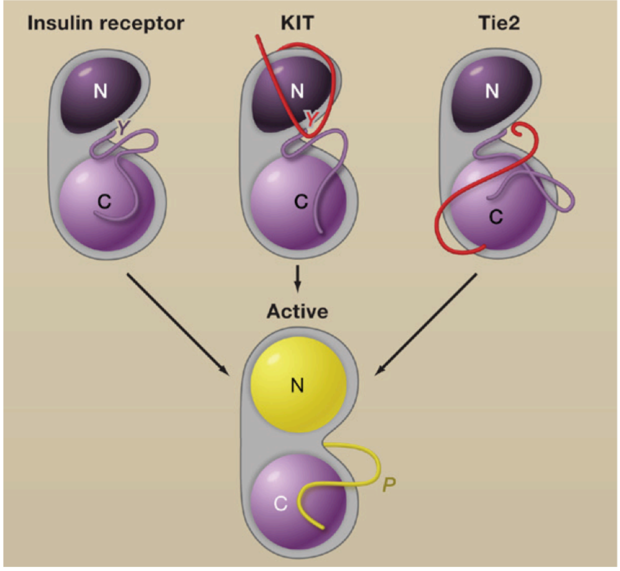

Figure 5: Schematic illustration of inactive and active kinase conformations. Insulin receptor-like (activation loop inhibition). In FGFR, insulin receptor, and IGF1 receptor, the activation loop interacts directly with the active site of the kinase and blocks access to protein substrates (in FGFR) or to both ATP and protein substrates (in insulin and IGF1 receptors). Phosphorylation of key tyrosines (“Y”) disrupts these autoinhibitory interactions and allows the kinase to “relax” to the active state. KIT-like (juxtamembrane inhibition). In KIT, PDFGR, and Eph receptors, the juxtamembrane region (red) interacts with elements within the active site of the kinase (including the αC helix and the activation loop) to stabilize an inactive conformation. Phosphorylation of key tyrosines in the juxtamembrane region destabilizes these autoinhibitory interactions and allows the TKD to resume an active conformation. Tie2-like (C-terminal tail inhibition). In Tie2 (and possibly Met and Ron), the C-terminal tail (red) interacts with the active site of the TKD to stabilize an inactive conformation (Shewchuk et al., 2000). Figure from Lemmon and Schlessinger, 2010.

Growth factors are required to induce a three-dimensional conformation change promoting active dimers or oligomers. All RTKs share a similar architecture consisting of an extracellular domain that binds specific ligands, a transmembrane domain and a cytoplasmic region that contains a tyrosine kinase domain plus additional regulatory elements.

Contrasting with the remarkable motif conservations, RTKs differ sometimes substantially in the inactive kinase domain conformation, which reflects a large source of diversity of regulatory mechanisms (Lemmon and Schlessinger, 2010). For example, a tyrosine in the activation loop interacts directly with the active site (cis autoinhibition) of the kinase of both the insulin receptor and the FGF-receptor 1 (FGFR1). In the first case it blocks access to both ATP and protein substrate, in the second case only to the protein substrate (FGFR1) (Figure 5). As soon as the receptors become activated by ligands, tyrosine trans-phosphorylation of the activation loop interrupts the cis-autoinhibitory conformation, so that the activation segment and the helix-αC can fold to their characteristic active shape.

Another mechanism for kinase regulation is the juxtamembrane autoinhibition in which the tyrosine kinase domain (TKD) is auto-inhibited *in cis* by elements outside of the TKD itself (Figure 5). Well-understood examples for juxtamembrane inhibition are MuSK, Flt3, Kit and Eph-family RTKs. The detailed mechanisms differ slightly among the receptors. Yet, in each case tyrosines in the juxtamembrane region interact with the kinase domain and stabilize the inactive conformation (Figure 5). Ligand induced receptor dimerization and therefore trans-phosphorylation of the juxtamembrane tyrosine disrupts the cis-autoinhibition and promotes activation (Lemmon and Schlessinger, 2010).

Tie2 shows a third mechanism of activation loop inhibition (Figure 5). Here the activation loop exists in an activated-like shape but the carboxyl terminus of Tie2 adopts an inactive conformation and blocks substrate access to the catalytic subunit. Autophosphorylation of the C-terminal tail induces activation. Altogether, phosphorylation of the activation loop plays the key role in kinase activation, because the particular phosphorylation destabilizes the cis-autoinhibition and stabilizes the active conformation (Nolen et al., 2004).

2.4.2 Fibroblast Growth Factor Receptors

All fibroblast growth factor receptors (FGFRs) are receptor tyrosine kinases. The FGFR family comprises four receptors (FGFR1, FGFR2, FGFR3 and FGFR4). Moreover, several splice variants can be generated from each receptor, some of which also become secreted (Mason, 2007). All four receptors consist of extracellular immunoglobulin loops, a trans-membrane domain and an intracellular tyrosine kinase domain (Figure 6).

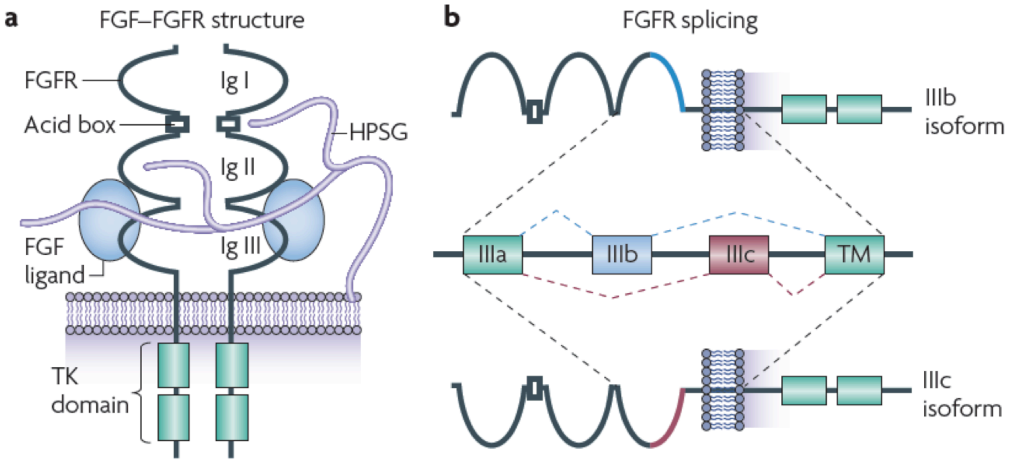

Figure 6: Structure of the Fibroblast growth factor receptor (FGFR). a) All isoforms of the four vertebrate FGFRs consist of extracellular immunoglobulin (IG) domains and one acid box, a transmembrane domain, and intracellular domains including a split tyrosine kinase (TK) domain. Ligand binding occurrs at the C-terminal part of IgII and the N-terminal portion of IgIII. b) The alternatively spliced sequences in IgIII distinguish the 'b' and 'c' isoforms of FGFR1–3. Figure from Turner and Grose, 2010.

Ligand specificity is mainly mediated by the four receptors and alternative splicing e.g. the third immunoglobulin loop of FGFR1-3 generates IIIb or IIIc isoforms (Figure 6) and the mesenchymal IIIc-β variant differs from full length IIIc-α by skipping exon 2 (IgG1 loop). Furthermore, FGFR signaling is modulated endogenously by several adaptor proteins, which facilitate the downstream signaling cascade. The docking proteins FRS2 and Grb2 mediate to the Ras pathway. Ultimately, Ras is mainly activating the mitogen activated protein kinase (MAPK) pathway and, in a cell type specific manner, the p38 and Jun kinase(Mason, 2007).

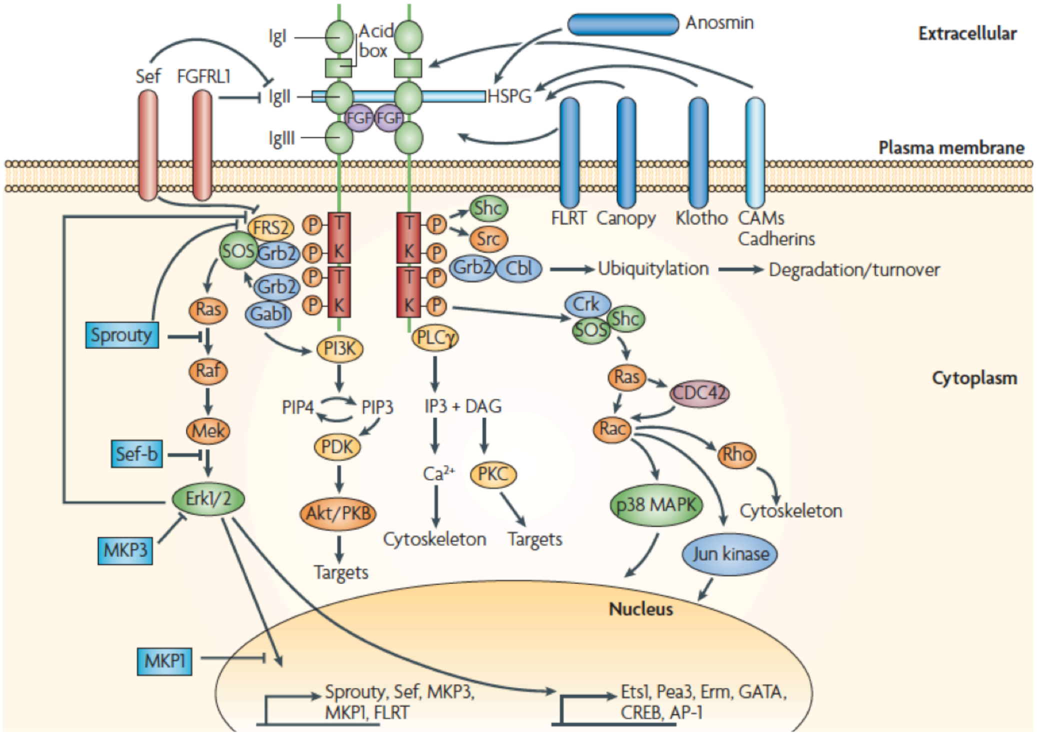
Anosmin
Extracellular
IgI
Acid box
Sef
FGFRL1
IgII
HSPG
FGF
FGF
IgIII
Plasma membrane
FRS2
SOS
Grb2
Grb2
Gab1
P
T
K
Shc
Src
Grb2
Cbl
Ubiquitylation
Degradation/turnover
FLRT
Canopy
Klotho
CAMs
Cadherins
Crk
Shc
SOS
Ras
Sprouty
Raf
PI3K
PLCγ
Ras
CDC42
Cytoplasm
PIP4
PIP3
IP3 + DAG
Rac
Mek
PDK
Sef-b
Rho
Ca2+
PKC
Erk1/2
Akt/PKB
p38 MAPK
Cytoskeleton
MKP3
Cytoskeleton
Targets
Jun kinase
Targets
Nucleus
MKP1
Sprouty, Sef, MKP3, MKP1, FLRT
Ets1, Pea3, Erm, GATA, CREB, AP-1

Figure 7: Signaling through fibroblast growth factor receptors (FGFRs). This diagram illustrates the multiplicity of signaling pathways that are activated downstream of FGFRs together with the endogenous agonists and antagonists that have been identified both, upstream and downstream of the receptor. CAM, cell adhesion molecule; CREB, cyclic AMP response element binding protein; FLRT, fibronectin leucine-rich transmembrane proteins; FRS, FGF receptor substrate; HSPG, heparan sulphate proteoglycan; Ig, immunoglobulin; IP3, inositol tris phosphate; MAPK, mitogenactivated protein kinase; MKP, MAPK phosphatase; PI3K, phosphatidylinositol-3-kinase; PIP3, phosphatidylinositol-3-phosphate; PIP4, phosphatidylinositol-4-phosphate; PKB, protein kinase B; PLCγ, phospholipase Cγ; SOS, son of sevenless; TK, tyrosine kinase. Figure from Mason, 2007.

Activation of MAPK pathway feeds into a negative feedback loop controlled by the docking protein FRS2 and Erk (Lax et al., 2002). Furthermore, Grb2 can recruit Gab1 leading to the activation of phosphatidylinositol 3 kinase (PI3K) and therefore to the AKT dependent anti-apoptotic pathway. Other responses include the activation of phospholipase C (PLC), Src, STAT and the recruitment of Shc, which have the potential to activate several other downstream pathways (Mason, 2007). In addition, there are several other intrinsic mechanisms and ligands, which are able to enhance or decrease

FGFR mediated signaling (Figure 7). For example, heparan sulphate proteoglycans (HSPGs) are necessary for efficient binding of most FGFs in an FGF-FGFR-HSPG ratio of 2:2:1, while intrinsic Klotho expression is only necessary for FGFs 19, 21 and 23 (Mason, 2007).

Due to the wide range of regulatory mechanisms, FGFRs play fundamental roles in a wide range of different signaling pathways, for instance regulation of cellular proliferation, differentiation, angiogenesis and development (Mason, 2007; Turner and Grose, 2010). These mechanisms lead to a wide range of aberrant FGF signaling. Therefore, oncogenic FGFR signaling is an essential part of the pathogenesis of multiple tumor types. A full-scale study sequencing the coding exons of 518 kinases from 210 different cancer types discovered that the FGF signaling pathway showed the highest enrichment of non-synonymous mutations (Greenman et al., 2007). In more detail, *FGFR1* is amplified in lung (squamous cell carcinoma 20%), breast (10%), ovarian (5%) and bladder (3%) cancer as well as in rhabdomyosarcoma (3%) (Courjal et al., 1997; Gorringe et al., 2007; Missiaglia et al., 2009; Simon et al., 2001; Weiss et al., 2010). In addition, it is rarely mutated in the lung (e.g. P252T), melanoma (e.g. P252S) and glioblastoma (e.g. N546K and K656E) (Greulich and Pollock, 2011). Intrestingly, activating mutations of FGFR1 are most frequent within the extracellular ligand-binding IgII and IgIII domain. These mutations enhance ligand binding or may lead to unspecific FGF binding and therefore ligand induced receptor activation. Oncogenic kinase mutations, which provoke continuous activation of the kinase domain, are quiet rare and can only be found in glioblastoma. In the end, *FGFR1* is found to be translocated in stem cell leukemia and lymphoma syndrome, resulting in the *ZNF198-FGFR1* or *BCR-FGFR1* fusion gene (Turner and Grose, 2010).

Similar to *FGFR1*, *FGFR2* amplifications and mutations occur in several tumor types. However, activating point mutations are much more frequent in *FGFR2*. They mainly occur in the extracellular ligand binding domain. *FGFR2* mutations are by far most frequent in endometrial cancer (12%; e.g. S252W, P253R, N550K). Next to this, *FGFR2* mutations are rarely found in gastric, lung and cervical cancer. Furthermore, *FGFR2* is amplified in approximately 10 % of gastric cancer and in about 1% of breast cancer (Greulich and Pollock, 2011; Turner and Grose, 2010).

In contrast to that, *FGFR3* amplifications are either absent among various cancer types or only inadequately described. The only described amplification occurs in relapsed multiple myeloma (Greulich and Pollock, 2011). However, *FGFR3* mutations are frequently reported in several cancer types. Since the first FGFR3 translocation was found in multiple myeloma, several other cancer types were found to contain FGFR3 mutations (e.g. Y373C, K650E or K650M). Up to 25% of myeloma incidents exhibit translocations of the immunoglobulin heavy chain (*IGH*) and *FGFR3*. These translocations result in high expression of *FGFR3* but do not significantly increase protein expression. Therefore, it is controversially discussed to which degree these mutations drive tumorgenesis. However, 10% of these translocations harbor additional somatic point mutations (Greulich and Pollock, 2011). Furthermore, activating *FGFR3-TACC3* fusions are frequently found in bladder cancer (Network, 2014). Activating FGFR3 point mutations are found in multiple myeloma (up to 10% in translocations), bladder cancer (50-60% non-invasive, 10-15% invasive type), cervical cancer (5%), prostate (3%) and spermatocytic seminoma (7%). Interestingly, mutations in the kinase domain of FGFR3 are much more frequent than in case of FGFR1, 2 or 4 (Greulich and Pollock, 2011; Turner and Grose, 2010).

Not much is known about *FGFR4* and no amplifications have been described. Yet, somatic mutations of the extra cellular domain are described for breast cancer and recurrent somatic kinase mutations have recently been discovered in 8% of rhabdomyosarcoma (e.g. N535D/K, V550E/L) (Greulich and Pollock, 2011; Turner and Grose, 2010).

2.5 Growth Factors

Cellular growth factors (GFs) are relatively small proteins. They describe numerous kinds of proteins, which regulate a variety of cellular processes and enable a cell to pass information within a living tissue. All ligands, which bind to receptor tyrosine kinases, are growth factors. However, growth factors can also be steroid hormones. Sometimes growth factors are also termed as cytokines or mitogens.

Cytokines are proteins referring mainly to hematopoietic cells and immunomodulators such as interferons (Huse and Kuriyan, 2002; Reiner, 2007). They are involved in multiple regulatory pathways, e.g. the cytokine Fas is involved in apoptosis pathway (Nagata, 1997).

Mitogens refer to a group of proteins, which mainly trigger the mitogen-activated protein kinase (MAPK) signaling pathway and drive mitosis (cell division) (Liebmann, 2001).

However, usually GFs are released by cells or secreted from specialized cells. They make their way through intercellular space and eventually impinge on other cells carrying specific biological messages (The biology of cancer, p. 121). It is termed “paracrine signaling”, if the acceptor cell is near the transmitting cell, and “endocrine signaling”, if the acceptor cell is in a distant tissue. Thus, GFs are carried for example through the blood stream to the target tissue.

GFs which are frequently involved in tumor pathogenesis are for example PDGF, EGF, NGF, FGF, HGF, VEGF and IGF. All these growth factors stimulate cell growth and can bind to their own specific receptor, which are all kinases (Beenken and Mohammadi, 2009; Lemmon and Schlessinger, 2010). Moreover, GFs can act as oncogenes themselves and are frequently altered. EGF for example is overexpressed in NSCLC, breast, head, neck, stomach, collateral, esophageal, prostate, bladder, renal, pancreatic and ovarian carcinomas. Another example is FGF which can be mutated or overexpressed in multiple myeloma, bladder and cervical carcinomas. Furthermore, tumor cells produce their own growth factors and at the same time express the receptors for these ligands to stimulate themselves (autocrine signaling). For example certain lung cancer cells produce TGF-α, SCF, IGF as well as the associated receptor tyrosine kinases EGFR, Kit and IGF-R1 (The biology of cancer, p.133).

2.5.1 Fibroblast Growth Factors

Fibroblast growth factors (FGFs) belong to the family tree of growth factors (GFs). They predominantly bind to fibroblast growth factor receptors (FGFRs) in conjugation with heparin sulfate proteoglycans (HSPGs). The FGF-Family consists of 23 homologs, although only 18 mammalian FGFs bind specifically to FGFRs (Beenken and Mohammadi, 2009; Mason, 2007). The FGF homologous factors (FGF11-14) do not function as FGFR ligands and the FGF15/19 is an orthologue (mouse FGF15 is the human FGF19). The FGFs are classified in six subfamilies based on their homology (Figure 8).

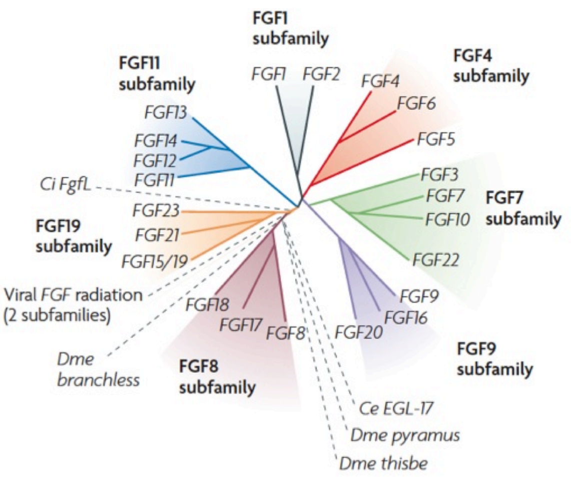
FGF1 subfamily
FGF1
FGF2
FGF4 subfamily
FGF4
FGF6
FGF5
FGF11 subfamily
FGF13
FGF14
FGF12
FGF11
Ci FgfL
FGF3
FGF7
FGF10
FGF7 subfamily
FGF22
FGF23
FGF21
FGF15/19
FGF19 subfamily
Viral FGF radiation (2 subfamilies)
FGF18
FGF17
FGF8
FGF20
FGF9
FGF16
FGF9 subfamily
Dme branchless
FGF8 subfamily
Ce EGL-17
Dme pyramus
Dme thisbe

Figure 8: The phylogenetic relationship of FGFs. Figure from Mason, 2007.

The FGF1-subfamily consists of FGF1 and FGF2. The physiological role of FGF1 and 2 is not established yet. Though, both FGFs are able to bind and activate FGFR1, 2, 3 and 4 to varying degrees (Xu, 1996). FGF1/2 double knockout mice apparently have a viable and normal phenotype. However, they show dissimilarities in wound healing and neuron organization of the frontal motor cortex (Miller et al., 2000). Even though knockout mice show normal vascularization, the angiogenic role of FGF1/2 is well known.

Microvascular branching as well as anti-apoptotic activity is shown for endothelial cells, if incubated with FGF1. FGF2 stimulates migration and proliferation in endothelial cells. Furthermore, FGF2 shows antiapoptotic and mitogenic effects in smooth muscle cells. Targeting the FGF1-subfamily has therapeutic potential, varying from cardiovascular disorders and cartilage homeostasis via cancer treatments to patients suffering from depressive disorder (Beenken and Mohammadi, 2009).

The FGF4-subfamily comprises of FGF4, 5 and 6 and has extensive functions in relation to cardiac valve formation, limb development, hair growth and myogenesis (Beenken and Mohammadi, 2009). All members of the FGF4-subfamily are able to activate FGFR1 and 2, although with different intensity. Furthermore, FGF4 is capable to activate FGFR3 and 4, while FGF6 promotes further FGFR4 activation (Xu, 1996). FGF4 knockout mice are embryonically lethal because of insufficient trophoblastic proliferation (Feldman et al., 1995). FGF5 knockout mice display abnormally long hair (Hébert et al., 1994), whereas FGF6 knockout mice show fibrosis and defective skeletal muscle fiber regeneration (Floss et al., 1997).

The FGF7-subfamily involves FGF3, 7, 10 and 22. FGF3, 10 and 22 are able to activate FGFR1 and 2, though in distinctive intensity (Zhang et al., 2006). FGF7 binds and activates FGFR2 and 4. It is especially expressed in the mesenchyme and highly upregulated after cutaneous bladder and kidney injury. Furthermore, FGF7 knockout mice demonstrate matted hair and significantly fewer nephrons (Beenken and Mohammadi, 2009). FGF3 is involved in inner ear development. Mutations of this gene (310 C>T, 466 T>C and 616 del G) relate to inherited deafness accompanied by slight dental defects (Tekin et al., 2007). FGF10 (also known as Kgf2) is involved in morphological branching. Mutations in this gene (409 A>T and 467 T>G) are responsible for the lacrimo-auriculo-dento-digital (LADD) syndrome (Milunsky et al., 2006). Knockout mice are perinatally lethal and lack limb and lung development (Min et al., 1998). Not much is known about the physiological role of FGF22. Nevertheless, FGF22 is a presynaptic organizer in the mammalian brain (Umemori et al., 2004).

The FGF8-subfamily consists of FGF8, 17 and 18. All members of the FGF8-subfamily are able to bind and activate FGFR2, 3 and 4 with a highly varying degree. FGF8 and 17 are also able to activate FGFR1 (Zhang et al., 2006). It has been shown that FGF8 has several responsibilities and is involved during brain, limb, ear and eye development. Together with FGF17 it is necessary for patterning of the embryonic forebrain (Beenken and Mohammadi, 2009). Loss of function mutations in FGF8 (e.g. P26L, R127G, etc.) lead to altered FGFR1 binding and cause Kallmann's syndrome (Falardeau et al., 2008). In contrast, a monoclonal antibody neutralizing the FGF8b isoform showed anti-tumor activity in prostate cancer (Maruyama-Takahashi et al., 2008). Complete FGF8 knockout mice are embryonic lethal during gastrulation. However, knockout mice with a hypomorphic and a null allele show disorders in cardiac, craniofacial, forebrain, midbrain and cerebellar development (Meyers et al., 1998). The physiological role of FGF17 is specialized in cerebral and cerebellar development. Knockout mice reveal defects in the development of the cerebellar vermis (Xu et al., 2000). Injection of FGF18 into rats appears to increase cartilage formation. Furthermore, FGF8 plays a significant role for cell proliferation during bone development. Knockout mice show disorders during ossification (Beenken and Mohammadi, 2009).

The FGF9-subfamily comprises FGFs9, 16 and 20. The binding to FGFR2 and 3 varies considerably for the FGF9-subfamily. Furthermore, FGF20 binds to FGFR1 and both FGF9 and FGF20 bind to FGFR4 (Zhang et al., 2006). The FGF9-subfamily primarily signals from the epithelium to the mesenchyme, in opposition to the FGF7-subfamily which signals from the mesenchyme to the epithelium. FGF9 encourages mesenchymal proliferation and promotes FGF7-subfamily ligand production. Consequently, FGF9 knockdown leads to disruption of the mesenchymal-epithelial signaling loop.

Reduced mesenchymal proliferation promotes reduced FGF7-subfamily ligand production, which results in pulmonary hypoplasia (Beenken and Mohammadi, 2009). FGF9 knockout mice show lung and testicular hypoplasia, male to female sex reversal, and postnatal death (Colvin et al., 2001). Moreover, early embryonic death results in FGF16 knockout mice because of congenital heart anomalies (Lu et al., 2008). Also, FGF20 polymorphism is associated to Parkinson's disease (van der Walt et al., 2004).

The FGF19-subfamily involves FGF15/19, 21 and 23. This subfamily differs from all other FGF-subfamilies mainly due to poor binding of heparan sulphate proteoglycans (HSPGs), which can interact with protein ligands and affect for example metabolism and information transfer (Bishop et al., 2007). All members of the FGF19-subfamily can easily diffuse into the blood and circulate around the body. The endocrine FGFs have less ability to bind their receptors. They need the expression of α-klotho or β-klotho in the target tissues for proper ligand-receptor interaction (Beenken and Mohammadi, 2009). However, all members of the FGF19-subfamily are still able to entirely activate all FGFRs (Zhang et al., 2006). FGF15/19 (FGF15 is the orthologue of human FGF19) predominantly activates FGFR4. It is mainly expressed in the small intestine and circulates to the liver where it inhibits the expression of cholesterol 7alpha-hydroxylase (CYP7A1), an enzyme that is essential in bile acid synthesis (Inagaki et al., 2005). Furthermore, FGF15 knockout mice show increased expression of CYP7A1, a similar phenotype observed for β-klotho deficient mice (Ito et al., 2005). Therefore, FGF19 is mainly involved in the gut-liver signaling pathway as well as in regulation of energy provision (Beenken and Mohammadi, 2009). FGF21 is a metabolic glucose uptake regulator and primarily expressed in the liver, thymus and β-cells in the pancreas (Kharitonenkov et al., 2005). It causes expressional up-regulation of the glucose transporter GLUT1, stimulates glucose uptake and improves insulin sensitivity. Additionally, it activates the MAPK and Akt pathway in β-cells and protects them from apoptosis. PPARα is one of the main transcriptional regulators of FGF21. Knockdown of FGF21 in mice leads to fatty liver, lipemia, and reduced serum ketones (Badman et al., 2007). FGF23 is a key regulator in calcium and phosphorus homeostasis. It is highly expressed in the bones and the ventrolateral thalamic nuclei. FGF23 knockout mice suffer from hypophosphatemia, underdeveloped reproductive organs and encouraged serum triglyceride (Beenken and Mohammadi, 2009).

2.6 Transcription Factors

Transcription factors are key proteins for transcriptional activation and its regulation. Transcription is known as the process where DNA is copied by RNA polymerases into RNA. All transcription factors share the same feature of one ore more DNA-binding domains (DBD), a trans-activation domain (TAD), and an optional signal-sensing domain (SSD) (Latchman, 1997). Approximately 1200 transcription factors are known (Lee and Young, 2013). However, more than 2600 proteins are identified that contain DNA-binding domains (Babu et al., 2004). The DBDs lead to bonding of specific regions in the genome, so-called transcription factor-binding sites, and drive gene specific DNA transcription. Therefore, DBDs differ widely in their construction. Prominent DBDs are the basic helix-loop-helix, basic-leucine zipper, helix-turn-helix, or zinc finger family (Laity et al., 2001; Murre et al., 1994; Vinson et al., 2002; Wintjens and Rooman, 1996).

While DBDs are responsible for particular binding of gene-promoters the TAD contains binding sites for transcriptional co-regulating proteins. The TAD is able to recruit co-regulators and initiate transcription. In contrast to TADs that are mainly reliable for transcriptional activation, SSDs sensitize the transcriptional complex for up- or down-regulation of gene expression. It is common that SSDs are protein domains of the transcriptional co-regulator proteins and not part of the transcription factor itself.

p53 and MYC are the transcription factors which are most frequently altered in cancer are (Dang, 2012; Green and Kroemer, 2009; Wheeler and Wang, 2013). They act in completely different directions.

p53 is the highest prominent, most fundamental and best-understood tumor suppressor. People who harbor a mutated *TP53* gene will most likely develop cancer (Green and Kroemer, 2009). The wild-type protein is a homotetrameric transcription factor that is involved in response to many forms of cellular stress including DNA damage, osmotic shock, oxidative stress and even oncogene activation (Sherr, 2004). Furthermore, it has cytoplasmic effects like centrosome duplication, apoptosis induction via mitochondria outer membrane permeabilization (MOMP) and inhibition of autophagy (Green and Kroemer, 2009). The *TP53* gene harbors inactivating mutations in more than in 50 % of all cancer types. Most mutations occur within the DBD, leading to insufficient DNA binding. Therefore p53 is not able to trigger transcriptional cell cycle control via p21, 14-3-3σ and Reprimo or apoptosis via Bax, PUMA, Noxa, CD95, Apaf1 etc. Furthermore, it is largely deactivated through direct negative regulators or by inactivating downstream targets. For example, c-terminal oncogenic mutations of ARF lead to p53 depletion and abolishment of MOMP. Similar inactivating effects can be observed in nearly all tumor malignancies (Green and Kroemer, 2009).

On the contrary, *MYC* is a proto-oncogene that promotes growth-related transcriptional responses. MYC belongs to a family also including MYCL and MYCN. It is a junction of many growth related signal transduction pathways, an early response gene downstream of many ligand-membrane receptor complexes and mediates most of its function by dimerization with Max. The MYC transcription factor contains a basic helix-loop-helix and leucine zipper domain. It is one of the most frequent amplified genes among many different human cancers and its dependent serum responses are largely involved in nucleotide metabolism, ribosome biogenesis, RNA processing, and DNA replication. Therefore, MYC is highly regulated in normal cells and its overexpression initiates ARF and p53 activation (Dang, 2012).

2.7 Kinase Inhibitors and Targeted Therapy

It is well known that cancer and several other diseases, for example diabetes, are deregulated in their signaling network (Blume-Jensen and Hunter, 2001; Lemmon and Schlessinger, 2010). In many cancer types growth related protein kinases are permanently in the active conformation shape. These decontrolled kinases are perfect for targeted cancer therapy because tumors are heavily dependent on such growth related signaling cascades (Mok et al., 2009; Solit et al., 2005). Despite high homology among the different kinases, the ATP-binding pocket shows sufficient diversity to develop target specific small molecules (Lemmon and Schlessinger, 2010; Noble, 2004; Paul and Mukhopadhyay, 2004). In contrast to normal chemotherapy, kinase inhibitors and monoclonal antibodies are highly target specific. Therefore, the precise underlying genotypic characteristics of a tumor must be known before starting a targeted cancer therapy.

Three types of small molecules are known. Type I inhibitors have higher affinity to the ATP-binding pocket and therefore interrupt the transfer of the phosphate. Thus, the kinase dependent signal cascade is interrupted. Type II inhibitors bind to the hinge region in a hydrophobic pocket next to the ATP-binding pocket. The hinge region presents higher diversity among different kinase families than the ATP pocket itself. Of note the hydrophobic pocket is only present in the inactive kinase conformation and the kinase is consequently shifted into such conformation. In contrast to Type I and II inhibitors, Type III inhibitors do not bind to the ATP binding pocket. They are allosteric inhibitors and block the shift towards the active kinase conformation. In general, all types of inhibitors can bind reversibly or irreversibly by forming covalent bonds (Davis et al., 2011).

Monoclonal antibodies bind to specific receptor tyrosine kinases (RTKs) and affect their activation. According to antibody binding, the immune system destructs cells expressing such RTKs. Currently approved monoclonal antibodies demonstrated limited efficiency as single agents but are highly effective in combination with conventional chemotherapy. Several therapeutic antibodies demonstrate weak inhibitory effects of oncogenic RTKs with activating mutations in their tyrosine kinase domain (Lemmon and Schlessinger, 2010).

3 Objective of this study

Lung cancer is one of the most deadly diseases due to late diagnosis and inadequate treatment options (Robert-Koch-Institut, 2013). However, in recent years a variety of small molecule kinase inhibitors have been developed which can prevent oncogenic kinase signaling and lead to tumor regression. These inhibitors can be used for targeted cancer therapy in the clinic, though, for a successful response to kinase inhibitor therapy, it is important to understand the precise genotypic characteristics of a distinct tumor entity (Mok et al., 2009; Verma et al., 2012).

FGFR1 is claimed to be the main target of frequent 8p12 amplifications, which arise among several different tumors. However, targeting FGFR1 in recent clinical trials had generally no excessive results (Andre et al., 2013, Sequist et al., 2014). Therefore, it was asked how 8p12 amplifications differ from other well treatable amplifications and whether *FGFR1* is the main target. Furthermore, it was questioned if *FGFR1* alone causes oncogenicity and what are potential co-modulators predicting FGFR1 dependency.

In this thesis several computational and biochemical approaches were used to systematically describe 8p12 amplifications, FGFR1 function and oncogenicity as well as potential resistance mechanisms in lung cancer. The aim of the study was to discriminate and identify 8p12-amplified lung tumors which clearly depend on FGFR1 signaling and therefore respond to targeted FGFR therapy.

4 Material and Methods

4.1 Reagents

Compounds were obtained from Selleck Chemicals, Tocris Bioscience, Merck Millipore, Sigma Aldrich or as a kind gift from Lead Discovery Center GmbH. They were diluted in DMSO, aliquoted and stored as 10mM stocks at -80°C. Fibroblast Growth Factor (FGFs) proteins were provided by ProSpec, dissolved in water and stored at -20°C. Heparin solution (0.2%) was purchased from StemCell Technologies and stored at 4°C.

4.2 Apoptosis assays

For analysis of apoptosis, the Annexin V-FITC Apoptosis Detection Kit I (BD Biosciences) was used. H1581, HCC15 or retrovirally transduced (pBabe) NIH3T3 cells were seeded in 6 cm dishes at 30% confluence in cell culture medium containing puromycine (3µg/ml). After 24 hours supernatant was refreshed and cells were treated with PD173074 (1µM) and DMSO respectively for 72 hours. Subsequently, cells were detached by trypsin, washed with cold PBS, incubated with accutase solution (Sigma Aldrich) for one minute, and resuspended in Annexin-V binding buffer (BD Biosciences). Finally, cells were stained with FITC-labeled Annexin V antibody and Propidium Iodide (PI) and incubated in the dark for 20 minutes. Analysis was performed on a FACS Gallios Flow Cytometer (Beckman Coulter) measuring at least 100,000 events per probe. For calculation of apoptosis, changes from DMSO control to treated samples were evaluated by setting appropriate gate in Kaluza analysis software (Beckman Coulter).

4.3 cDNA Transcription

RNA was isolated from 5-10 x 106 cancer cell lines or from NIH3T3 cells using 1ml TRIZOL reagent (Invitrogen). Suspension was incubated for 5 minutes at room temperature. Then, 200 µl chloroform was added and suspension was shaken for 20 seconds and incubated for 3 minutes at room temperature. Afterwards it was centrifuged at 13.000 rpm for 10 minutes at 4°C (Eppendorf, Centrifuge 5402). The upper phase was pipetted into a clean tube and 0.5 ml isopropanol per ml TRIZOL was added. After an incubation time of 10 minutes composite was centrifuged for 30 minutes at 4°C at 13.000 rpm. Supernatant was discarded and RNA pellet was washed in 80% ice cold ethanol, followed by 5 minutes centrifugation at 13.000 rpm. Supernatant was discarded and RNA was cleaned up using the RNeasy MinElute Cleanup Kit (Qiagen) following the manufacturer's protocol. Finally, 1 µg of RNA was transcribed into cDNA using Superscript III reverse transcriptase (Invitrogen, #18064) following the manufacture's protocol.

4.4 Cell Line Stimulation

Cell lines were starved from bovine serum for 24 hours and stimulated by a collection of 6 FGF-ligands (1 ng/ml) and heparin (10 µg/ml) for 20 minutes. Additionally, the FGFR inhibitor PD173074 (1 µM) was added 40 minutes before stimulation by FGF-1 and FGF-2. Phosphorylation of FGFR, ERK, AKT and the FGFR1 signaling adapter protein FRS2α as well as total expression of ERK and FGFR1 were assessed by immunoblotting.

4.5 Cell lines

All cancer cell lines, HEK293T and NIH3T3 cells were purchased from American Type Culture Collection (ATCC) and the German Resource Centre for Biological Material (DSMZ) and cultured using either RPMI (for cancer cell lines) or DMEM High Glucose media (for Hek293T or NIH3T3 cell lines), supplemented with 10% fetal calf serum (FCS). Adherent cells were routinely passaged when 70 to 90% confluence was reached by washing with phosphate buffered saline (PBS) buffer and by subsequent incubation in Trypsin/EDTA or Accutase. Trypsin or Accutase was inactivated by addition of culture medium and cells were plated or diluted accordingly. Suspension cell lines were passaged by suitable dilution of the cell suspension. All cells were cultured at 37°C and 5% CO^2. The identity of all cell lines included in this study was authenticated by genotyping (SNP 6.0 arrays, Affymetrix) and they were tested for infection with mycoplasma (MycoAlert, Lonza). Furthermore, the identity of the H1581 cell line was ensured by STR profiling (DNA fingerprinting).

4.6 Computational Analysis

In total, segmented copy number data of a collection of 306 primary squamous cell lung cancer samples from the Clinical Lung Cancer Project (The Clinical Lung Cancer Genome Project (CLCGP) and Network Genomic Medicine (NGM), 2013) and 132 primary squamous cell lung cancer samples from the Cancer Genome Atlas were analyzed (http://cancergenome.nih.gov). Recurrence of copy number aberrations was analyzed by using the GenePattern Platform of the Broad institute, specially the Genomic Identification of Significant Targets in Cancer (GISTIC) algorithm (http://genepattern.broadinstitute.org/gp/pages/login.jsf).

Copy number data were displayed by integrative genome viewer (IGV). Representative screenshots (12-14 Mbp range) of segmented CLCGP copy number data containing *EGFR* (7p12), *FGFR1* (8p12) and *CCND1* (11q13) were taken. The same analysis was similarly done for segmented TCGA copy number data. Samples were sorted by the genomic coordinate of the highest copy number value and positions of the genes were highlighted. Work was performed using a 2.8 GHz Intel Core i7 Processor with 8GB DDR3 Memory on Mac OS X Version 10.7.5 operating system.

4.7 ELISA Assay

Cell lines (HCC15, H1581, H358, HCC1599, DMS114, HCC95, A427, SW1271, SBC7, H520 and H1703) were seeded as triplicates with 70% confluence at 10 cm dishes and incubated over night under normal cell culture conditions. Then, medium was removed and replaced by 10 ml normal cell culture medium (10% FCS), starved medium (0.01% FCS) or starved medium with FGFR inhibitor (0.01% FCS, 1µM PD173074) for each cell line. After 48-hour incubation supernatants were collected and centrifuged for 5 minutes at 200g. Next, supernatants were concentrated through Viaspin 20 (3.000 MWCO PES, Sartorius stedim) by centrifugation 2 x 30 min at 4200g. Volume of medium was measured before and after concentration for normalization. Additionally, protein was extracted from cells, collected in equal amounts of lysis buffer (Cell Signaling) and measured by Bradford assay (Pierce). Supernatants were analyzed for FGF2 and FGF4 concentration by ELISA (Abcam) following the manufacturer's instructions.

4.8 FGFR1 Cloning and Site-Directed Mutagenesis

cDNA of H1581 cells (100ng) was used to amplify FGFR1 by attB-overhang primers and flipped into pDONR.221 using the BP-clonase (Invitrogen). Bacterial transformation of the competent E. coli strain DH5α (Invitrogen) was carried out according to the manufacturer's instructions. Single clones were sequenced from mini-preparation of plasmid DNA using the NucleoSpin Mini Kit (Machery Nagel). For midi-preparation of plasmid DNA, the NucleoBond Xtra Midi EF Kit (Machery Nagel) was used. pDONR-FGFR1α and β were flipped into the retroviral vector backbones of pBabe-puro, -neo or -hygro gateway (GW) using the LR Clonase Kit (Invitrogen).

For site directed mutagenesis of the pBabe-puro-FGFR1β plasmid, QuickChange II XL Site-Directed Mutagenesis Kit (Agilent) was used in order to integrate the following point mutations: V472M, L76T plus V472M, A78L plus V472M, K83E plus V472M, D157N plus V472M, D193N plus V472M and Q195E plus V472M.

4.9 Immunoblotting

Cells were seeded and incubated over night, washed with cold PBS, lysed in lysis buffer (Cell Signaling) and supplemented with protease (Roche) and phosphatase inhibitor (Calbiochem) cocktails. After 20 minutes of incubation on ice, lysates were centrifuged at 18,000g for 25 minutes. Protein concentration in supernatants was measured using BCA Protein Assay (ThermoScientific). Equivalent amounts of protein (30–60µg) were denatured for 5 minutes at 95°C and separated on 4–12% SDS-PAGE gels and after blotting on nitrocellulose membranes (Amersham Hybond-C Extra). The following antibodies were used for immunoblotting: β-actin (MP Bioscience), phospho-FGFR (Tyr653, Tyr654), phospho-FRS2 (Tyr196), phospho-AKT (Ser473), AKT, phospho-ERK, and ERK, c-myc (Cell Signaling Technology), total FGFR1 (Epitomics / Abcam), caspase-3 (Cell Signaling 9662S), cyto-chrom C (BD Pharmingen, mouse), cyclin D1 (Santa Cruz), conjugated antibodies to rabbit and mouse (Millipore).

4.10 Immunohistochemistry

Tissues were fixed in 4% PBS-buffered formalin and embedded in paraffin (FFPE). Immunohistochemistry was performed as described previously (Heukamp et al., 2003) on 3 µm slides with specific antibodies for pFGFR1 (Abnova, Y154) and MYC (Abcam). Staining intensities were individually evaluated by 3 independent observers, using a 4-tier scoring system. The areas of highest staining intensity were scored. Examples of nuclear MYC and cytoplasmic and membranous pFGFR1 staining are exemplarily shown. Statistical analysis was performed using a Fisher's exact test.

4.11 Quantitative Real-Time PCR

Quantitative real-time PCR was performed using a 7300 Real-Time PCR System (Applied Biosystems) and Power SYBR Green PCR Master Mix (Applied Biosystems) with primer pairs (primer table) specific for GAPDH (QT01192646, Qiagene) (58°C), AKT2 (58°C), CCND1 (58°C), REL (58°C), SOX (58°C), MYC (58°C), DYRK1K (58°C), FGFR1 (56°C), FGFR2 (56°C), FGFR3 (56°C) and FGFR4 (56°C). ΔCt-values were determined using the 7300 System Software (Applied Biosystems) using GADPH as reference control. Gene expression was calculated by ΔΔCt-method.

4.12 RNAi and Stable Transduction

Cancer cell lines were transduced by lentiviral supernatants at equal titers in the presence of polybrene (10µg/ml) for 24 hours and selected by puromycine (1 - 3µg/ml). Relative cell survival was calculated as ratio to the empty-vector construct (Addgene). Knockdown efficacy was validated by immunoblotting. The following target sequences were used for MYC and FGFR2, respectively: CCTGAGACAGATCAGCAACAA (shMYC).

4.13 Soft-Agar Assay

All soft-agar experiments were performed as triplicates in 96-well plates. For bottom agar 50 µl of growth medium per well (10% FCS; 1.0% agar) were added and allowed to solidify at 4°C for 10 minutes. Cells were detached by trypsin and cell number was determined by using the Z2-coulter counter (Beckman Coulter). Re-suspended cell pellets were solved in growth media containing 10% FCS and 0.6% agarose type IX ultra low (Sigma Aldrich).1000 cells in 50 µl per well were plated on pre-warmed bottom agar. Plates were incubated at 4°C for 10 minutes for solidification and transferred to a 37°C incubator. The next day, soft agar was covered with 150 µL cell culture medium. After 3-4 weeks of incubation at 37°C and 5% CO^2, colonies were either analyzed by Scanalyzer imaging system (LemnaTec) or counted by hand.

4.14 Stable cDNA Expression

Cancer cell lines and NIH3T3 cells were transduced by retroviral supernatants in the presence of polybrene (10µg/ml) for 24 hours and selected by puromycine (3 µg/ml), G418 (800 µg/ml) or hygromycine (400 µg/ml), respectively, for 2-3 weeks. NIH3T3 cells transduced with FGFR1 were incubated with 15ng/ml FGF2 and 2µg/ml heparin (StemCell). Expression of the respective cDNA was confirmed by immunoblotting or quantitative real-time PCR. Finally, cells were expanded and frozen in liquid nitrogen for long-term storage.

4.15 Viability Assays and Compound Activity Prediction

Cell lines were plated as triplicates into sterile 96-well plates at 1500 cells/well density, as described previously. After 24 hours of incubation, compounds were added at increasing dosages, ranging from 30µM to 0.005 µM together with a separate DMSO control. After 96 hours, relative cell viability was determined by comparing the ATP-content of each well - assessed by CellTiter Glo Assay (Promega, US) - to the content of the DMSO control. Finally, half-maximal growth inhibitory concentrations (GI50) were calculated by the package “ic50” (R programming language) (Sos et al., 2009b).

4.16 Virus Production

HEK293T cells were plated on 6 cm dishes in DMEM + 10% FCS and incubated over night at 37 °C. After 24 hours, the cells were 80% confluent and transfected with retroviral plasmids. For this, 12µl TransIT-LT1 (Mirus) were added drop-wise to 400 µl OptiMem medium (Invitrogen). In a separate tube, 4 µg of pBabe expression plasmid was mixed with 4 µg of pCL-eco or pCL-ampo packaging plasmid in 400 µl OptiMem medium. After 5 minutes of incubation, both tubes were mixed carefully and incubated at room temperature for 20 minutes. Subsequently, this mixture was added to HEK293T cells. The next day, medium was removed and changed to DMEM + 30% FCS. After 24 hours and 48 hours, supernatants were collected and centrifuged at 200 g for 5 minutes, filtered, aliquoted and stored at -80 °C.

Similarly, replication-incompetent lentivirus was produced from pLKO.1-puro vector containing a short hairpin RNA (shRNA), specific for the respective target gene. For this, HEK293T cells were co-transfected with Δ8.9, pMGD2 and pLKO.1 vector, as described previously (Sos et al., 2009b). Viral titers were determined by transduction of NIH3T3 cells (ATCC) at increasing virus dilutions. Hereby the virus titer was calibrated equally for all samples.

4.17 Whole Transcriptome Sequencing (RNAseq)

Total RNA was extracted from fresh-frozen lung tumor tissue containing at least 60% tumor cells. Depending on the tissue size, 15–30 slides were cut using a cryostat (Leica) at –20 °C. Material for RNA extraction was disrupted and homogenized for 2 minutes at 20 Hz by Tissue Lyser (Qiagen). RNA was extracted using the Qiagen RNeasy Mini kit following the manufacturer's instructions. RNA quality was assessed by a Bioanalyzer. Samples showing an RNA integrity number (RIN) > 8 were retained for transcriptome sequencing. cDNA strands of 250 bp were cloned into a sequencing library, allowing the sequencing of 95-bp paired-end reads without overlap. All RNAseq libraries were analyzed on the Illumina Genome Analyzer IIx.

Gene coverage was used to differentiate splice variants of FGFR1. Mesenchymal splice variants of FGFR1 were differentiated by coverage of exon 2, whereas coverage of tissue specific exons 8 (IIIb/IIIc) distinguished epithelial (IIIb) from mesenchymal (IIIc) forms.

4.18 Xenograft Mouse Models

All animal procedures were approved by the local animal protection committee and the local authorities. Transduced NIH3T3 and tumor cells were resuspended in RPMI or DMEM medium and injected (5 x 106 cells per tumor) subcutaneously into the flanks of 8 to 15 week old male nude mice (Rj:NMRI-nu (nu/nu), Janvier Europe) under 2.5% isoflurane anesthesia.

In order to assess the effect of FGFR inhibitors in vivo, NVP-BGJ 398 (Novartis) was dissolved in a vehicle solution (33% PEG300, 5% glucose) for xenograft application. Tumor size was monitored every second day by measurement of perpendicular diameters by an external caliper and calculated by use of the modified ellipsoid formula (V = 1/2 (Length x Width2)). Oral therapy was started when tumors reached a volume of 100mm^3. Mice daily received either BGJ398 (15mg/kg) or vehicle solution. After 14 (NIH3T3 FGFR1β + MYC), 16 (NIH3T3 EML4-ALK, KRAS G12V) or 25 (NIH3T3 e.V., FGFR1α/β) days of therapy, respectively, mice were killed by intraperitoneal injection of Ketamin/Xylazine (300/60 mg/kg).

In order to examine ligand dependency in vivo, AdCMV-null virus (Vector Biolabs) and AdsFGFR virus (titer: 1x1010, contributed as a kind gift by Gerhard Christofori) were mixed with tumor cells in DMEM medium for subcutaneous injection. Tumor formation was monitored daily or twice a week by careful visual inspection and palpation of the skin. As soon as tumors became palpable, diameters were measured by an external caliper in order to determine tumor volumes. Additionally, animal weights were documented weekly. Eight weeks after injection of H1581 and A549 tumor cells, animals were killed.

Subcutaneous tumors as well as livers were resected and fixed in 4% formaldehyde for IHC staining and virus detection, respectively.

4.19 Primer List

	Name	**Sequence**
1	F_CCND1_RT_1	GGCGGAGGAGAACAAACAGA
2	F_CCND1_RT_2	GACCCCGCACGATTTCATTG
3	F_CCND1_RT_3	CAATGACCCCGCACGATTTC
4	R_CCND1_RT_1	TGTGAGGCGGTAGTAGGACA
5	R_CCND1_RT_2	GAGGCGGTAGTAGGACAGGA
6	R_CCND1_RT_3	CACTCTGGAGAGGAAGCGTG
7	R_SOX2_RT_1	TGTGCATCTTGGGGTTCTCC
8	R_SOX2_RT_2	GCTTCTCCGTCTCCGACAAA
9	R_SOX2_RT_3	TTAGCCTCGTCGATGAACGG
10	F_REL_RT_1	TTGAACAACCCAGGCAGAGG
11	F_REL_RT_2	GCACAGCACAGACAACAACC
12	F_REL_RT_3	GCACAGACAACAACCGAACA
13	R_REL_RT_1	AGTAGCCGTCTCTGCAGTCT
14	R_REL_RT_2	TGAATGGATTGATTCCTGCCT
15	R_REL_RT_3	CATTGAATGGATTGATTCCTGCCT
16	F_DYRK1B_RT_1	CATCAGACCCAGGAGCTTGT
17	F_DYRK1B_RT_2	GTGGCCATCAAGATCATCAA
18	F_DYRK1B_RT_3	GAGCTGATGAACCAGCATGA
19	R_DYRK1B_RT_1	CTTGAGGTCGCAGTGAATGA
20	R_DYRK1B_RT_2	CTTGAGGTCGCAGTGAATGA
21	R_DYRK1B_RT_3	CTGCCGAAGTCCACAATCTT
22	F_AKT2_RT_1	TATACCGCGACATCAAGCTG

23	F_AKT2_RT_2	GCAGAGATTGTCTCGGCTCT
24	F_AKT2_RT_3	AGCTGGAAAACCTCATGCTG
25	R_AKT2_RT_1	TGGGTGTGGTCATGTACGAG
26	R_AKT2_RT_2	TCTGCTTGGGGTCCTTCTTA
27	R_AKT2_RT_3	CTCTGCTTGGGGTCCTTCTT
28	F_FGFR1_326296	AAAAAGCAGGCTTCACCATGTGGAGCTGGAAGTGC
29	R_FGFR1_397108	AGAAAGCTGGGTC TCAGCGGCGTTTGAGTC
30	F1_FGFR1_326296	ATGTGGAGCTGGAAGTGC
31	R1_FGFR1_397108	TCAGCGGCGTTTGAGTC
32	h Gapdh	TGACAACTTTGGTATYCGTGGAAGG
33	h Gapdh	AGGCAGGGATGATGTTCTGGAGAG
34	F_FGFR1	ATGTGGAGCTGGAAGTGC
35	R_FGFR1	TCAGCGGCGTTTGAGTC
36	F_FGFR1_326296	AAAAAGCAGGCTTCACCATGTGGAGCTGGAAGTGC
37	R_FGFR1_397108	AGAAAGCTGGGTC TCAGCGGCGTTTGAGTC
38	attB1_F_adapter	G GGG ACA AGT TTG TAC AAA AAA GCA GGC T
39	attB2_R_adapter	GGGGACCACTTTGTACAAGAA AGC TGG GT
40	Myc_RT_PCR_F	CAGCTGCTTAGACGCTGGATT
41	Myc_RT_PCR_R	GTAGAAATACGGCTGCACCGA
42	Myc_RT_PCR_F2	AATGAAAAGGCCCCCAAGGTAGTTATCC
43	Myc_RT_PCR_R2	GTCGTTTCCGCAACAAGTCCTCTTC
44	Myc_RT_PCR_F4	CTGGTGCTCCATGAGGAGA
45	Myc_RT_PCR_R4	GTGAGGAGGTTTGCTGTGG
46	FGFR2_Human_F2_HF1	TGTTGAAAGATGATGCCACAG
47	FGFR2_Human_F2_HR2	TGACATAGAGAGGCCCATCC
48	FGFR2_Human_F2_HF3	CAGGGGTCTCCGAGTATGAA
49	FGFR2_Human_F2_HR4	ACTTGCCCAAAGCAACCTT
50	FGFR3_Human_F3_HF1	GTGACAGACGCTCCATCCTC

51	FGFR3_Human_F3_HR2	CAGCTTGATGCCTCCAATG
52	FGFR3_Human_F3_HF3	CCGACGAGTACCTGGACCT
53	FGFR3_Human_F3_HR4	GTGGGCAAACACGGAGTC
54	FGFR4_Human_F4_HF1	GCTGCTTTGGCCAGGTAGTA
55	FGFR4_Human_F4_HR2	CACCAAGCAGGTTGATGATG
56	FGFR4_Human_F4_HF3	AGCACCCTACTGGACACACC
57	FGFR4_Human_F4_HR4	ACGCTCTCCATCACGAGACT
58	FGFR1_Primer 1	CTGGTCACAGCCACACTCTG
59	FGFR1_Primer 2	TGGAAGTGGAGTCCTTCCTG
60	FGFR1_Primer 3	TGCTGGTTACGCAAGCATAG
61	FGFR1_Primer 4	TGCATGCAATTTCTTTTCCA
62	FGFR1_Primer 5	AGGAGGGGAGAGCATCTGA
63	FGFR1_Primer 6	GACCTTGCCTGAACAAGATGCTC
64	FGFR1_Primer 7	GCACTGCATGCAATTTCTTTTCC
65	FGFR1_Primer 8	GCCTGAACAAGATGCTCTCC
66	FGFR1_Primer 9	TGCATGCAATTTCTTTTCCA
67	FGFR1_Primer 10	GGAGCTGGAAGTGCCTCCT
68	FGFR1_Primer 11	GAGGGGAGAGCATCTTGTTC
69	FGFR1_Primer 12	CTTGAAGCATTCGGGGATTA
70	FGFR1_Primer 13	GCACAGGTCTGGTGACAGTG
71	FGFR1_Primer 14	CCTCTCTTCCAGCACAGGTC
72	FGFR1_Primer 15	CCCAGACAACCTGCCTTATG
73	FGFR1_Primer 16	ACCACCGACAAAGAGATGGA
74	FGFR1_Primer 17	GCAGAGTGATGGGAGAGTCC
75	FGFR1_Primer 18	GTACAGGGGCGAGGTCATC
76	FGFR1_Primer 19	TTCCTCATCTCCTGCATGGT
77	FGFR1_Primer 20	CATGGATGCACTGGAGTCAG
78	FGFR1_Primer 21	AAGGGCAACTACACCTGCAT

79	FGFR1_Primer 22	TCGATGTGCTTTAGCCACTG

5 Results

5.1 Heterogenic Amplification Pattern of the 8p12 Locus

As a first step to evaluate 8p12 (*FGFR1*) amplification events, we analyzed 306 single-nucleotide polymorphism (SNP) array data from squamous cell carcinomas (SCC) of the clinical lung cancer genome project (CLCGP), using GISTIC (Genomic Identification of Significant Targets in Cancer). The integrative genome viewer (IGV) helped in identifying significantly amplified regions (q=0.05) (Beroukhim et al., 2007; The Clinical Lung Cancer Genome Project (CLCGP) and Network Genomic Medicine (NGM), 2013).

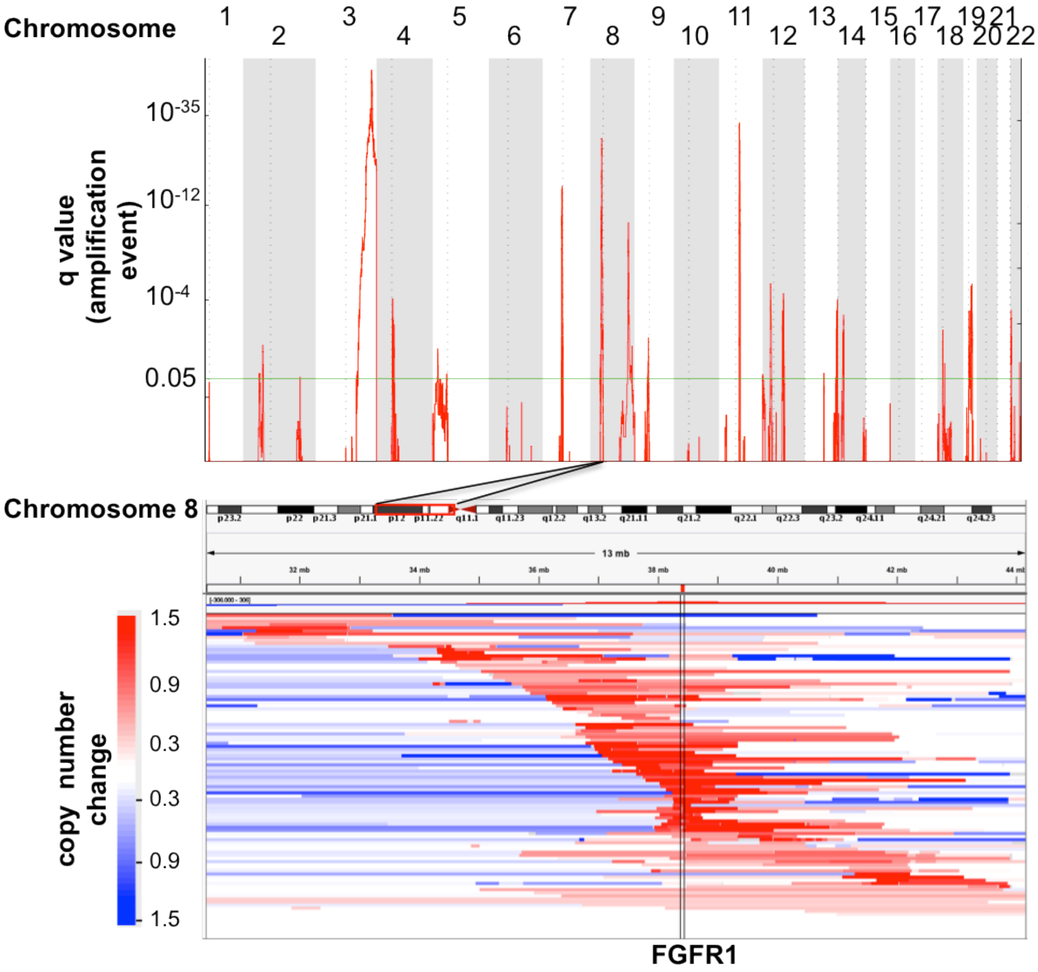

Figure 9: Genomic heterogeneity of the 8p12 amplicon in squamous-cell lung cancer. Analysis of 306 raw copy number data of the CLCGP dataset by GISTIC (top). Visualized CLCGP copy number data by IGV demonstrates heterogenic amplification pattern at the 8p12 locus (bottom; n=79).

We detected twenty-five significantly amplified regions within the SCC genome, which was previously described (Figure 9) (Hammerman et al., 2012; Weiss et al., 2010). Furthermore, we found that in contrast to well-known amplification events like 7p11 (*EGFR*) or 11q13 (*CCND1*, *FGF4*, *FGF19*) the 8p12 locus is characterized by genomic heterogeneity, which results in multiply amplified centers (Figure 9). Only about 25% of 8p12 amplifications were actually centered on *FGFR1*. Additionally, most copy number changes of the 8p12 locus occur within a range of 13 Mbp. Copy number changes of other significantly amplified regions are completely centered on respective oncogenes like *EGFR* (7p11) or *CCND1* (11q13) (Figure 10).

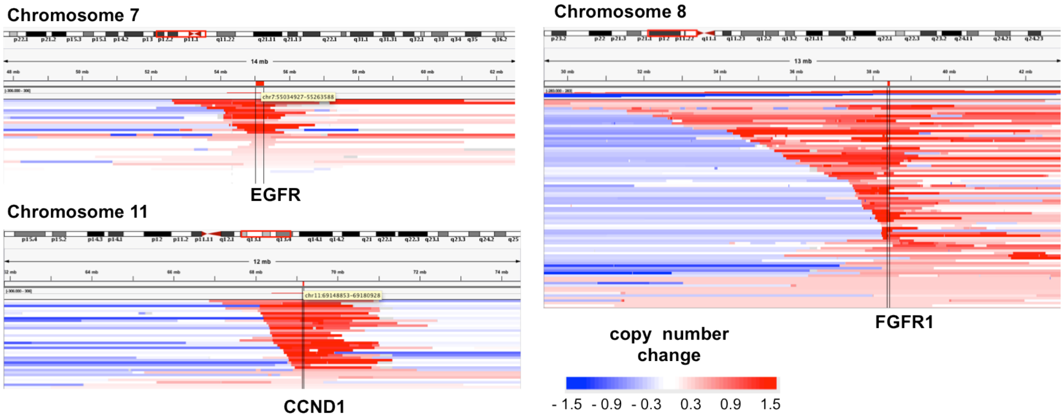

Figure 10: IGV screenshots of recurrently amplified regions in squamous-cell lung cancer. CLCGP data demonstrates homogeneity of 7p11 (top left; n=29) and 11q13 (bottom left; n=35) amplified SCC tumors. TCGA data demonstrates heterogenic amplification pattern at the 8p12 locus (right; n=68).

These homogeneous amplification events revealed breakpoints within a region of only 5 Mbp. Using The Cancer Genome Atlas (TCGA) dataset of 299 squamous cell lung cancer specimens as an independent validation, we observed similar heterogenic amplification patterns of the 8p12 locus (Figure 10).

In summary, the 8p12 amplicon in SCC is profoundly heterogeneous on the genomic level. The 8p12 locus is characterized by multiple amplification centers. Thus, only in a fraction of amplified tumors, *FGFR1* lies within the epicenter. In some tumor specimens *FGFR1* was not even included in the amplicon, suggesting that the geographic extension is biologically relevant for diagnostic purposes.

5.2 Activation of the MAPK Pathway by FGFs

Autocrine growth stimulation by FGF is well known for non-EGFR driven lung cancer cell lines (Marek et al., 2008). Although FGFR1 signaling stimulates ERK activation, activating mutations are rare (Hammerman et al., 2012; Weiss et al., 2010). Thus, it was unclear if FGFR1 downstream signaling cascade is ligand dependent or independent. We therefore tested FGFs for FGFR1 activation (Mason, 2007).

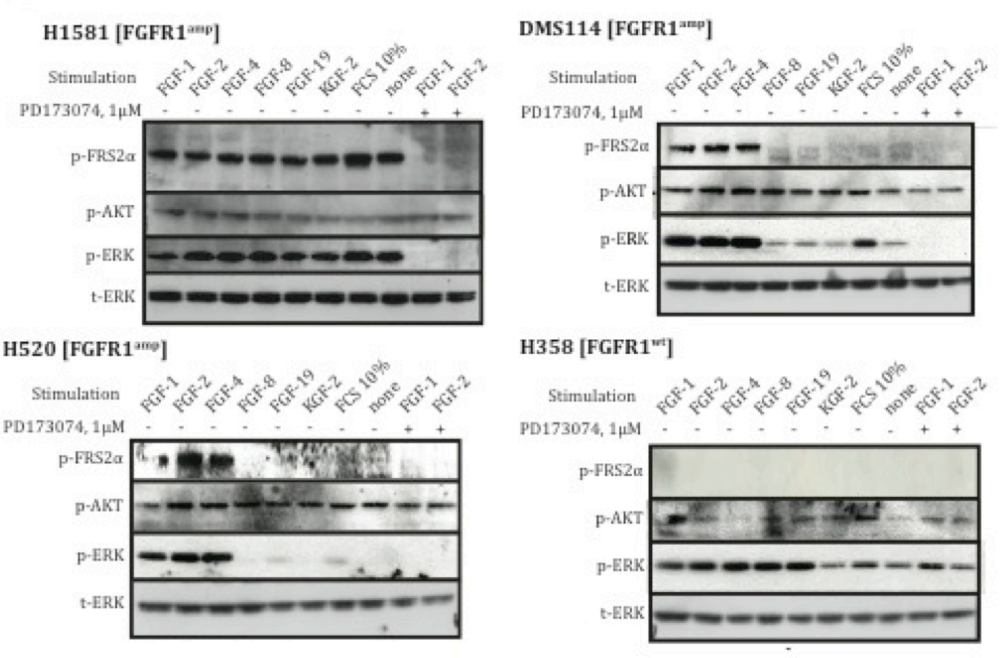
H1581 [$FGFR1^{amp}$]
DMS114 [$FGFR1^{amp}$]
H520 [$FGFR1^{amp}$]
H358 [$FGFR1^{wt}$]
Stimulation
FGF-1
FGF-2
FGF-4
FGF-8
FGF-19
KGF-2
FCS 10%
none
FGF-1
FGF-2
PD173074, 1µM
- - - - - - - - + +
p-FRS2α
p-AKT
p-ERK
t-ERK

Figure 11: Immunoblots of FGF stimulated cell lines. Immunoblots of three FGFR1-amplified cell lines H1581, DMS114 and H520 (in order of FGFR inhibition sensitivity) and one NRAS mutated control cell line H358 demonstrate different entities of ERK phosphorylation through FGF stimulation.

All *FGFR1*-amplified cell lines showed FRS2 and ERK activation when stimulating with FGF1, FGF2, and FGF4 at relatively low concentrations (1ng/ml) (Figure 11). However, FGFR inhibition completely antagonized stimulation. Furthermore, we found that H1581 cells, which are the most sensitive cells to FGFR inhibition, showed high basal activation of ERK even after 24 hours of starvation. Interestingly, basal stimulation decreases in order of FGFR inhibitor sensitivity from H1581 (IG50; 180 nmol), over DMS114 (IG50; 460 nmol) to H520 (IG50; 4.5 μmol) (Figure 11).

These results can be interpreted in two different ways. In order of inhibitor sensitivity, either FGFR1 amplification activates FGFR1 downstream signaling independent of FGF ligands, or FGF ligands are secreted from the cells themselves to activate FGFR1. Second would indicate that FGFR-dependent lung tumor cells may be sustained in their growth through an FGF autocrine and/or paracrine activation loop.

5.3 Secretion of FGF2 and 4 by *FGFR1*-amplified Tumor Cells

The production and secretion of growth factors as proliferation circuits is one hallmark of cancer (Hanahan and Weinberg, 2011). In order to assess FGFR1 activation in vitro under cell culture conditions, we analyzed FGF2 and FGF4 concentrations in supernatants of 11 cancer cell lines by ELISA.

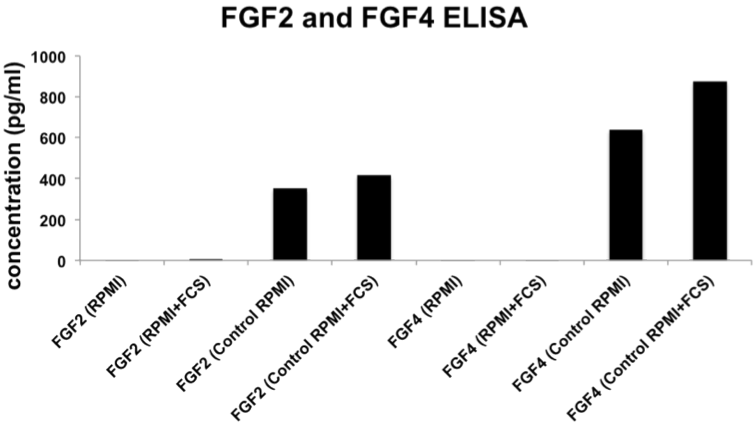

Figure 12: FGF2 and FGF4 are not detectable in medium or fetal calf serum. Relative FGF2 and FGF4 concentrations of medium (RPMI) or fetal calf serum (FCS) were examined by ELISA.

We detected FGF2 and 4 in the cell culture supernatants of all tested cell lines. By contrast, FGFs were undetectable in both the growth medium and the RPMI supplemented with 10% FCS (Figure 12). Furthermore, starvation of cells in combination with FGFR inhibition treatment led to significantly increased FGF2 (p=0.009) and FGF4 (p=0.04) secretion for *FGFR1*-amplified cancer cell lines, compared to controls (Figure 13).

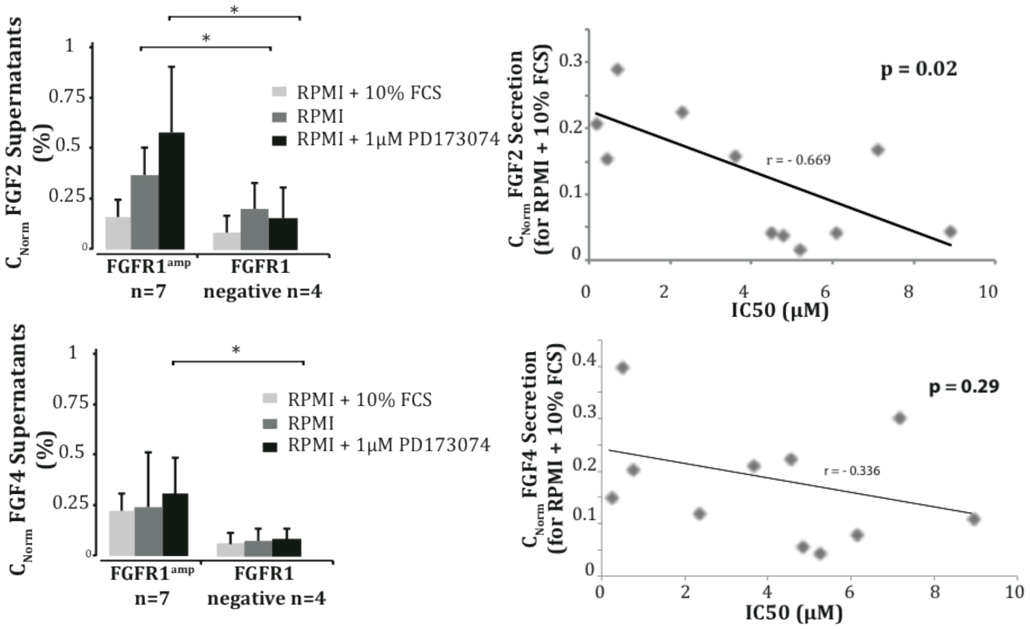

Figure 13: FGF2 and 4 concentrations are upregulated by withdrawal of 10% fetal calf serum and FGFR inhibition. Secretion of normalized FGF2 (top left) and FGF4 (bottom left) concentrations (cNorm) by 48-hour normal culture conditions (RMPI + 10 % FCS), serum starvation (RPMI) or FGFR inhibited conditions (RPMI + 1µM PD173074). Cell lines were grouped for *FGFR1*-amplified (H1581, DMS114, HCC1599, SBC-7, H520, HCC95 and H1703) or *FGFR1* non-amplified (A427, SW1271, H358 and HCC15), respectively, to compare normalized FGF concentrations by t-test. Correlation of FGFR sensitivity (PD173074 GI50, x-axis) and normalized FGF-2 (top left) and FGF-4 (bottom left) concentrations (y-axis) under normal culture conditions (RMPI + 10 % FCS). Significant ($p < 0.05$) differences were marked by (*). Error bars display standard deviation within the respective groups.

This observation indicates the presence of a positive feedback loop. Interestingly, the cell lines H1581 (IG50; 180 nmol), DMS114 (IG50; 460 nmol) and HCC1599 (IG50; 600 nmol) which are most sensitive to FGFR inhibition, showed the highest secretion of FGF2 during starvation. Remarkably, there was a correlation between FGF2 secretion and FGFR inhibitor sensitivity (p=0.02) under normal cell culture conditions (Figure 13).

This result supports the notion that *FGFR1*-amplified and FGFR inhibitor sensitive cancer cells secrete FGFs for auto-stimulation.

5.4 Ligand Dependency of H1581 Cells

Next we tested the exigency of extracellular ligands for viability of FGFR1 dependent cell lines (Figure 14). Andre Richters and Felix Dietlein provided technical support and acquisition of data.

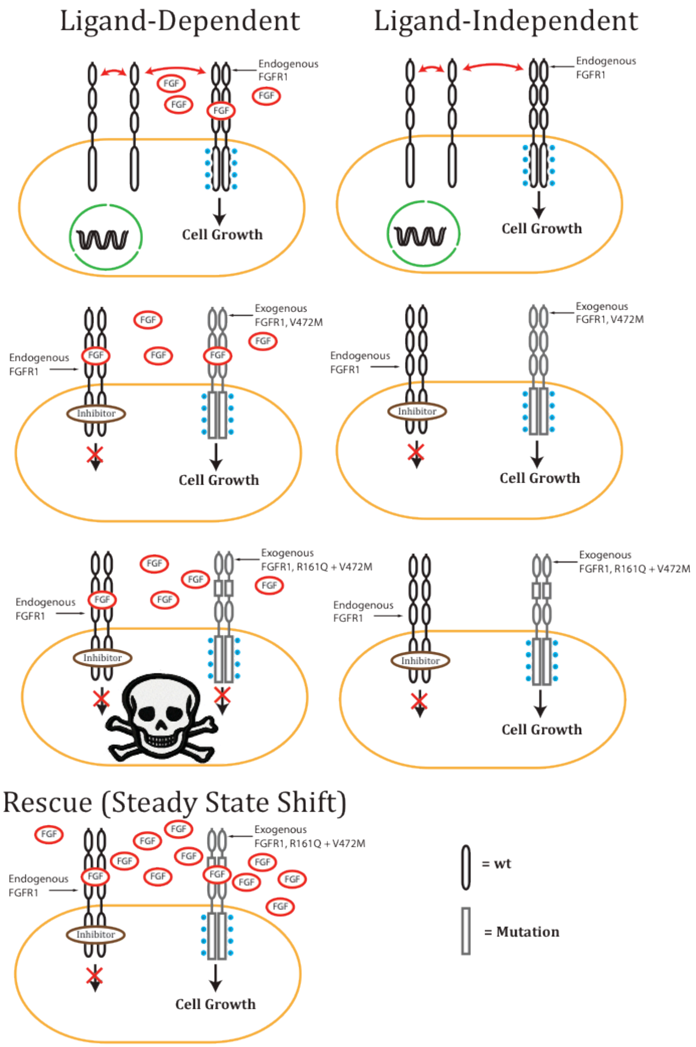
Ligand-Dependent
Ligand-Independent
Endogenous FGFR1
FGF
Cell Growth
Exogenous FGFR1, V472M
Inhibitor
Exogenous FGFR1, R161Q + V472M
Rescue (Steady State Shift)
= wt
= Mutation

Figure 14: Experimental draft for H1581 Ligand Dependency in vitro. Ligand-Dependent: Endogenous receptor binds FGF, dimerizes and activates downstream signaling. Exogenous receptor with gatekeeper mutation (FGFR1, V472M) takes over signaling during FGFR-inhibitor treatment. Exogenous double mutated receptor (FGFR1, R161, V472M) canot take over signaling during treatment (lack of FGF binding). Reconstitution of FGFR1 signaling through FGF stimulation. Ligand-Independent: Endogenous receptor dimerizes and activates downstream signaling. Exogenous receptor with gatekeeper mutation (FGFR1, V472M) takes over signaling during FGFR-inhibitor treatment. Exogenous double mutated receptor (FGFR1, R161, V472M) still signals during therapy (lack of FGF binding).

A loss-of-function mutation of FGFR2 was previously described in melanoma (Gartside et al., 2009). According to an analysis with PolyPhen the analogous R161Q mutation was also predicted to potentially impact the secondary structure of FGFR1 (http://genetics.bwh.harvard.edu/pph2/) (Figure 15).

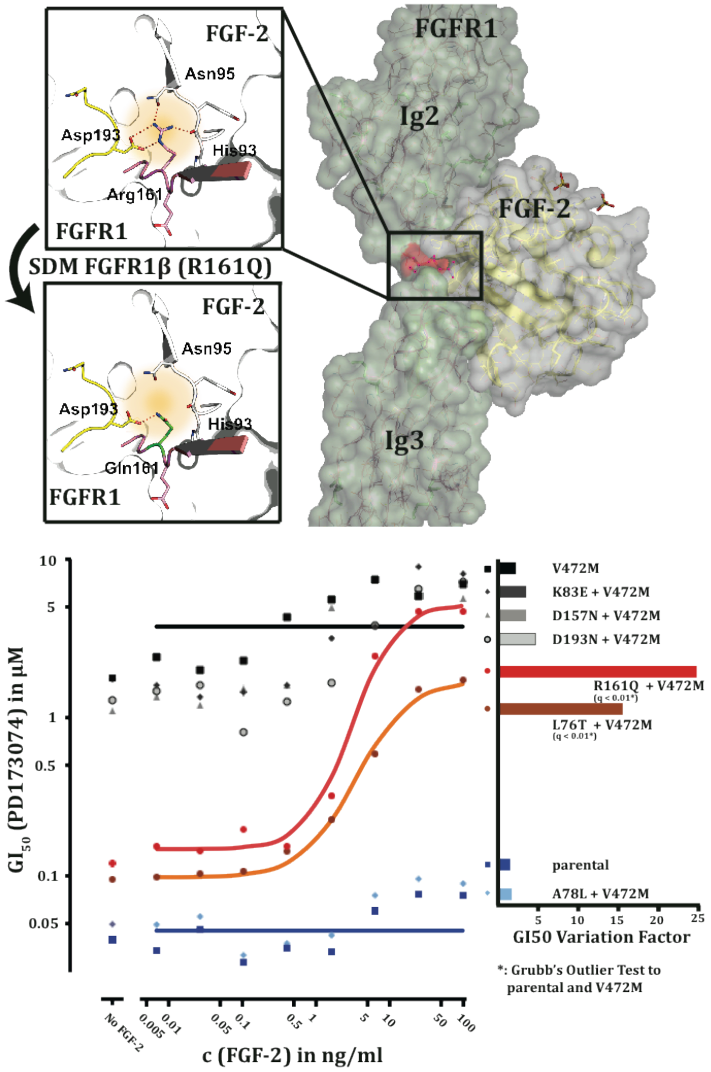

Figure 15: Ligand binding is essential for signaling perpetuation of FGFR-dependent H1581 cells. Interaction of the Ig2-Ig3-interloop domain of FGFR1β Arg161 with the FGF-2 Asn95 and His93 as derived from crystal structures (top). Visualization with the PyMOL software implicates loss-of-interaction if Arg161 is substituted (site directed mutagenesis, SDM) by Gln161 (top). For each FGFR1β mutant, FGFR-dependency (PD173074) was assessed under increasing concentrations of FGF-2 (x-axis, logarithmic) by 96-hour cell titer glo assay (bottom). FGF-2-GI50-dependencies (y-axis, logarithmic) were fitted to logistic functions. Andre Richters, TU Dortmund, Germany, generated the structural image with PyMOL.

Starting from here, we designed and cloned mutants of FGFR1β that we predicted to be deficient in ligand binding, L76T, A78L, K83E, D157N and D193N. Furthermore, all constructs also contained the gatekeeper mutation V472M in the intracellular kinase domain of the receptor, inducing FGFR inhibitor resistance (Weiss et al., 2010). We introduced the FGFR1 mutants to H1581 cells and treated them with the FGFR inhibitor PD173074 (Figure 15). By doing so, we repressed signaling from the endogenous FGFR1 receptors, as in the presence of drug the cells switched to the ectopically expressed drug-resistant mutants (Weiss et al., 2010).

We found that the receptors with the V472M and additional K83E, D157N, D193N mutations showed the same resistance phenotype as the single mutated V472M receptor (Figure 15). Resistance to PD173074 was given but ligand dependency was not detectable. Thus, these transduced cells are capable of rescuing FGFR1 signaling without further FGF stimulation. By contrast, the A78L mutated receptor construct was sensitive to PD173074 treatment and could not respond to FGF stimulation, implicating a complete structural damage of the ligand-binding domain (Figure 15). The L76T and R161Q receptor constructs showed a distinct phenotype: at low FGF concentrations, mutants were not able to maintain FGFR1 signaling (t-test, p<0.01). However, increasing amounts of the ligand dose-dependently rescued receptor activities. These constructs may represent mutants, which partially impair ligand binding, whereby the steady state of FGF-FGFR1 interaction was shifted into the FGF bound conformation via addition of high amounts of FGF (Figure 14 and 15). Western blot of the double mutant L76T

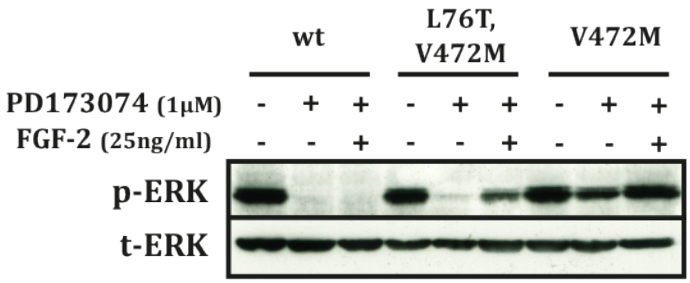
wt
L76T, V472M
V472M
PD173074 (1µM) - + + - + + - + +
FGF-2 (25ng/ml) - - + - - + - - +
p-ERK
t-ERK

Figure 16: Reconstitution of MAPK phosphorylation of ligand-binding-deficient mutations under high doses of FGF-2.

and V472M showed no pErk signaling under inhibited conditions, while the signal could be reconstituted with 25ng/ml FGF2 (Figure 16). Therefore, exogenously added ligands overcome the reduction in ligand affinity induced by L76T and R161Q.

These results further indicate that FGFR1 signaling is not induced due to spontaneous signaling as a result of overexpression. Moreover, FGFR1 activation seams to be entirely dependent on FGF ligand binding.

5.5 FGFs Requirement of H1581 Cells for Tumor Formation

As a next step, we analyzed the relevance of ligand dependency for tumor formation *in vivo*. To this end, we applied an adenovirus (AdsFGFR virus) expressing a soluble protein, which includes the extracellular domain of an FGF-receptor fused to an immunoglobulin heavy chain. This construct competes with cellular FGFRs for FGF ligands and served as a "FGF trap" (Celli et al., 1998). We subcutaneously injected the virus together with *FGFR1*-amplified H1581 cells or Kras-mutant A549 controls (Figure 17). Within twelve weeks, the AdsFGFR adenoviral infection inhibited tumor formation of H1581 cells but not of A549 cells. Infection with the control adenovirus had no impact on tumor growth (Figure 17). In contrast to the empty vector infection, AdsFGFR infected mice showed as expected delayed weight increase in both groups (H1581, $p = 0.04$ and A549, $p = 0.012$) (Beenken and Mohammadi, 2009). Furthermore, an adenovirus-specific PCR from fixed liver tissue confirmed efficiency of viral infection.

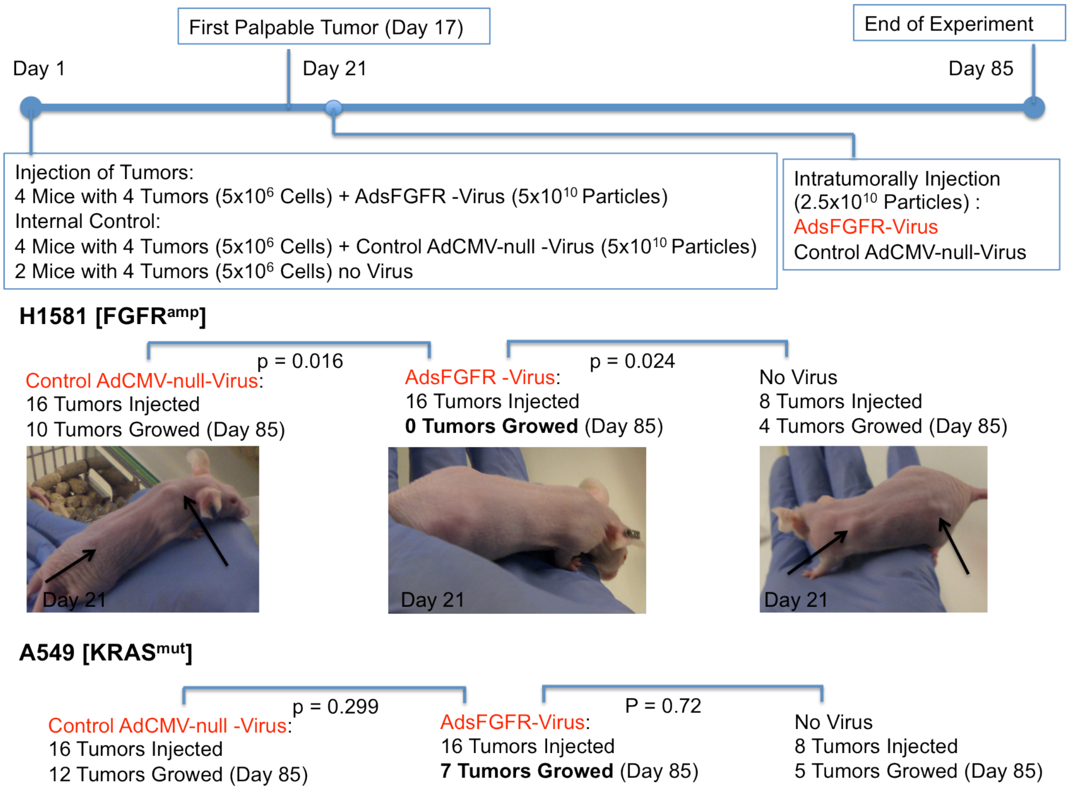
First Palpable Tumor (Day 17)
End of Experiment
Day 1
Day 21
Day 85
Injection of Tumors:
4 Mice with 4 Tumors (5x10⁶ Cells) + AdsFGFR -Virus (5x10¹⁰ Particles)
Internal Control:
4 Mice with 4 Tumors (5x10⁶ Cells) + Control AdCMV-null -Virus (5x10¹⁰ Particles)
2 Mice with 4 Tumors (5x10⁶ Cells) no Virus
Intratumorally Injection
(2.5x10¹⁰ Particles) :
AdsFGFR-Virus
Control AdCMV-null-Virus
H1581 [FGFRamp]
p = 0.016
p = 0.024
Control AdCMV-null-Virus:
16 Tumors Injected
10 Tumors Growed (Day 85)
AdsFGFR -Virus:
16 Tumors Injected
0 Tumors Growed (Day 85)
No Virus
8 Tumors Injected
4 Tumors Growed (Day 85)
Day 21
Day 21
Day 21
A549 [KRASmut]
p = 0.299
P = 0.72
Control AdCMV-null -Virus:
16 Tumors Injected
12 Tumors Growed (Day 85)
AdsFGFR-Virus:
16 Tumors Injected
7 Tumors Growed (Day 85)
No Virus
8 Tumors Injected
5 Tumors Growed (Day 85)

Figure 17: Tumor formation under depleted FGF conditions. Time schedule of the FGF-Trap experiment (top), with H1581 tumors (middle) and A549 (bottom). Mice were exposed to either control virus (AdCMV-null, left), FGF-trapping virus (AdsFGFR, middle), or noninfectious supernatants (right). Significant values were derived from the fisher's exact test. Experiment was done with support of Felix Dietlein, University of Cologne, Germany.

In summary, these results provide evidence that *FGFR1*-amplified and inhibitor-sensitive H1581 cells depend on FGF ligands *in vivo*.

5.6 FGF Signaling is Saturated in *FGFR1*-amplified Lung Cancer Cells

In order to determine if abundant supply of FGF ligands is beneficial for cell growth, we tested if external addition of FGF2 or 4 leads to increased cell proliferation. Therefore we stimulated four cell lines with externally added Heparin plus FGFs. Remarkably, constitutive activation of FGFR signaling by high dose FGF stimulation (10 ng/ml) did neither enhance proliferation of the

FGFR1-amplified cell lines H1581 and H520 nor influence growth of the HCC15 and PC9 control cell lines (Figure 18).

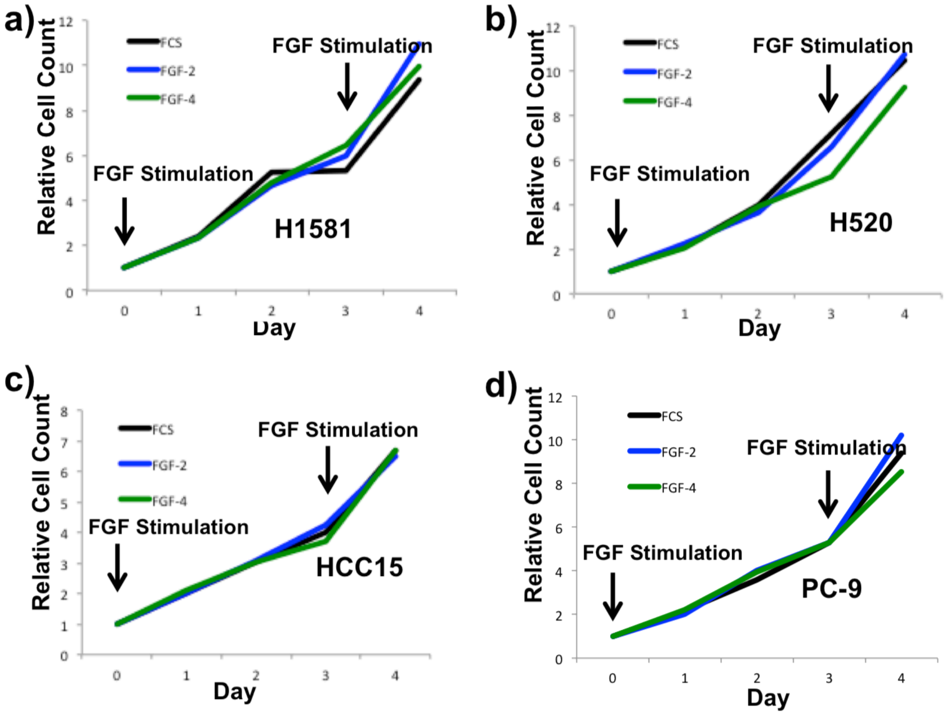

Figure 18: Constitutive activation of receptor signaling does not accelerate proliferation rate of *FGFR1*-amplified cells. a) H1581 [FGFR1amp], b) H520 [FGFR1amp], c) HCC15 [FGFR1del], d) PC-9 [EGFRmut] Cells were plated at low density and stimulated by heparin (10 µg/ml) and high doses of FGF-2 and FGF-4 (each: 10ng/ml), respectively, on day 0 and day 3. Average values normalized to day 0 are shown as growth curves.

This observation is in marked contrast to EGFR driven tumor cells, which clearly benefit from overdosed external ligand supply (Greulich et al., 2005).

Summarizing the results, FGF stimulation seems to be necessary for FGFR1 transformation while overstimulation through FGFs has no beneficial impact on cell proliferation. Thus, the FGFR signaling is saturated in *FGFR1*-amplified cells.

5.7 Identification of FGFR1 Splice Variants Expressed in 8p12-Amplified Tumors

The *FGFR1* gene is known to encode several splice variants (Beenken and Mohammadi, 2009; Turner and Grose, 2010).

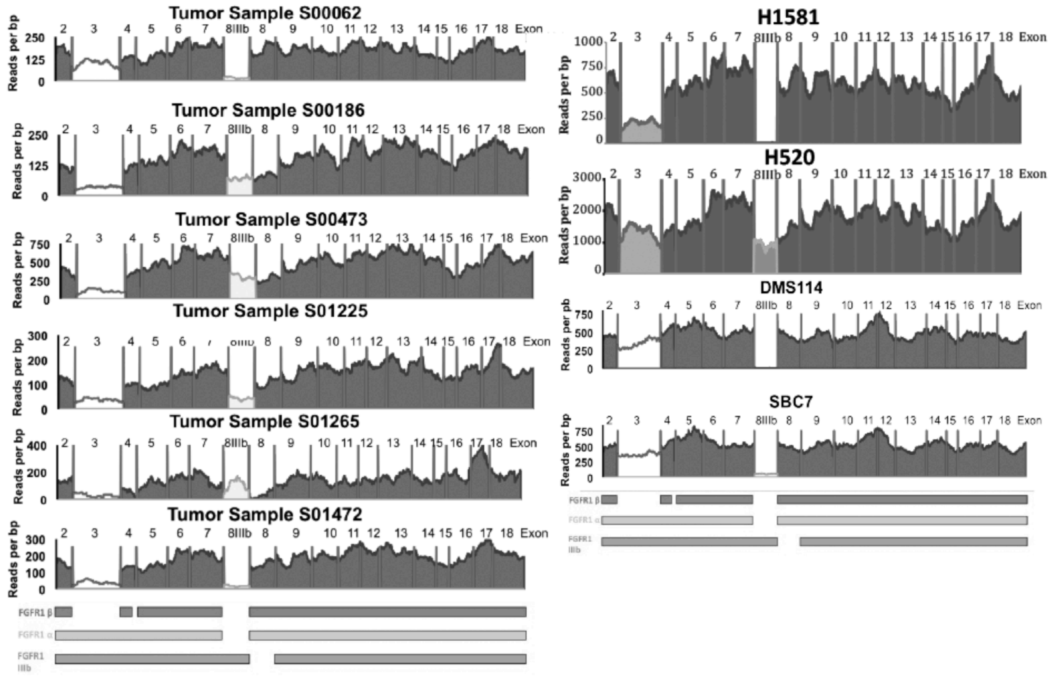

Figure 19: Whole transcriptome analysis demonstrates alternative FGFR1 splicing for amplified tumor samples. Collection of 6 Patient Samples (left) and four cell lines (right) with low coverage of exon 8 (IIIb) suggests dominance of mesenchymal IIIc splice variants, whereas small read density on exon 3 indicates dominance of IIIc-β variants. Coverage is highly affected by GC content. Analysis was developed and supported by Felix Dietlein, University of Cologne, Germany.

Whole transcriptome sequencing (RNAseq) of six SCC primary tumors and four lung cancer cell lines revealed that mesenchymal FGFR1-IIIc splice variants were most commonly expressed with a prevalence of approximately 75% (Figure 19). Alternative splicing of FGFR1-IIIc results in two isoforms: FGFR1-IIIc-α and FGFR1-IIIc-β. These two isoforms differ in their Ig1 domain, where FGFR1β, the most common variant, has a truncated Ig1 domain lacking exon 3 (Figure 19). In contrast to that, epithelial FGFR1 splice variants, such as FGFR1-IIIb, are less abundant (prevalence lower than 25%) and absent in the FGFR inhibitor-sensitive cell lines H1581 and DMS114 (Figure 19 and 20).

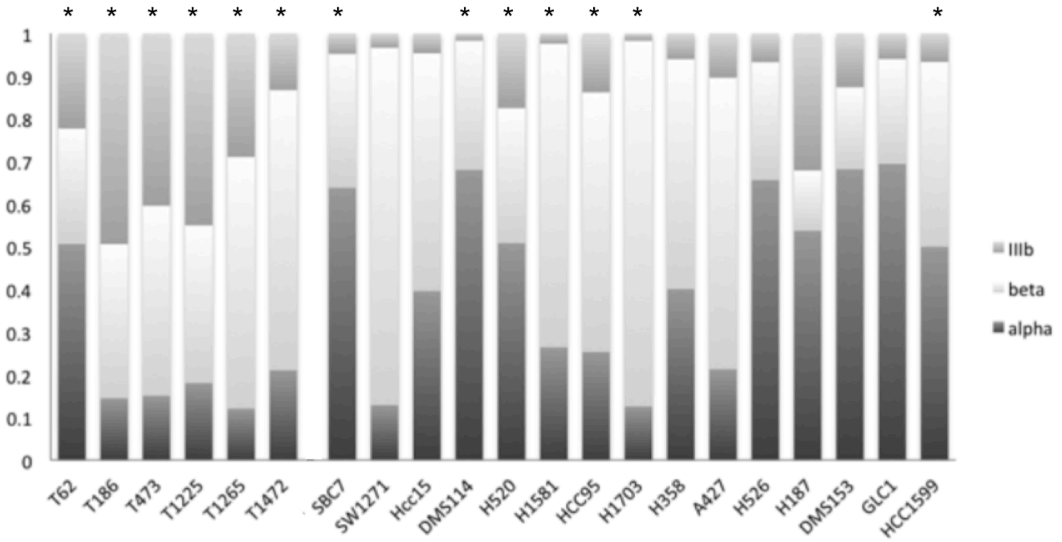

Figure 20: Validation of alternative FGFR1 splicing by real time PCR. Frequency (y-aches in %) of FGFR1 splice variants in a panel of 6 patient samples and 15 lung cancer cell lines (x-aches) were validated. *FGFR1*-amplified samples are indicated (*). Quantitative real time PCR for detection of alternative FGFR1 splice variants was performed using 12 FGFR1-specific primer pairs. Relative expression was derived by ΔΔC_t method.

Real-time PCR (RT-PCR) confirmed the identified splice variants. Furthermore, we analyzed the occurrence of the FGFR1 isoforms in 15 other cancer cell lines (Figure 20). Thereby we found, that mesenchymal splice variants of FGFR1 were also predominantly expressed in FGFR inhibitor-resistant cell lines like H1703.

Altogether, FGFR1 mesenchymal splice variants are commonly expressed isoforms in *FGFR1*-amplified cell lines. However, quantification of mesenchymal splice variant expression is not sufficient for FGFR inhibitor-sensitivity prediction.

5.8 *MYC* Induced Transformation Supported by Oncogenic FGFR1 Expression

We analyzed the oncogenicity of overexpressed wild-type mesenchymal FGFR1 in soft agar assays. Therefore, we cloned the coding sequences of FGFR1-IIIc-α and β variants from H1581 cells. They were ectopically expressed in NIH3T3 cells alone or in combination with six genes that are found in or close to recurrent amplicons in squamous-cell lung cancer (*REL*, *SOX2*, *MYC*, *CCND1*, *DYRK1B*, *AKT2*). The expression was confirmed by RT-PCR (Figure 21).

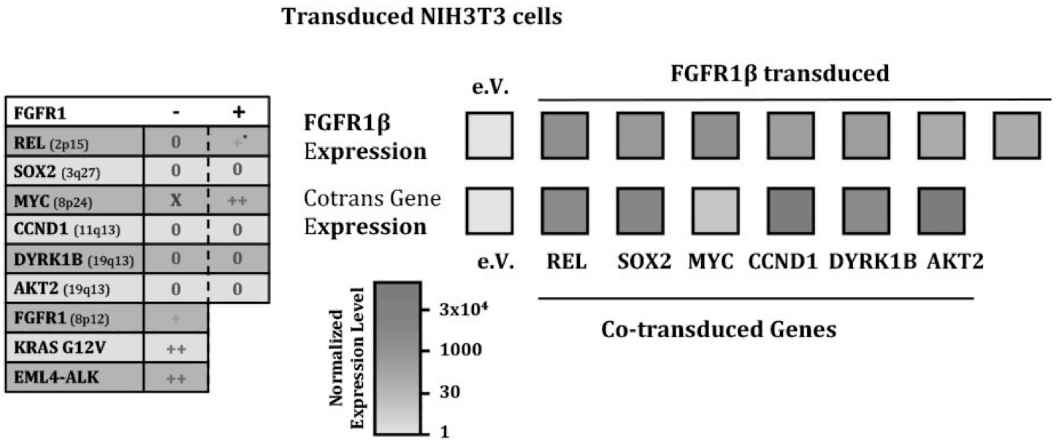

FGFR1	-	+
REL (2p15)	0	+*
SOX2 (3q27)	0	0
MYC (8p24)	X	++
CCND1 (11q13)	0	0
DYRK1B (19q13)	0	0
AKT2 (19q13)	0	0
FGFR1 (8p12)	+	
KRAS G12V	++	
EML4-ALK	++	

Figure 21: Colony formation experiments indicate oncogenic properties of *FGFR1* and its supporting role for *MYC* transformation. NIH3T3 cells were retrovirally (pBabe) (co)-transduced with *FGFR1* and eight further cancer genes. Colony formation in 21-day soft agar assay was compared to empty vector controls by Benjamini-Hochberg corrected t-testing and classified into strong (++), mild (+; < 10 colonies per well) and no (0) transformation. NIH3T3 cells did not survive transduction with *MYC* alone (X). * Benjamini-Hochberg correction is not significant. Validation of gene expression was done by quantitative real time PCR (right). Color intensities indicate expression levels in transduced NIH3T3 cells as assessed by quantitative real time PCR specific for *FGFR1* or the genes annotated below. For each gene, three independent primer pairs were used.

NIH3T3 cells transformed with FGFR1-IIIc formed few but significant numbers of colonies ($p<0.0001$). *MYC* transduced NIH3T3 cells showed an apoptotic phenotype, indicating that high MYC expression cannot be tolerated in these cells. The other genes were not able to transform 3T3s (Figure 21).

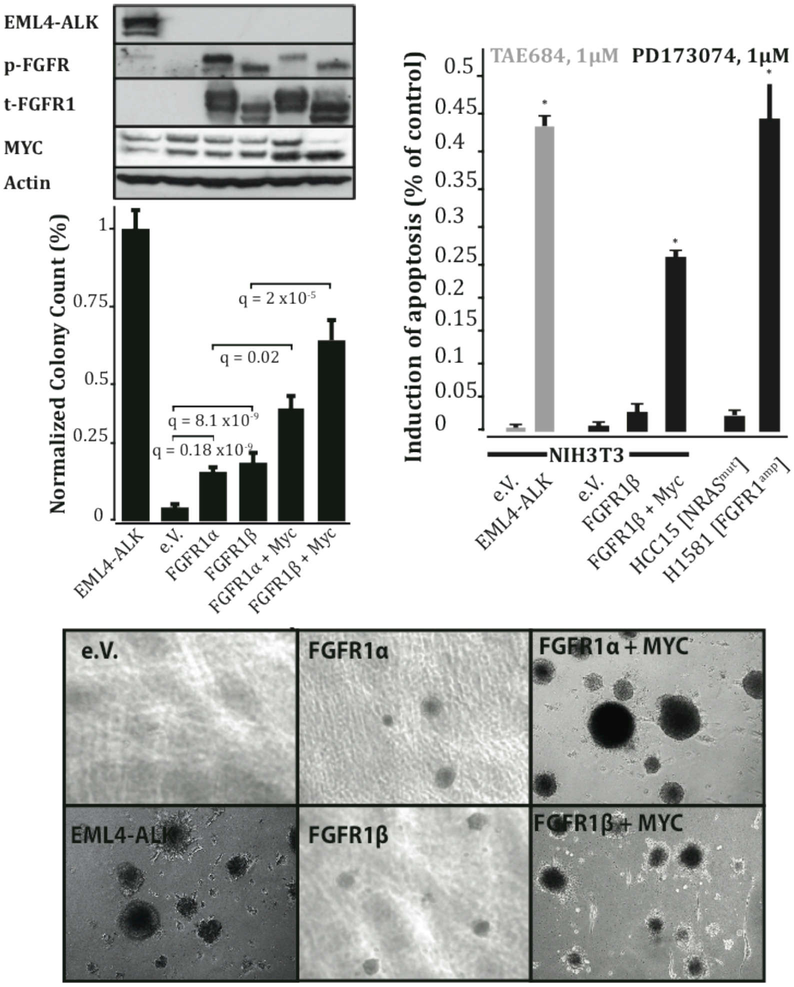

Figure 22: Protein expression and phosphorylation of transduced NIH3T3 cells were analyzed by immunoblotting (top left). Mesenchymal FGFR1α (full length) can be differentiated from FGFR1β by protein size. Relative colony counts of 21-day soft agar assay were compared by Benjamini-Hochberg corrected t-testing. Error bars display standard deviation of average counts of three independent experiments. Induction of apoptosis (Annexin-V/PI, flow cytometry) in NIH3T3 cells (top right), (co-) transduced with FGFR1β ± MYC, by 72-hour FGFR inhibition (PD173074 ,1µM). FGFR-dependent H1581 cells (PD173074, 1µM) as well as ALK-dependent NIH3T3-EML4-ALK cells (TAE684, 1µM) were used as positive controls. Resistant HCC15 and NIH3T3-e.V. cells served as negative controls. * Significant induction of apoptosis ($p<0.01$). Representative pictures of the NIH3T3 colony formation experiment (bottom).

However, co-expression of *FGFR1* and *MYC* resulted in colony formation in soft agar amounting to bigger size and higher number. This result implies synergistic effects of FGFR1 and MYC on colony formation in soft agar (Figure 22). Similar to FGFR1-dependent H1581 cells (Weiss et al., 2010), treatment with the FGFR inhibitor PD173074 induced apoptosis in NIH3T3 FGFR1 – MYC co-transduced cells, but not in cells expressing FGFR1 alone (Figure 22).

Thus, *FGFR1*-amplified cells co-expressing MYC may be more susceptible to FGFR inhibition, which has been similarly reported for FGFR2 mutations in breast cancer (Ota et al., 2009).

5.9 Initiation of Tumor Formation by FGFR1

We next tested if FGFR1 overexpression is able to drive tumor formation in xenograft mouse models. Injection of NIH3T3 cells expressing FGFR1-IIIc-α and –β induced tumors after a median of 20 days in vivo. Intravenous injection of NIH3T3 FGFR1α cells led to tumor growth in the lung (Figure 23). Similarly, injection of FGFR1α transduced Hek293T cells into nude mice formed palpable subcutaneous tumors within 20 days (Figure 23). This was entirely dependent on the *FGFR1* oncogene, since we disabled tumor growth through treatment with BGJ398, a highly specific FGFR inhibitor (Figure 24). Of note, treatment of tumors co-expressing FGFR1 and MYC led to significant regression of the tumors. This was in line with our previous observation, that NIH3T3 cells are sensitized for FGFR inhibition if FGFR1 and MYC are co-expressed (Figure 22).

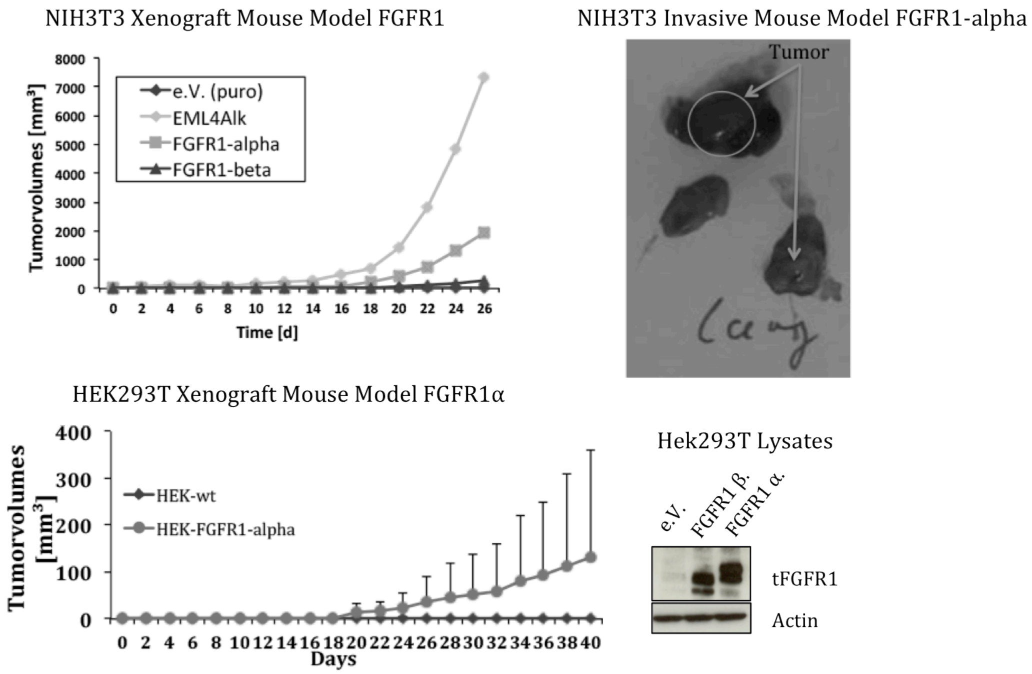

Figure 23: Nude mice, engrafted with retrovirally transduced empty vector, EML4-Alk, FGFR1α or FGFR1β NIH3T3 cells form palpable tumors after 20 days (top left). No tumor formation was observed for empty vector transduced NIH3T3 cells. Nude mice with intravenous injected FGFR1α cells form tumors in the lung (top right). Nude mice were subcutaneously engrafted with wild type Hek293T cells and retrovirally transduced HEK-FGFR1α cells (bottom left). Protein expression of transduced cells was analyzed by immunoblotting (bottom right). Experiments were supported by Jakob Schöttle, University of Cologne, Germany.

Interestingly, mouse tumors generated from NIH3T3 cells expressing FGFR1 alone exhibited some nuclear expression of MYC as well ($p < 0.001$) (Figure 24). Nevertheless, MYC was expressed at much higher nuclear levels in the double-transduced cells. In contrast, mouse tumors generated from NIH3T3 cells expressing EML4-Alk or K-Ras-G12V proteins were neither sensitive to FGFR inhibitors, nor expressed elevated levels of MYC (Figure 24).

In conclusion, FGFR1-expressing tumors upregulate MYC in vivo, but only very high levels of MYC expression sensitize cells to FGFR inhibition.

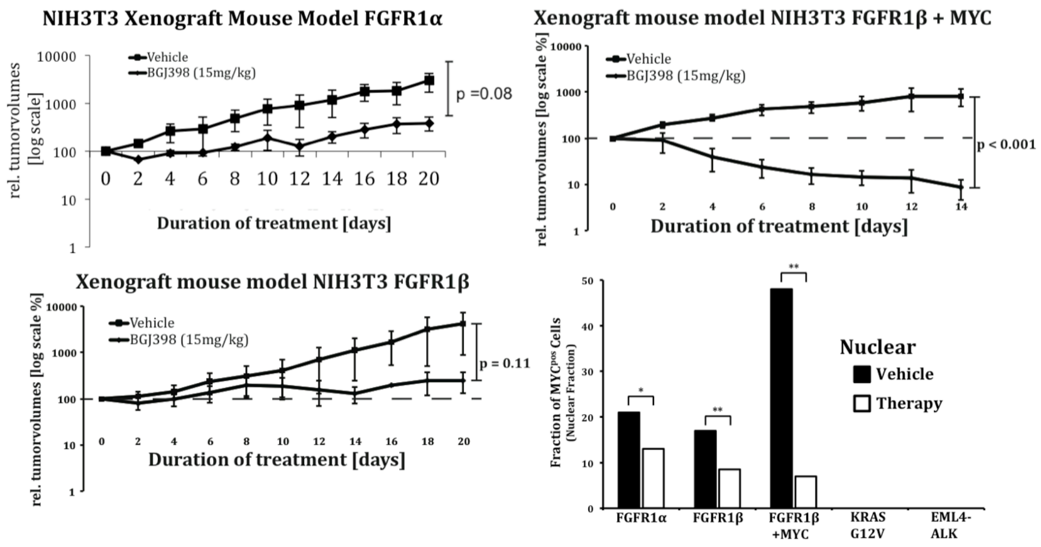

Figure 24: Nude mice, engrafted with retrovirally transduced NIH3T3 cells, received BGJ398 (15 mg/kg, q.d., lower curve) or 5% glucose (upper curve), respectively, upon formation of palpable tumors. Volumes of tumors formed by NIH3T3-FGFR1α (top left), NIH3T3-FGFR1β cells (bottom left) and NIH3T3-FGFR1β-MYC cells (top right) were assessed every second day and compared by t-testing. Error bars display standard deviation of three independent experiments. Tumors explanted from mice were examined for MYC expression by immunohistochemistry prior (black) and post (white) therapy (bottom right). Average fractions of cells, which display positive MYC stains in their nucleus, are shown as bar plot. At least 1,000 tumor cells in 10 independent fields were counted for each sample. Significant (*; p<0.05) and strongly significant (; p<0.01) differences are marked by asterisks. Experiments were supported by Jakob Schöttle, University of Cologne, Germany.**

5.10 Regulation of MYC in FGFR1-Depended Cell Lines

Based on the observation that MYC was found to be involved in the NIH3T3-FGFR1 tumor formation model, the question arose, whether MYC regulation is a common mechanism in FGFR1-dependent cell lines. Therefore, we performed immunoblotting using the FGFR inhibitor sensitive cell lines H1581 and DMS114, treated for 2, 8, 16 and 24 hours with the FGFR inhibitor PD173074. As expected, treatment interrupted ERK signaling (Weiss et al., 2010). Treatment with 1µM of inhibitor led to a continuous reduction of total MYC protein (Figure 25). Furthermore, we found protein reduction of MYC regulated genes, such as Cyclin D1.

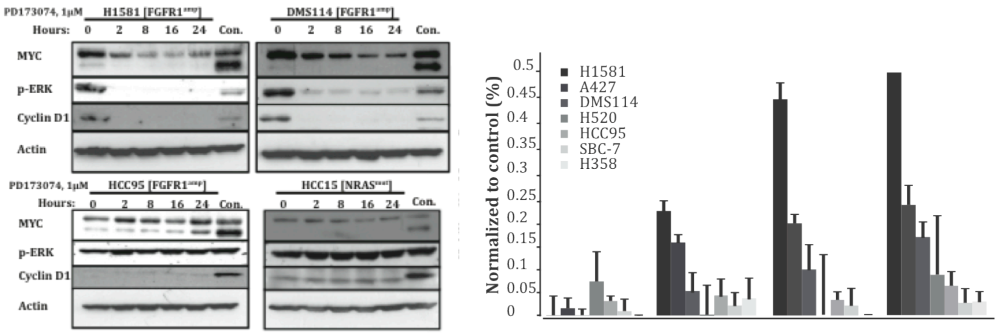

Figure 25: Protein expression levels of MYC and Cyclin D1 are regulated by FGFR signaling in PD173074 sensitive cell lines. Two FGFR1-amplified, inhibitor sensitive cell lines (H1581 and DMS114; IC50 < 500 nM), one FGFR1-amplified, insensitive cell line (HCC95; IC50 > 5 µM) and one control (NIH3T3-FGFR1β-MYC cells) were treated with the FGFR inhibitor PD173074 for 0, 2, 8, 16 and 24 hours, respectively (left). Expression levels of MYC, Cyclin D1 and ERK phosphorylation were analyzed by immunoblotting. A panel of seven cell lines was treated with PD173074 (1 µM) and DMSO for 24, 48, 72 and 96 hours, respectively. Breakdown of mitochondrial potential was examined by comparison of JC-1 stains flow cytometrically (right).

By contrast, protein levels remained relatively stable in both *FGFR1*-amplified HCC95 cells, which are resistant to FGFR inhibition (Weiss et al., 2010) and in the NRAS mutant HCC15 cells. Measuring the mitochondrial membrane potential using JC-1 flow cytomentry imaging, FGRF1 inhibition resulted in apoptosis. This was only detectable after 48 hours of treatment, indicating that the induced apoptotic mechanism is of slow kinetics (Figure 25).

We found that FGFR inhibition affected MYC and its downstream-regulated genes in FGFR1-dependent cells. Bearing in mind the slow and unspecific kinetics of apoptosis, the data is compatible with an involvement of MYC in apoptotic signaling (Soucie et al., 2001).

5.11 Prediction of FGFR Inhibitor Sensitivity by FGFR1 and MYC Expression

The NIH3T3 soft agar and xenograft experiment indicated the mutual influence of FGFR1 and MYC (Figure 22 and 24). FGFR1-dependent cell lines substantiated these results (Figure 25). In order to evaluate the significance of given observations, we preformed RT-PCR quantification of FGFR1 and MYC expression in seven *FGFR1*-amplified, three *FGFR1* copy neutral and four *FGFR1* deleted cancer cell lines (n=14).

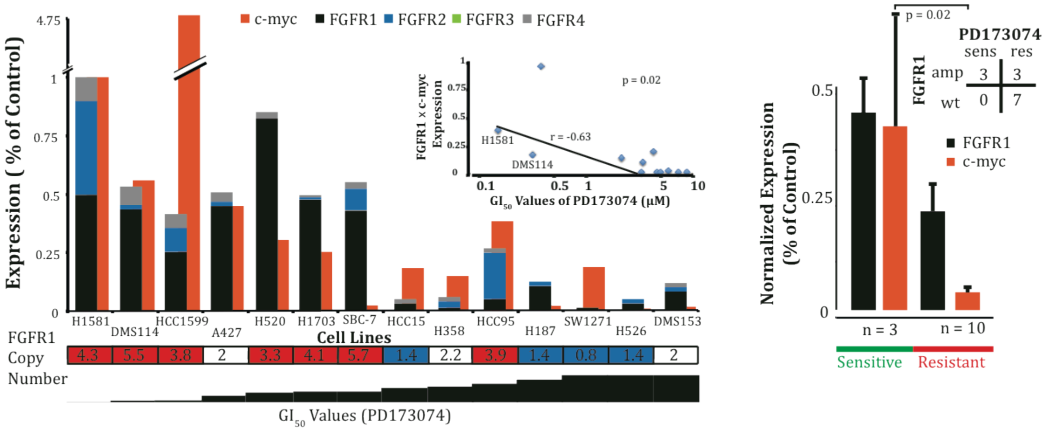

Figure 26: Relative RNA expression levels of FGFR1-4 (black to grey) and MYC (light grey) in a cohort of 14 cancer cell lines enriched for FGFR1 amplification (left). Correlation of FGFR dependency and FGFR1 x MYC expression levels (inset). Significance of correlation was derived from Student t distribution. Segregation of FGFR1 amplification with RNA expression-levels of MYC (right). Cancer cell lines were divided into an FGFR-dependent (H1581, DMS114, and HCC1599) GI 50 < 500 nM, PD173074) versus FGFR-resistant group (A427, H520, H1703, HCC15, H358, HCC95, H187, SW1271, H526, and DMS153 cells). Expression levels were compared by the student t test.

In order to assess potential influence of other FGFR members, we furthermore analyzed all cell lines for FGFR2, 3 and 4 expression (Figure 26). We detected sensitivity to the FGFR inhibitor only in samples where high levels of FGFR1 correlated with elevated MYC expression (p = 0.02). Thus, measuring amplification of *FGFR1* in combination with MYC expression predicts FGFR1 dependency (Figure 26).

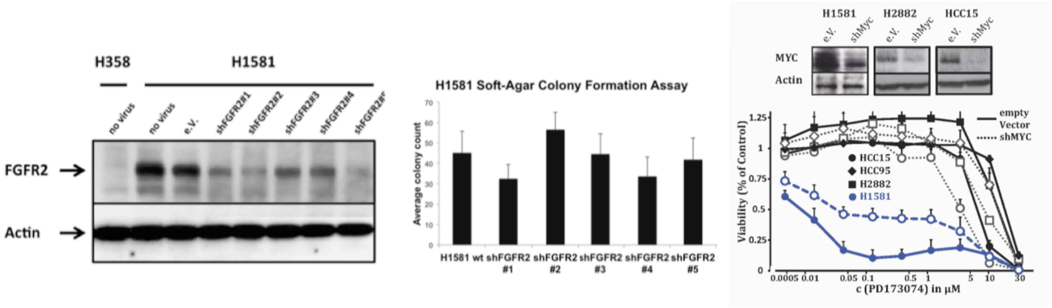

Figure 27: Silencing of FGFR2 preserves the transforming phenotype of H1581 cells. Immunoblot analysis of FGFR2 expression after stable lentiviral transduction of H1581 cells with 5 independent FGFR2 hairpin constructs (left). Relative colony numbers of H1581-shFGFR2 cells in soft agar assay (middle). Protein expression of MYC was silenced by stable lentiviral transduction of FGFR1 dependent H1581 cells and HCC15, H2882, HCC95 controls (right). Knockdown efficiency was validated by immunoblotting for H1581, H2882, and HCC15 cells (inset). FGFR dependency was determined by measuring cellular ATP content after 96 hours (bottom right).

FGFR 2, 3 and 4 were not abundantly expressed in the analyzed cell lines. Only H1581 and HCC95 expressed FGFR2 exceedingly. However, silencing of FGFR2 in H1581 cells did neither lead to an impaired growth pattern nor did it affect the cellular phenotype of colony formation in soft agar (Figure 27). On the contrary, silencing FGFR1 expression in H1581 cells is lethal (Weiss et al., 2010). Stable repression of MYC expression in H1581 cells by lentiviral MYC short-hairpin DNAs did not influence cell viability, but resulted in FGFR inhibitor resistance (Figure 27). Unfortunately, DMS114 cells did not tolerate MYC knock down.

Altogether, multiple approaches highlighted the interplay of FGFR1 and MYC in context of oncogenicity. MYC expression may thus be evaluated as a clinical marker to predict FGFR inhibitor sensitivity in *FGFR1*-amplified tumors.

5.12 FGFR1 and MYC Expression in Primary 8p12-Amplified Lung Tumors

In order to assess the cellular expression pattern of FGFR1, we conducted immunohistochemistry (IHC) staining of primary lung tumors. We screened a large cohort of 306 squamous cell lung cancer biopsies for the presence of *FGFR1* amplification using FISH (Schildhaus et al., 2012). Alexandra Florin mainly did the IHC and Lukas C. Heukamp supported the analysis of data.

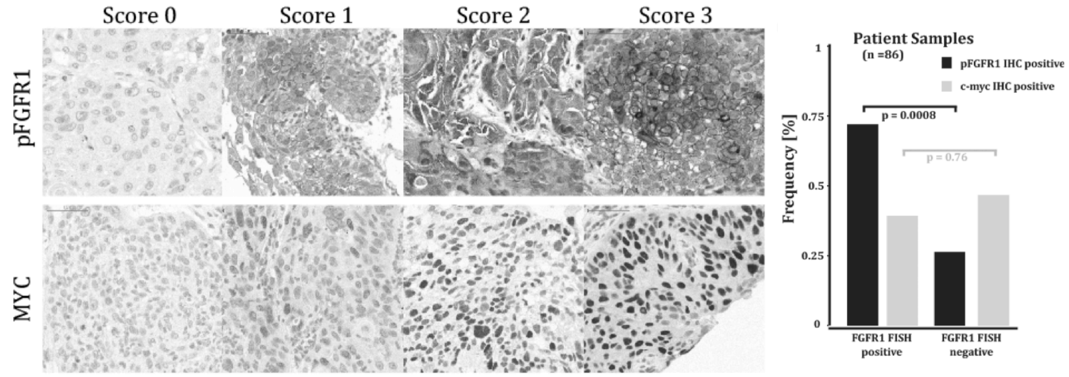

Figure 28: MYC expression in primary *FGFR1*-amplified squamous cell lung carcinomas. Phospho-FGFR (top left) and MYC (bottom left) IHC stains were scored from 0 to 3. A representative sample is shown for each score. Enrichment of FGFR1 phosphorylation, independent of MYC expression in a cohort of 86 *FGFR1*-amplified lung cancer patients (right). Tumor biopsies were analyzed by FGFR1 FISH and stained for MYC expression as well as FGFR1 phosphorylation. Frequencies of positive stains were compared by Fisher's exact test. Experiments were supported by Alexandra Florin and Lukas Heukamp, Institute of Pathology, University of Cologne, Germany.

We further analyzed a group of 86 samples of this cohort, which was enriched for *FGFR1*-amplified samples (78%), for FGFR1 phosphorylation and high MYC expression. We grouped the phosphorylation and expression pattern of FGFR1 and MYC in 4 different scores (0-3) (Figure 28). Phosphorylated FGFR1 was predominantly expressed along the plasma membrane, shown by a phospho-specific FGFR1 antibody. Furthermore, 8p12-amplified tumors significantly and constitutively phosphorylated FGFR1 (score 2 or 3; p=0.0008) (Figure 28). However, the heterogenic 8p12 amplification event and the poor specificity of *FGFR1* FISH might explain why only 74% of amplified cases present high levels of FGFR1 phosphorylation. High nuclear MYC levels did not segregate with amplification status of 8p12 (p=0.76). In line with this observation, RNAseq data from primary tumors revealed high MYC expression, only if the 8p12 amplification event was centered on *FGFR1* (Figure 29).

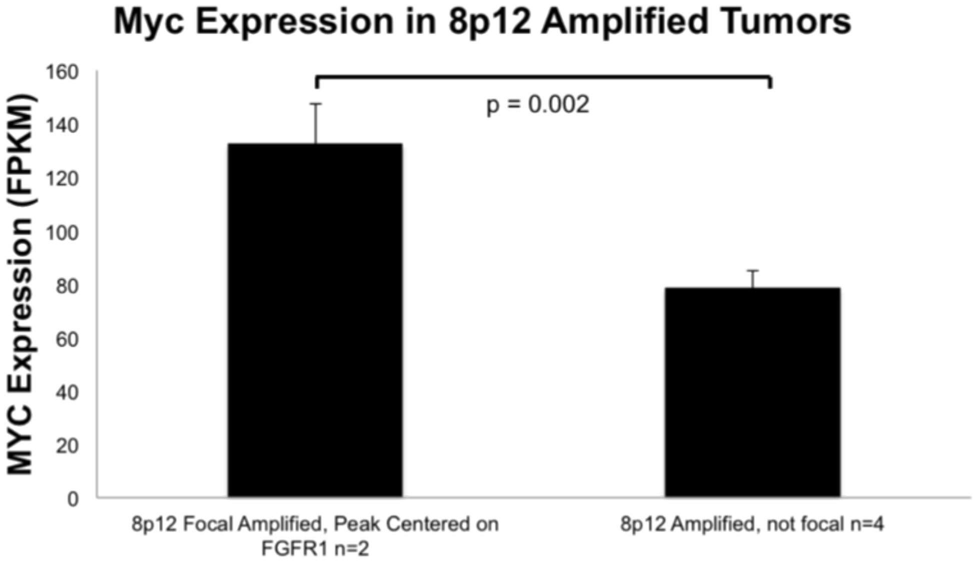

Figure 29: MYC expression is upregulated in centrally *FGFR1*-amplified tumor samples. Average FPKM-normalized (whole transcriptome sequencing) values of MYC expression were compared by t-test. Error bars display standard deviation within the respective groups.

Thus, most *FGFR1*-amplified squamous cell lung cancers exhibited phosphorylated FGFR1. Only a fraction of these cases also showed nuclear MYC expression. Therefore it is likely that only a minority of *FGFR1*-amplified lung tumors respond to FGFR inhibition (Andre et al., 2013, Sequist et al., 2014).

5.13 Clinical Case

Preliminary data from clinical trials including patients with progressive disease in spite of FISH confirmed *FGFR1* (8p12) amplification have shown that the efficacy of FGFR inhibition in lung cancer is inconsistent (Andre et al., 2013, Sequist et al., 2014). This observation is consistent with the finding, that only a minority of *FGFR1*-amplified lung tumors are likely to respond to FGFR inhibition.

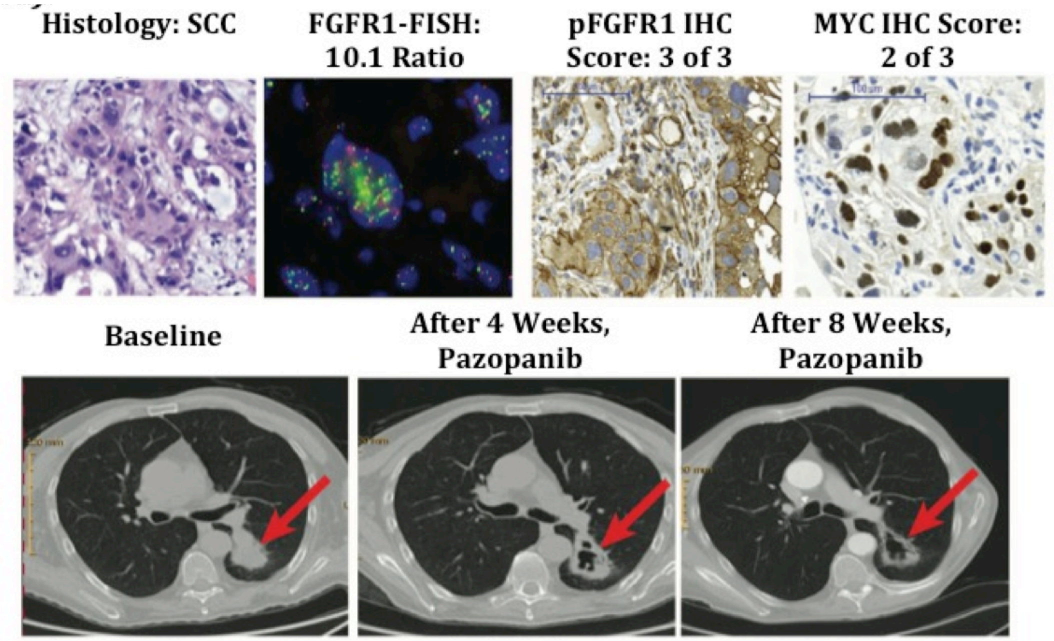

Figure 30: Pathological examination of a tumor biopsy of the pazopanib responder before therapy. After SCC diagnosis (top left), the sample was scored by FGFR1 FISH (top left middle) , phospho-FGFR1 IHC (top right middle) as well as nuclear staining of MYC IHC (top right). Dual colour FISH was performed with *FGFR1* (green) and CEN8 (red) probes in order to derive a normalized copy number ratio for *FGFR1* amplification. Baseline computer tomographic (CT) scan with tumor in the left lung (bottom left); CT after 4 weeks (bottom middle) and 8 weeks (bottom right) of pazopanib, showing tumor regression with cavitation. Arrows highlight target lesions for evaluation of tumor response. Acquisition and interpretation of data was supported by Oliver Gautschi and Joachim Diebold, Medical Oncology, Cantonal Hospital, Switzerland.

We detected clinical evidence of *FGFR1* dependency based on 8p12 amplification in combination with high MYC expression (Figure 30). We identified a 79 year old man, who was referred to the medical oncology institution of the cantonal hospital Luzern with a mass in the right shoulder. The patient showed a tumor in the left lung and metastasis in the right deltoid muscle found by combined 18F-Fluordesoxyglucose Positron-Emissions-

Tomography and computer tomography (FDG-PET/CT). He was a former smoker with a history of superficial urinary bladder carcinoma. After biopsy he was diagnosed with stage M1b metastatic squamous cell lung cancer (Figure 30). Sequencing of *DDR2* exon 18, *PIK3CA* exon 10 and 21, and *PTEN* exon 7 was negative (Hammerman et al., 2011; Janku et al., 2013; Sos et al., 2009a). Fluorescent in situ hybridization (FISH) of *FGFR1* revealed high-level 8p12 amplification with an average of 10.1 signals per cell and high MYC expression with a score of 2 (Figure 30). The patient refused chemotherapy, but consented to a combined therapy with pazopanib off-label use (Hurwitz et al., 2009; Kumar et al., 2009) and analgesic radiotherapy to the right shoulder. After cardiac assessment and baseline thoracic CT, treatment with pazopanib 800 mg per day was started. Four and eight weeks after the start of the therapy, CT showed tumor regression with cavitation (Figure 30). Pazopanib had moderate gastrointestinal side effects. Therefore, after 4 weeks the dose was reduced to 400 mg per day. Because of further grade 2 fatigue and stomatitis side effects, the patient decided to stop pazopanib after 6 months. At that time, no clinical or radiologic signs of tumor progression were present. Of note, the inhibitory profile of pazopanib and the pseudocavernous response are compatible with a predominant antiangiogenic effect. However, in light of the preclinical findings, we speculate that the patient response might also be attributable to FGFR inhibition in the context of a MYC-expressing *FGFR1* -amplified lung cancer.

6 Discussion

This is the first genetic study describing molecular mechanisms underlying FGFR1-dependency in lung cancers with amplification of 8p12. We identified an important role for a complex interplay of cofactors, genetic alterations, receptor splice variants and extracellular ligands in FGFR1-driven tumors. Furthermore, frequent 8p12 amplification in squamous cell lung cancer (SCC) is markedly heterogenic and occurs during broad genome breakpoint events. In approximately 25% of these cases *FGFR1* is the likely oncogenic driver. Thus, in approximately 75% of 8p12 amplification events the role of *FGFR1* is unclear at least. Therefore other genes might be more important for oncogenic transformation. It is likely that *BRF2*, *NRG1* or *WHSC1L1* are other important players in the 8p12 amplicon (Fernandez-Cuesta et al., 2014; Lockwood et al., 2010; Travis et al., 2011). Therefore the 8p12 amplification event possibly has multiple functions for tumor formation and has to be studied in much more detail. One should bear in mind that most 8p12-amplified tumors express FGFR1. Furthermore, FGFR kinase domains are conserved and therefore kinases inhibitors are hardly able to distinguish among the FGFR family. Consequently, antibodies targeting the extracellular FGFR1 domain could substitute unspecific kinase inhibition. This would possibly enhance efficacy and reduce undesirable clinical side effects. Likewise, a specific FGFR2-IIIb antibody therapy has been established for *FGFR2*-amplified breast and gastric cancer (Bai et al., 2010).

The present study and others demonstrate that the tested FGF panel is representative to explain that FGFR1 predominantly activates the MAPK pathway upon extracellular stimulation (Gartside et al., 2009; Tomlinson and Knowles, 2010; Xu, 1996). As FGF1 is a pan-FGFR activator it was concluded that FGF2 and 4 are most specific for the FGFR1 signaling pathway. This observation is similarly described in the literature (Mason, 2007). The ligand-receptor interaction occurs predominantly at the extracellular immunoglobulin domains Ig2, Ig3 and at the junction domain Ig2-Ig3 (Plotnikov et al., 2000). The latter is highly conserved between the different

FGF-Receptors (Beenken and Mohammadi, 2009). Of note, almost all receptor variants have a pronounced autoinhibitory Ig1-loop and an acid box. These functional domains are likely to play a role in blocking spontaneous activation of the receptor in the absence of its ligand (Kalinina et al., 2012). However, we identified predominantly expressed splice variants from 8p12-amplified cell lines and primary tumors but we were unable to correlate FGFR1 splicing and FGFR1 dependency. Moreover, autocrine/paracrine FGF secretion was related to FGFR-inhibitor response rates in cell lines. The importance of FGFs for FGFR1 dependent transformation, shown by multiple approaches, indicates ligand induced FGFR1 activation. This observation is in marked contrast to *ErbB2* amplification in breast cancer where spontaneous dimerization and activation of downstream signaling is described (Harari and Yarden, 2000). These results raise the possibility that FGFs could be actionable targets for both diagnostics and therapy.

The oncogenic property of *FGFR1* is highly complex and not comprehensively described as it is e.g. for *EGFR* (Sharma et al., 2007). We were able to prove oncogenic characteristics of overexpressed mesenchymal FGFR1 splice variants, which are expressed by 8p12-amplified tumors. However, expression of *FGFR1* alone in NIH3T3 cells was not sufficient to promote FGFR1 dependency and full-blown transformation. Likewise, FGFR1 phosphorylation was found in a representative group of *FGFR1*-amplified primary tumors (n=86, p<0,002) but not sufficient to predict FGFR1-addiction. Signaling into the MAPK pathway via FRS2 could be one critical key point, because of the negative feedback loop of MAPK on FRS2 (Lax et al., 2002). Hence, *FGFR1* amplification defines an important first step towards precancerous lesions, but does probably not convey ultimate oncogenic advantage. Yet, it was shown that only co-expression of *MYC* significantly enhanced oncogenic properties and predicts *FGFR1* dependency. Furthermore, the role of high-level MYC expression to mediate FGFR-dependency was further strengthened by clinical observation of a patient with *FGFR1*-amplified and highly MYC-expressing squamous-cell lung cancer, who responded to the multi-kinase inhibitor pazopanib (Hurwitz et al., 2009; Kumar et al., 2009). Therefore, MYC expression status itself leads to a clinically assessable marker for therapy response prediction. In spite of clinical trials, these findings explain the equivocal results using FGFR inhibitors and may define a subgroup of lung cancer patients who benefit from FGFR inhibition (Andre et al., 2013, Sequist et al., 2014). Finally, as FGFR1 resistance could be induced by MYC knockdown in vitro, negative regulatory mechanisms of MYC are a potential form of acquired resistance.

Altogether, different entities and etiologies of 8p12-amplified tumors explain why only a selected subset of *FGFR1*-amplified lung cancer patients profit from a direct FGFR kinase inhibition. We hope that our findings help to select patients who clearly benefit from treatment with FGFR inhibitors.

7 Summary

Globally lung cancer accounts for million deaths per year and squamous-cell carcinoma (SCC) reports for 15-25% of all lung cancers. SCC is most strongly associated with cigarette smoking and has a lag for targeted cancer therapy. Current advances in genome characterization and sequencing technologies have enabled systematic efforts to characterize complex genomic alterations, mutations, genomic rearrangements and copy number alterations of SCC suggesting potential therapeutic strategies. The fibroblast growth factor receptor 1 gene (*FGFR1*) is located within the 8p12 locus and is one of the most common amplified genes in human cancer and frequently found to be amplified in different tumor types such as breast, ovarian, bladder and squamous cell lung cancer. Therefore, FGFR1 is a promising therapeutic target but recent clinical trials for lung cancer patients highlighted that only a selected subset profit from an FGFR therapy. Thus, response rates cannot be predicted by sole analysis of FGFR1 amplification via FISH.

This study shows, that only the minority of 8p12 amplifications FGFR1 lay within the epicenter. Interestingly, overexpressed FGFR1 had only limited transforming capacities and is strongly ligand dependent. Co-expression of FGFR1 and MYC in NIH3T3 cells induce strong dependency on FGFR1. Furthermore, xenograft tumors generated from FGFR1 transduced NIH3T3 cells overexpressed MYC by themselves and additional MYC expression resulted in strong tumor regression during FGFR therapy. Whereas FGFR1 and MYC expression predicted FGFR inhibitor sensitivity in tumor cell lines, MYC knockdown caused FGFR inhibitor resistance. In the end a clinical case demonstrated the importance of FGFR1 amplification and MYC expression due to tumor response.

Altogether, an oncogenic transformation model of amplified FGFR1 tumors was provided, wherein both cell-autonomous and non-cell autonomous mechanisms dictate, whether these tumors are dependent on FGFR1 and thus are susceptible to FGFR inhibitor treatment.

8 References

Babu, M.M., Luscombe, N.M., Aravind, L., Gerstein, M., and Teichmann, S.A. (2004). Structure and evolution of transcriptional regulatory networks. Current Opinion in Structural Biology *14*, 283–291.

Badman, M.K., Pissios, P., Kennedy, A.R., Koukos, G., Flier, J.S., and Maratos-Flier, E. (2007). Hepatic Fibroblast Growth Factor 21 Is Regulated by PPARα and Is a Key Mediator of Hepatic Lipid Metabolism in Ketotic States. Cell Metabolism *5*, 426–437.

Bai, A., Meetze, K., Vo, N.Y., Kollipara, S., Mazsa, E.K., Winston, W.M., Weiler, S., Poling, L.L., Chen, T., Ismail, N.S., et al. (2010). GP369, an FGFR2-IIIb-Specific Antibody, Exhibits Potent Antitumor Activity against Human Cancers Driven by Activated FGFR2 Signaling. Cancer Research *70*, 7630–7639.

Beenken, A., and Mohammadi, M. (2009). The FGF family: biology, pathophysiology and therapy. Nat Rev Drug Discov *8*, 235–253.

Beroukhim, R., Getz, G., Nghiemphu, L., Barretina, J., Hsueh, T., Linhart, D., Vivanco, I., Lee, J.C., Huang, J.H., Alexander, S., et al. (2007). Assessing the significance of chromosomal aberrations in cancer: methodology and application to glioma. Proc. Natl. Acad. Sci. U.S.a. *104*, 20007–20012.

Bishop, J.R., Schuksz, M., and Esko, J.D. (2007). Heparan sulphate proteoglycans fine-tune mammalian physiology. Nature *446*, 1030–1037.

Blume-Jensen, P., and Hunter, T. (2001). Oncogenic kinase signalling. Nature *411*, 355–365.

Buettner, R., Wolf, J., and Thomas, R.K. (2013). Lessons Learned From Lung Cancer Genomics: The Emerging Concept of Individualized Diagnostics and Treatment. Journal of Clinical Oncology *31*, 1858–1865.

Celli, G., LaRochelle, W.J., Mackem, S., Sharp, R., and Merlino, G. (1998). Soluble dominant-negative receptor uncovers essential roles for fibroblast growth factors in multi-organ induction and patterning. Embo J. *17*, 1642–1655.

Colvin, J.S., Green, R.P., Schmahl, J., Capel, B., and Ornitz, D.M. (2001). Male-to-female sex reversal in mice lacking fibroblast growth factor 9. Cell *104*, 875–889.

Courjal, F., Cuny, M., Simony-Lafontaine, J., Louason, G., Speiser, P., Zeillinger, R., Rodriguez, C., and Theillet, C. (1997). Mapping of DNA amplifications at 15 chromosomal localizations in 1875 breast tumors: definition of phenotypic groups. Cancer Research *57*, 4360–4367.

Dang, C.V. (2012). MYC on the Path to Cancer. Cell *149*, 22–35.

Davis, M.I., Hunt, J.P., Herrgard, S., Pietro Ciceri, Wodicka, L.M., Pallares, G., Hocker, M., Treiber, D.K., and Zarrinkar, P.P. (2011). Comprehensive analysis of kinase inhibitor selectivity. Nature Biotechnology *29*, 1046–1051.

Detterbeck, F.C., Postmus, P.E., and Tanoue, L.T. (2013). The stage classification of lung cancer: Diagnosis and management of lung cancer, 3rd ed: American College of Chest Physicians evidence-based clinical practice guidelines. Chest *143*, e191S–210S.

Ding, L., Getz, G., Wheeler, D.A., Mardis, E.R., McLellan, M.D., Cibulskis, K., Sougnez, C., Greulich, H., Muzny, D.M., Morgan, M.B., et al. (2008). Somatic mutations affect key pathways in lung adenocarcinoma. Nature *455*, 1069–1075.

Falardeau, J., Chung, W.C.J., Beenken, A., Raivio, T., Plummer, L., Sidis, Y., Jacobson-Dickman, E.E., Eliseenkova, A.V., Ma, J., Dwyer, A., et al. (2008). Decreased FGF8 signaling causes deficiency of gonadotropin-releasing hormone in humans and mice. J. Clin. Invest. *118*, 2822–2831.

Feldman, B., Poueymirou, W., Papaioannou, V.E., DeChiara, T.M., and Goldfarb, M. (1995). Requirement of FGF-4 for postimplantation mouse development. Science *267*, 246–249.

Fernandez-Cuesta, L., Plenker, D., Osada, H., Sun, R., Menon, R., Leenders, F., Ortiz-Cuaran, S., Peifer, M., Bos, M., DaBler, J., et al. (2014). CD74-NRG1 fusions in lung adenocarcinoma. Cancer Discovery.

Floss, T., Arnold, H.H., and Braun, T. (1997). A role for FGF-6 in skeletal muscle regeneration. Genes & Development *11*, 2040–2051.

FRCS, P.P.G., FRANZCR, P.D.B., MD, J.R.J., Le Chevalier MD, T., FRCS, E.L., FRCPath, P.A.G.N., and MD, F.A.S. (2011). Non-small-cell lung cancer. The Lancet *378*, 1727–1740.

Garraway, L.A., and Lander, E.S. (2013). Lessons from the Cancer Genome. Cell *153*, 17–37.

Gartside, M.G., Chen, H., Ibrahimi, O.A., Byron, S.A., Curtis, A.V., Wellens, C.L., Bengston, A., Yudt, L.M., Eliseenkova, A.V., Ma, J., et al. (2009). Loss-of-Function Fibroblast Growth Factor Receptor-2 Mutations in Melanoma. Molecular Cancer Research *7*, 41–54.

Gorringe, K.L., Jacobs, S., Thompson, E.R., Sridhar, A., Qiu, W., Choong, D.Y.H., and Campbell, I.G. (2007). High-Resolution Single Nucleotide Polymorphism Array Analysis of Epithelial Ovarian Cancer Reveals Numerous Microdeletions and Amplifications. Clinical Cancer Research *13*, 4731–4739.

Green, D.R., and Kroemer, G. (2009). Cytoplasmic functions of the tumour suppressor p53. Nature *458*, 1127–1130.

Greenman, C., Stephens, P., Smith, R., Dalgliesh, G.L., Hunter, C., Bignell, G., Davies, H., Teague, J., Butler, A., Stevens, C., et al. (2007). Patterns of somatic mutation in human cancer genomes. Nature *446*, 153–158.

Greulich, H., and Pollock, P.M. (2011). Targeting mutant fibroblast growth factor receptors in cancer. Trends in Molecular Medicine *17*, 283–292.

Greulich, H., Chen, T.-H., Feng, W., Jänne, P.A., Alvarez, J.V., Zappaterra, M., Bulmer, S.E., Frank, D.A., Hahn, W.C., Sellers, W.R., et al. (2005). Oncogenic Transformation by Inhibitor-Sensitive and -Resistant EGFR Mutants. Plos Med *2*, e313.

Gustafsson, B.I., Kidd, M., Chan, A., Malfertheiner, M.V., and Modlin, I.M. (2008). Bronchopulmonary neuroendocrine tumors. Cancer *113*, 5–21.

Hammerman, P.S., Sos, M.L., Ramos, A.H., Xu, C., Dutt, A., Zhou, W., Brace, L.E., Woods, B.A., Lin, W., Zhang, J., et al. (2011). Mutations in the DDR2 Kinase Gene Identify a Novel Therapeutic Target in Squamous Cell Lung Cancer. Cancer Discovery *1*, 78–89.

Hammerman, P.S., Lawrence, M.S., Voet, D., Jing, R., Cibulskis, K., Sivachenko, A., Stojanov, P., McKenna, A., Lander, E.S., Gabriel, S., et al. (2012). Comprehensive genomic characterization of squamous cell lung cancers. Nature *489*, 519–525.

Hanahan, D., and Weinberg, R.A. (2011). Hallmarks of Cancer: The Next Generation. Cell *144*, 646–674.

Harari, D., and Yarden, Y. (2000). Molecular mechanisms underlying ErbB2/HER2 action in breast cancer. Oncogene *19*, 6102–6114.

Heukamp, L.C., Schröder, D.-W., Plassmann, D., Homann, J., and Büttner, R. (2003). Marked clinical and histologic improvement in a patient with type-1 Gaucher's disease following long-term glucocerebroside substitution. A case report and review of current diagnosis and management. Pathol. Res. Pract. *199*, 159–163.

Hébert, J.M., Rosenquist, T., Götz, J., and Martin, G.R. (1994). FGF5 as a regulator of the hair growth cycle: evidence from targeted and spontaneous mutations. Cell *78*, 1017–1025.

Hurwitz, H.I., Dowlati, A., Saini, S., Savage, S., Suttle, A.B., Gibson, D.M., Hodge, J.P., Merkle, E.M., and Pandite, L. (2009). Phase I Trial of Pazopanib in Patients with Advanced Cancer. Clinical Cancer Research *15*, 4220–4227.

Huse, M., and Kuriyan, J. (2002). The conformational plasticity of protein kinases. Cell *109*, 275–282.

Ihde, D.C. (1992). Chemotherapy of lung cancer. N Engl J Med *327*, 1434–1441.

Inagaki, T., Choi, M., Moschetta, A., Peng, L., Cummins, C.L., McDonald, J.G., Luo, G., Jones, S.A., Goodwin, B., Richardson, J.A., et al. (2005). Fibroblast growth factor 15 functions as an enterohepatic signal to regulate bile acid homeostasis. Cell Metabolism *2*, 217–225.

Ito, S., Fujimori, T., Furuya, A., Satoh, J., Nabeshima, Y., and Nabeshima, Y.-I. (2005). Impaired negative feedback suppression of bile acid synthesis in mice lacking βKlotho. J. Clin. Invest. *115*, 2202–2208.

Janku, F., Wheler, J.J., Naing, A., Falchook, G.S., Hong, D.S., Stepanek, V.M., Fu, S., Piha-Paul, S.A., Lee, J.J., Luthra, R., et al. (2013). PIK3CA Mutation H1047R Is Associated with Response to PI3K/AKT/mTOR Signaling Pathway Inhibitors in Early-Phase Clinical Trials. Cancer Research *73*, 276–284.

Kalinina, J., Dutta, K., Ilghari, D., Beenken, A., Goetz, R., Eliseenkova, A.V., Cowburn, D., and Mohammadi, M. (2012). The Alternatively Spliced Acid Box Region Plays a Key Role in FGF Receptor Autoinhibition. Structure/Folding and Design *20*, 77–88.

Kar, G., Keskin, O., Gursoy, A., and Nussinov, R. (2010). Allostery and population shift in drug discovery. Current Opinion in Pharmacology *10*, 715–722.

Kharitonenkov, A., Shiyanova, T.L., Koester, A., Ford, A.M., Micanovic, R., Galbreath, E.J., Sandusky, G.E., Hammond, L.J., Moyers, J.S., Owens, R.A., et al. (2005). FGF-21 as a novel metabolic regulator. J. Clin. Invest. *115*, 1627–1635.

Khuder, S.A. (2001). Effect of cigarette smoking on major histological types of lung cancer: a meta-analysis. Lung Cancer *31*, 139–148.

Koboldt, D.C., Fulton, R.S., McLellan, M.D., Schmidt, H., Kalicki-Veizer, J., McMichael, J.F., Fulton, L.L., Dooling, D.J., Ding, L., Mardis, E.R., et al. (2012). Comprehensive molecular portraits of human breast tumours. Nature *490*, 61–70.

Kumar, R., Crouthamel, M.-C., Rominger, D.H., Gontarek, R.R., Tummino, P.J., Levin, R.A., and King, A.G. (2009). Myelosuppression and kinase selectivity of multikinase angiogenesis inhibitors. British Journal of Cancer *101*, 1717–1723.

Laity, J.H., Lee, B.M., and Wright, P.E. (2001). Zinc finger proteins: new insights into structural and functional diversity. Current Opinion in Structural Biology *11*, 39–46.

Latchman, D.S. (1997). Transcription factors: an overview. Int. J. Biochem. Cell Biol. *29*, 1305–1312.

Lax, I., Wong, A., Lamothe, B., Lee, A., Frost, A., Hawes, J., and Schlessinger, J. (2002). The docking protein FRS2alpha controls a MAP kinase-mediated negative feedback mechanism for signaling by FGF receptors. Mol. Cell *10*, 709–719.

Lee, T.I., and Young, R.A. (2013). Transcriptional Regulation and Its Misregulation in Disease. Cell *152*, 1237–1251.

Lemmon, M.A., and Schlessinger, J. (2010). Cell Signaling by Receptor Tyrosine Kinases. Cell *141*, 1117–1134.

Lengauer, C., Kinzler, K.W., and Vogelstein, B. (1998). Genetic instabilities in human cancers. Nature *396*, 643–649.

Liebmann, C. (2001). Regulation of MAP kinase activity by peptide receptor signalling pathway: paradigms of multiplicity. Cell. Signal. *13*, 777–785.

Lockwood, W.W., Chari, R., Coe, B.P., Thu, K.L., Garnis, C., Malloff, C.A., Campbell, J., Williams, A.C., Hwang, D., Zhu, C.-Q., et al. (2010). Integrative Genomic Analyses Identify BRF2 as a Novel Lineage-Specific Oncogene in Lung Squamous Cell Carcinoma. Plos Med *7*, e1000315.

Lu, S.Y., Sheikh, F., Sheppard, P.C., Fresnoza, A., Duckworth, M.L., Detillieux, K.A., and Cattini, P.A. (2008). FGF-16 is required for embryonic heart development. Biochemical and Biophysical Research Communications *373*, 270–274.

Manning, G. (2002). The Protein Kinase Complement of the Human Genome. Science *298*, 1912–1934.

Mantovani, A., Allavena, P., Sica, A., and Balkwill, F. (2008). Cancer-related inflammation. Nature *454*, 436–444.

Marek, L., Ware, K.E., Fritzsche, A., Hercule, P., Helton, W.R., Smith, J.E., McDermott, L.A., Coldren, C.D., Nemenoff, R.A., Merrick, D.T., et al. (2008). Fibroblast Growth Factor (FGF) and FGF Receptor-Mediated Autocrine Signaling in Non-Small-Cell Lung Cancer Cells. Molecular Pharmacology *75*, 196–207.

Maruyama-Takahashi, K., Shimada, N., Imada, T., Maekawa-Tokuda, Y., Ishii, T., Ouchi, J., Kusaka, H., Miyaji, H., Akinaga, S., Tanaka, A., et al. (2008). A neutralizing anti-fibroblast growth factor (FGF) 8 monoclonal antibody shows anti-tumor activity against FGF8b-expressing LNCaP xenografts in androgen-dependent and -independent conditions. Prostate *68*, 640–650.

Mason, I. (2007). Initiation to end point: the multiple roles of fibroblast growth factors in neural development. Nat Rev Neurosci *8*, 583–596.

McWhirter, J.R., Galasso, D.L., and Wang, J.Y. (1993). A coiled-coil oligomerization domain of Bcr is essential for the transforming function of Bcr-Abl oncoproteins. Mol. Cell. Biol. *13*, 7587–7595.

Meyers, E.N., Lewandoski, M., and Martin, G.R. (1998). An Fgf8 mutant allelic series generated by Cre- and Flp-mediated recombination. Nat Genet *18*, 136–141.

Miller, D.L., Ortega, S., Bashayan, O., Basch, R., and Basilico, C. (2000). Compensation by fibroblast growth factor 1 (FGF1) does not account for the mild phenotypic defects observed in FGF2 null mice. Mol. Cell. Biol. *20*, 2260–2268.

Milunsky, J.M., Zhao, G., Maher, T.A., Colby, R., and Everman, D.B. (2006). LADD syndrome is caused by FGF10 mutations. Clinical Genetics *69*, 349–354.

Min, H., Danilenko, D.M., Scully, S.A., Bolon, B., Ring, B.D., Tarpley, J.E., DeRose, M., and Simonet, W.S. (1998). Fgf-10 is required for both limb and lung development and exhibits striking functional similarity to Drosophila branchless. Genes & Development *12*, 3156–3161.

Missiaglia, E., Selfe, J., Hamdi, M., Williamson, D., Schaaf, G., Fang, C., Koster, J., Summersgill, B., Messahel, B., Versteeg, R., et al. (2009). Genomic imbalances in rhabdomyosarcoma cell lines affect expression of genes frequently altered in primary tumors: An approach to identify candidate genes involved in tumor development. Genes Chromosom. Cancer *48*, 455–467.

Mok, T.S., Wu, Y.-L., Thongprasert, S., Yang, C.-H., Chu, D.-T., Saijo, N., Sunpaweravong, P., Han, B., Margono, B., Ichinose, Y., et al. (2009). Gefitinib or Carboplatin–Paclitaxel in Pulmonary Adenocarcinoma. N Engl J Med *361*, 947–957.

Murre, C., Bain, G., van Dijk, M.A., Engel, I., Furnari, B.A., Massari, M.E., Matthews, J.R., Quong, M.W., Rivera, R.R., and Stuiver, M.H. (1994). Structure and function of helix-loop-helix proteins. Biochim. Biophys. Acta *1218*, 129–135.

Nagata, S. (1997). Apoptosis by death factor. Cell *88*, 355–365.

Network, T.C.G.A.R. (2014). Comprehensive molecular characterization of urothelial bladder carcinoma. Nature *507*, 315–322.

Noble, M.E.M. (2004). Protein Kinase Inhibitors: Insights into Drug Design from Structure. Science *303*, 1800–1805.

Nolen, B., Taylor, S., and Ghosh, G. (2004). Regulation of protein kinases; controlling activity through activation segment conformation. Mol. Cell *15*, 661–675.

Nussinov, R., and Tsai, C.-J. (2013). Allostery in Disease and in Drug Discovery. Cell *153*, 293–305.

Ogino, S., Gulley, M.L., Dunnen, den, J.T., and Wilson, R.B. (2007). Standard Mutation Nomenclature in Molecular Diagnostics. The Journal of Molecular Diagnostics *9*, 1–6.

Ota, S., Zhou, Z.Q., Link, J.M., and Hurlin, P.J. (2009). The role of senescence and prosurvival signaling in controlling the oncogenic activity of FGFR2 mutants associated with cancer and birth defects. Human Molecular Genetics *18*, 2609–2621.

Paul, M.K., and Mukhopadhyay, A.K. (2004). Tyrosine kinase - Role and significance in Cancer. Int J Med Sci *1*, 101–115.

Peifer, M., Fernández-Cuesta, L., Sos, M.L., George, J., Seidel, D., Kasper, L.H., Plenker, D., Leenders, F., Sun, R., Zander, T., et al. (2012). Integrative genome analyses identify key somatic driver mutations of small-cell lung cancer. Nat Genet *44*, 1104–1110.

Petersen, I. (2011). The morphological and molecular diagnosis of lung cancer. Dtsch Arztebl Int *108*, 525–531.

Plotnikov, A.N., Hubbard, S.R., Schlessinger, J., and Mohammadi, M. (2000). Crystal structures of two FGF-FGFR complexes reveal the determinants of ligand-receptor specificity. Cell *101*, 413–424.

Reiner, S.L. (2007). Development in Motion: Helper T Cells at Work. Cell *129*, 33–36.

Robert-Koch-Institut (2013). Krebs in Deutschland 2009/2010. 1–150.

Rubin, H. (2011). The early history of tumor virology: Rous, RIF, and RAV. Proc. Natl. Acad. Sci. U.S.a. *108*, 14389–14396.

Schaffer, B.E., Park, K.S., Yiu, G., Conklin, J.F., Lin, C., Burkhart, D.L., Karnezis, A.N., Sweet-Cordero, E.A., and Sage, J. (2010). Loss of p130 Accelerates Tumor Development in a Mouse Model for Human Small-Cell Lung Carcinoma. Cancer Research *70*, 3877–3883.

Schildhaus, H.-U., Heukamp, L.C., Merkelbach-Bruse, S., Riesner, K., Schmitz, K., Binot, E., Paggen, E., Albus, K., Schulte, W., Ko, Y.-D., et al. (2012). Definition of a fluorescence in-situ hybridization score identifies high- and low-level FGFR1 amplification types in squamous cell lung cancer. *25*, 1473–1480.

Schiller, J.H., Harrington, D., Belani, C.P., Langer, C., Sandler, A., Krook, J., Zhu, J., Johnson, D.H., Eastern Cooperative Oncology Group (2002). Comparison of four chemotherapy regimens for advanced non-small-cell lung cancer. N Engl J Med *346*, 92–98.

Sharma, S.V., Bell, D.W., Settleman, J., and Haber, D.A. (2007). Epidermal growth factor receptor mutations in lung cancer. Nat Rev Cancer *7*, 169–181.

Sherr, C.J. (2004). Principles of tumor suppression. Cell *116*, 235–246.

Siegel, R., DeSantis, C., Virgo, K., Stein, K., Mariotto, A., Smith, T., Cooper, D., Gansler, T., Lerro, C., Fedewa, S., et al. (2012). Cancer treatment and survivorship statistics, 2012. CA: a Cancer Journal for Clinicians *62*, 220–241.

Simon, R., Richter, J., Wagner, U., Fijan, A., Bruderer, J., Schmid, U., Ackermann, D., Maurer, R., Alund, G., Knönagel, H., et al. (2001). High-throughput tissue microarray analysis of 3p25 (RAF1) and 8p12 (FGFR1) copy number alterations in urinary bladder cancer. Cancer Research *61*, 4514–4519.

Soda, M., Choi, Y.L., Enomoto, M., Takada, S., Yamashita, Y., Ishikawa, S., Fujiwara, S.-I., Watanabe, H., Kurashina, K., Hatanaka, H., et al. (2007). Identification of the transforming EML4–ALK fusion gene in non-small-cell lung cancer. Nature *448*, 561–566.

Solit, D.B., Garraway, L.A., Pratilas, C.A., Sawai, A., Getz, G., Basso, A., Ye, Q., Lobo, J.M., She, Y., Osman, I., et al. (2005). BRAF mutation predicts sensitivity to MEK inhibition. Nature *439*, 358–362.

Sos, M.L., Koker, M., Weir, B.A., Heynck, S., Rabinovsky, R., Zander, T., Seeger, J.M., Weiss, J., Fischer, F., Frommolt, P., et al. (2009a). PTEN Loss Contributes to Erlotinib Resistance in EGFR-Mutant Lung Cancer by Activation of Akt and EGFR. Cancer Research *69*, 3256–3261.

Sos, M.L., Michel, K., Zander, T., Weiss, J., Frommolt, P., Peifer, M., Li, D., Ullrich, R., Koker, M., Fischer, F., et al. (2009b). Predicting drug susceptibility of non–small cell lung cancers based on genetic lesions. J. Clin. Invest. *119*, 1727–1740.

Soucie, E.L., Annis, M.G., Sedivy, J., Filmus, J., Leber, B., Andrews, D.W., and Penn, L.Z. (2001). Myc potentiates apoptosis by stimulating Bax activity at the mitochondria. Mol. Cell. Biol. *21*, 4725–4736.

Sun, S., Schiller, J.H., and Gazdar, A.F. (2007). Lung cancer in never smokers — a different disease. Nat Rev Cancer *7*, 778–790.

Tekin, M., Hişmi, B.O., Fitoz, S., Ozdağ, H., Cengiz, F.B., Sirmaci, A., Aslan, I., Inceoğlu, B., Yüksel-Konuk, E.B., Yilmaz, S.T., et al. (2007). Homozygous mutations in fibroblast growth factor 3 are associated with a new form of syndromic deafness characterized by inner ear agenesis, microtia, and microdontia. Am. J. Hum. Genet. *80*, 338–344.

The Clinical Lung Cancer Genome Project (CLCGP) and Network Genomic Medicine (NGM), (2013). A Genomics-Based Classification of Human Lung Tumors. Science Translational Medicine *5*, 209ra153–209ra153.

Tomlinson, D.C., and Knowles, M.A. (2010). Altered Splicing of FGFR1 Is Associated with High Tumor Grade and Stage and Leads to Increased Sensitivity to FGF1 in Bladder Cancer. The American Journal of Pathology *177*, 2379–2386.

Travis, W.D. (2011). Pathology of Lung Cancer. Clinics in Chest Medicine *32*, 669–692.

Travis, W.D., Brambilla, E., Noguchi, M., Nicholson, A.G., Geisinger, K.R., Yatabe, Y., Beer, D.G., Powell, C.A., Riely, G.J., Van Schil, P.E., et al. (2011). International association for the study of lung cancer/american thoracic society/european respiratory society international multidisciplinary classification of lung adenocarcinoma. J Thorac Oncol *6*, 244–285.

Tsai, C.-J., del Sol, A., and Nussinov, R. (2009). Protein allostery, signal transmission and dynamics: a classification scheme of allosteric mechanisms. Mol. BioSyst. *5*, 207.

Turner, N., and Grose, R. (2010). Fibroblast growth factor signalling: from development to cancer. 1–14.

Umemori, H., Linhoff, M.W., Ornitz, D.M., and Sanes, J.R. (2004). FGF22 and its close relatives are presynaptic organizing molecules in the mammalian brain. Cell *118*, 257–270.

van der Walt, J.M., Noureddine, M.A., Kittappa, R., Hauser, M.A., Scott, W.K., McKay, R., Zhang, F., Stajich, J.M., Fujiwara, K., Scott, B.L., et al. (2004). Fibroblast growth factor 20 polymorphisms and haplotypes strongly influence risk of Parkinson disease. Am. J. Hum. Genet. *74*, 1121–1127.

Verma, S., Miles, D., Gianni, L., Krop, I.E., Welslau, M., Baselga, J., Pegram, M., Oh, D.-Y., Diéras, V., Guardino, E., et al. (2012). Trastuzumab Emtansine for HER2-Positive Advanced Breast Cancer. N Engl J Med *367*, 1783–1791.

Vinson, C., Myakishev, M., Acharya, A., Mir, A.A., Moll, J.R., and Bonovich, M. (2002). Classification of human B-ZIP proteins based on dimerization properties. Mol. Cell. Biol. *22*, 6321–6335.

Weiss, J., Sos, M.L., Seidel, D., Peifer, M., Zander, T., Heuckmann, J.M., Ullrich, R.T., Menon, R., Maier, S., Soltermann, A., et al. (2010). Frequent and Focal FGFR1 Amplification Associates with Therapeutically Tractable FGFR1

Dependency in Squamous Cell Lung Cancer. Science Translational Medicine *2*, 62ra93–62ra93.

Wheeler, D.A., and Wang, L. (2013). From human genome to cancer genome: The first decade. Genome Research *23*, 1054–1062.

Wintjens, R., and Rooman, M. (1996). Structural classification of HTH DNA-binding domains and protein-DNA interaction modes. J. Mol. Biol. *262*, 294–313.

Xu, J. (1996). Receptor Specificity of the Fibroblast Growth Factor Family. Journal of Biological Chemistry *271*, 15292–15297.

Xu, J., Liu, Z., and Ornitz, D.M. (2000). Temporal and spatial gradients of Fgf8 and Fgf17 regulate proliferation and differentiation of midline cerebellar structures. Development *127*, 1833–1843.

Yang, L., Luquette, L.J., Gehlenborg, N., Xi, R., Haseley, P.S., Hsieh, C.-H., Zhang, C., Ren, X., Protopopov, A., Chin, L., et al. (2013). Diverse Mechanisms of Somatic Structural Variations in Human Cancer Genomes. Cell *153*, 919–929.

Zakowski, M.F., Ladanyi, M., Kris, M.G., Memorial Sloan-Kettering Cancer Center Lung Cancer OncoGenome Group (2006). EGFR mutations in small-cell lung cancers in patients who have never smoked. N Engl J Med *355*, 213–215.

Zhang, X., Ibrahimi, O.A., Olsen, S.K., Umemori, H., Mohammadi, M., and Ornitz, D.M. (2006). Receptor Specificity of the Fibroblast Growth Factor Family: THE COMPLETE MAMMALIAN FGF FAMILY. Journal of Biological Chemistry *281*, 15694–15700.

8.1 Additional sources

Andre F, Ranson M, Dean E, Varga A, Van der Noll R, Stockman PK, et al. Results of a phase I study of AZD4547, an inhibitor of fibroblast growth factor receptor (FGFR), in patients with advanced solid tumors [Abstract]. *AACR* 2013.

Sequist LV, Cassier P, Varga A, Tabernero J, Schellens JHM, Delord JP, et al. Phase I study of BGJ398, a selective pan-FGFR inhibitor in genetically preselected advanced solid tumors [Abstract]. *AACR* 2014.

The biology of cancer; Weinberg, R. A. (2007).

The Emperor of All Maladies, A Biography of Cancer; Siddhartha, M. (2011).

https://www.destatis.de; Statistisches Bundesamt; March 2014

http://www.rki.de; Robert Koch Institut; March 2014

https://www.destatis.de/DE/ZahlenFakten/GesellschaftStaat/Gesundheit/Todesursachen/Tabellen/SterbefaelleInsgesamt.html; Statistisches Bundesamt; March 2014

http://www.krebsdaten.de/Krebs/DE/Home/homepage_node.html; Robert Koch Institut; March 2014

http://cancergenome.nih.gov; The Cancer Genome Atlas; December 2013

http://genepattern.broadinstitute.org/gp/pages/login.jsf; Broad Institute, MIT; Mai 2013

9 Publications

Malchers, F., Dietlein, F., Schöttle, J., Lu, X., Nogova, L., Albus, K., Fernandez-Cuesta, L., et al. (2014). Cell-Autonomous and Non-Cell-Autonomous Mechanisms of Transformation by Amplified FGFR1 in Lung Cancer. *Cancer discovery*, *4*(2), 246–57. doi:10.1158/2159-8290.CD-13-0323

Zhang, J., Zhang, L., Su, X., Li, M., Xie, L., **Malchers, F.**, Fan, S., et al. (2012). Translating the therapeutic potential of AZD4547 in FGFR1-amplified non-small cell lung cancer through the use of patient-derived tumor xenograft models. *Clinical cancer research : an official journal of the American Association for Cancer Research*, *18*(24), 6658–67. doi:10.1158/1078-0432.CCR-12-2694

Heuckmann, J. M., Balke-Want, H., **Malchers, F.**, Peifer, M., Sos, M. L., Koker, M., Meder, L., et al. (2012). Differential Protein Stability and ALK Inhibitor Sensitivity of EML4-ALK Fusion Variants. *Clinical cancer research : an official journal of the American Association for Cancer Research*, *18*(17), 4682–90. doi:10.1158/1078-0432.CCR-11-3260

Sos, M. L., Dietlein, F., Peifer, M., Schottle, J., Balke-Want, H., Muller, … **Malchers, F.**, et al. (2012). A framework for identification of actionable cancer genome dependencies in small cell lung cancer. *Proceedings of the National Academy of Sciences*. doi:10.1073/pnas.1207310109

Weiss, J., Sos, M. L., Seidel, D., Peifer, M., Zander, T., Heuckmann, J. M., … **Fischer, F.**, et al. (2010). Frequent and focal FGFR1 amplification associates with therapeutically tractable FGFR1 dependency in squamous cell lung cancer. *Science translational medicine*, *2*(62), 62ra93. doi:10.1126/scitranslmed.3001451

Sos, M. L., Rode, H. B., Heynck, S., Peifer, M., **Fischer, F.**, Klüter, S., Pawar, V. G., et al. (2010). Chemogenomic profiling provides insights into the limited activity of irreversible EGFR Inhibitors in tumor cells expressing the T790M EGFR resistance mutation. *Cancer research*, *70*(3), 868–74. doi:10.1158/0008-5472.CAN-09-3106

Sos, M. L., Koker, M., Weir, B. A., Heynck, S., Rabinovsky, R., Zander, T., … **Fischer, F.**, et al. (2010). PTEN Loss Contributes to Erlotinib Resistance in EGFR-Mutant Lung Cancer by Activation of Akt and EGFR. *Cancer research*, *69*(8), 3256–3261. doi:10.1158/0008-5472.CAN-08-4055.PTEN

Sos, M. L., Fischer, S., Ullrich, R., Peifer, M., Heuckmann, J. M., …**Fischer, F.**, et al. (2009). Identifying genotype-dependent efficacy of single and combined PI3K- and MAPK-pathway inhibition in cancer. *Proceedings of the National Academy of Sciences of the United States of America*, *106*(43), 18351–6. doi:10.1073/pnas.0907325106

Sos, M. L., Michel, K., Zander, T., Weiss, J., Frommolt, P., Peifer, M., Li, D., … **Fischer F.**, et al. (2009). Technical advance Predicting drug susceptibility of non – small cell lung cancers based on genetic lesions. *The Journal of Clinical Investigation*, *119*(6), 1727–1740. doi:10.1172/JCI37127DS1

Appendix

Ich versichere, dass ich die von mir vorgelegte Dissertation selbständig angefertigt, die benutzten Quellen und Hilfsmittel vollständig angegeben und die Stellen der Arbeit – einschließlich Tabellen, Karten und Abbildungen –, die anderen Werken im Wortlaut oder dem Sinn nach entnommen sind, in jedem Einzelfall als Entlehnung kenntlich gemacht habe; dass diese Dissertation noch keiner anderen Fakultät oder Universität zur Prüfung vorgelegen hat; dass sie – abgesehen von unten angegebenen Teilpublikationen – noch nicht veröffentlicht worden ist sowie, dass ich eine solche Veröffentlichung vor Abschluss des Promotionsverfahrens nicht vornehmen werde. Die Bestimmungen der Promotionsordnung sind mir bekannt. Die von mir vorgelegte Dissertation ist von Prof. Dr. Roman Thomas betreut worden.

Unterschrift

Curriculum vitae

Name: Florian Malchers (birth name: Fischer)

Address: Alter Traßweg 9, 51427 Bergisch-Gladbach

Date of birth: 04.09.1981, Bonn

Nationality: German

Marital status: Married, two children

Phone number: 0171 1056180

Email: Florian.Malchers@uni-koeln.de

Florian.Malchers@gmail.de

Academics:

05/2012 – now	PhD student at the University of Cologne, Department of Translational Genomics, Germany
05/2009 -05/2012	PhD position at the Max Planck Institute for Neurological Research in Cologne, Junior Research Group Cancer Genomics, Germany
10/2002 – 05/2009	Studies of life science at the University of Cologne, biochemistry, genetics and physics, final grate: 1.0
05/2008 – 05/2009	Diploma thesis at the Max Planck Institute for Neurological Research in Cologne, Germany, grade: 1.0
12/2007 – 07/2008	ERASMUS exchange, University of Manchester, England, clinical genetics, molecular biology of cancer and molecular evolution
08/2001 -05/2002	Alternative national service at the Katholische Studierende Jugend (KSJ) Cologne, Germany
08/1992 – 06/2001	Secondary school, Stätisches Gymnasium Köln-Deutz, Germany
08/1992 – 06/1998	Secondary school, BRO, Overath, Germany

Köln 18.03.2014